Eastern Research Group, Inc.

Brake and Tire Wear Emissions

Final Report

Revision 2

Prepared for:

California Air Resources Board

February 11, 2021

ERG 3982.03

Brake and Tire Wear Emissions
Project 17RD016

Final Report, Revision 2

2/11/21

Alan Stanard
Tim DeFries
Cindy Palacios
Sandeep Kishan
Eastern Research Group
In Cooperation with
LINK Testing Laboratories, Inc.

Prepared for the California Air Resources Board and the California Environmental Protection Agency

Disclaimer

The statements and conclusions in this Report are those of the contractor and not necessarily those of the California Air Resources Board. The mention of commercial products, their source, or their use in connection with material reported herein is not to be construed as actual or implied endorsement of such products.

Acknowledgment

ERG would like to acknowledge the work performed by Caltrans on the 2010-2012 California Household Travel Survey. The results of that survey are hosted and presented for public use by the National Renewable Energy Laboratory (NREL), and ERG would like to acknowledge the benefit to researchers by NREL maintaining and hosting the data. ERG would also like to thank the US Environmental Protection Agency's National Vehicle Fuel Emissions Laboratory (NVFEL) staff for their cooperative additional funding to the project that allowed additional types of measurements in support of the project's goals. ERG would also like to thank LINK staff for their efforts and dedication to this project.

ERG and LINK wish to acknowledge the significant contributions of Dan Berletchick from RAYLOC providing business intelligence and detailed vehicle and brake information; of Gregory Vyletel from Federal Mogul for review of the vehicle selection to validate it against common industry practices; of Jerry Forystek from Brake Parts International for the proper use of the replacement rate index.

This Report was submitted in fulfillment of Project 17RD016, Brake and Tire Wear, by ERG under the sponsorship of the California Air Resources Board. Work was completed as of 2/11/2021.

Table of Contents

Appendices

List of Figures

List of Tables

Abstract

As tailpipe emissions of particulate matter (PM) from the light-duty fleet have decreased significantly, non-tailpipe PM emissions, such as brake and tire wear have become a larger portion of the California light-duty PM emissions inventory. This research was conducted on behalf of CARB to inform the relative level of PM emissions from braking in the light-duty fleet, update EMFAC emission factors and speed correction cycles, and generally better understand the variables most significant in affecting brake emissions.

ERG partnered with LINK to perform emissions testing using a brake dynamometer in a constant velocity sampling (CVS) system. Based on temperature measurements during on-track testing, a temperature model was created to estimate light-duty brake temperatures based on speed data. This model was applied to California Household Travel Survey data, which contains 1Hz vehicle speed data from in-use operation. This dataset was used to generate a brake dynamometer cycle that is representative of in-use driving modes. The cycle included three segments representing different trip average speeds. Six different vehicle model assemblies, each with up to 3 different brake friction material types, were tested on the brake dynamometer over this cycle in 83 different tests. PM mass, particle counts, particle size distributions, and various other parameters were measured during testing. Testing also included the dynamometer modeling of the operation of a single regenerative-braking-equipped vehicle. Results tended to increase with increasing vehicle weight. The mass emissions were sensitive to the different pad material types as well as the regeneration function. Results are calculated and presented at the vehicle and vehicle class level for potential integration into EMFAC. The test results were sensitive to the various parameters in the test matrix. When in-use pad material rates are accounted for, the estimated PM emission rates vary from 3.3 mg/mi to 13.6 mg/mi depending on model. Metallic pad materials tended to emit higher PM masses and tended to have larger particles in their emitted size distributions. Mass emission rates on a per-mile basis were highest at medium average trip speeds and lower at high and low average trip speeds.

Executive Summary

Background

As tailpipe emissions of PM from the light-duty fleet have decreased significantly, non-tailpipe PM emissions, such as brake and tire wear have become more relevant and may be significantly impacting air quality near roadways. This research project was conducted to measure and analyze particulate matter (PM) emitted during light-duty vehicle braking to allow CARB to update emission factors in the Emission Factor inventory model (EMFAC) as well as to better understand the vehicle operational conditions associated with varying levels of brake PM emissions. This study utilized a LINK Engineering (LINK) brake dynamometer (in which the brake components of a single wheel are mounted and operated electronically) for the measurement of PM emissions over a prescribed driving cycle.

Objectives and Methods

Based on literature search, Eastern Research Group (ERG) and LINK determined that 4 parameters of a test cycle would be most likely to affect braking PM emissions: vehicle speed, deceleration rate, brake component temperature, and the duration of a given brake event. These four parameters formed the basis of the development of a new test cycle and procedure to test vehicle brake assemblies on the brake dynamometer.

Six test vehicles (with common cross-platform brake components) were selected to represent the range of vehicle types in the light-duty fleet. These vehicles were subject to track tests in which brake system temperatures were measured during standardized driving cycles. This temperature data was used to both inform a light-duty brake temperature model that ERG developed (temperature as a function of vehicle speed) and to select the cooling level used during brake dynamometer tests.

A new test cycle was developed to represent the operation of real-world vehicles in California based on the 2010-2012 Caltrans Household Travel Survey. This survey included speed data logged from over 2,000 vehicles operating throughout the state. ERG used the developed temperature model to estimate the distribution of brake temperatures encountered by these actual California trips. ERG developed a new test cycle to be as similar as possible to the speeds, deceleration rates, temperatures, and braking durations encountered by real vehicles. This new cycle is composed of three distinctive operation patterns characterized with 3 speed bins to facilitate resolving emission rates across different trip average speed ranges.

The LINK lab site included a constant volume sampling (CVS) system with an integrated brake dynamometer. The airflow through the CVS provides the medium for transferring brake particles to the point of sampling as well as the brake cooling. Cooling flowrates were selected for the front and rear brake for each model to match temperatures encountered during track testing. Measurements were made in batch and continuously by a variety of instruments including gravimetric sampling in parallel on coated aluminum impactors (TSI 100S4) as well as on 47mm Teflon filters. Instrumentation was also installed to measure particle size distributions, particle counts, and continuous particle mass. A test matrix was developed consisting of 85 single-day tests of different test parameters for the 6 selected vehicles and two tunnel blanks; brake friction materials, vehicle test weights, and front and rear axles were varied. All test parameter combinations were replicated in at least two different tests. One of the vehicles was equipped with regenerative braking and the dynamometer was programmed to simulate that regenerative braking function during testing of that model.

Results

Figure ES-1 presents the vehicle-level results for each of the 6 tested models by three different pad materials: Original Equipment Service non-asbestos organic (OES-NAO), aftermarket NAO, and aftermarket Low-Metallic (LM). Vehicle-level emissions for each pad type are calculated by doubling the average front and rear single-wheel emission rates for each pad material type and summing.

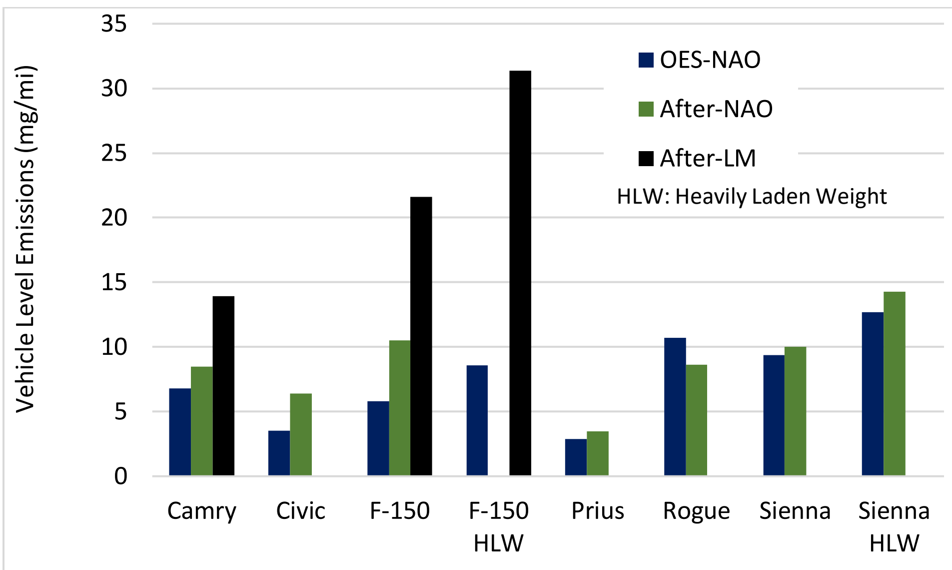

Figure ES-1. Vehicle level braking emissions by model and friction material

Vehicle-level emission rates trended with vehicle weight within each pad material type. Figure ES-2 presents the vehicle level PM mass emission rate against the simulated vehicle test weight. It can be seen that the OES-NAO fit has the shallowest increase in emissions with weight and the LM fit has the highest increase with weight.

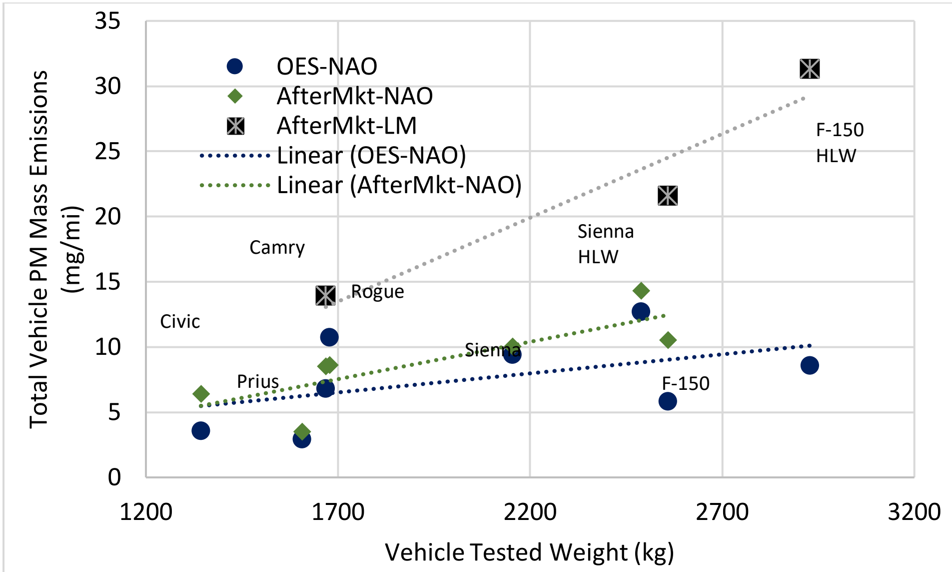

Figure ES-2. Vehicle level braking emissions vs vehicle test weight by pad material

Particle size distribution was also measured across two size ranges during all tests. Figure ES-3 presents the test-level particle size distribution for tests of the Civic front brakes in the range from 5.6 to 560 nm, and Figure ES-4 presents the size distribution measured (using a different measurement principle) for the range from 0.5 to 18 µm for the same tests. Distributions are shown by pad material. The Civic is shown in these plots as it was representative of most test results. All vehicles resulted in multimodal distributions with at least one peak found within each particle size range.

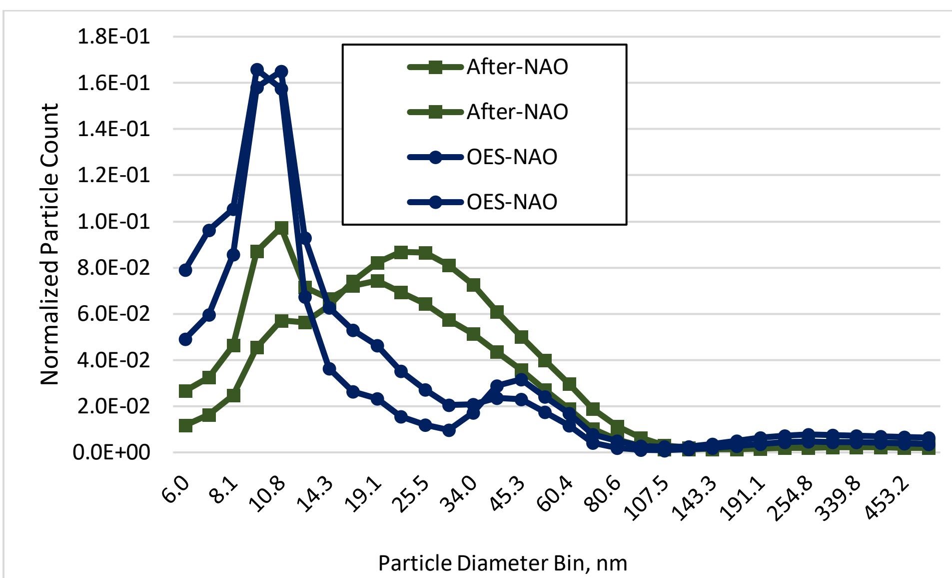

Figure ES-3. Particle size distribution for the Camry Front axle tests, 5.6-560 nm.

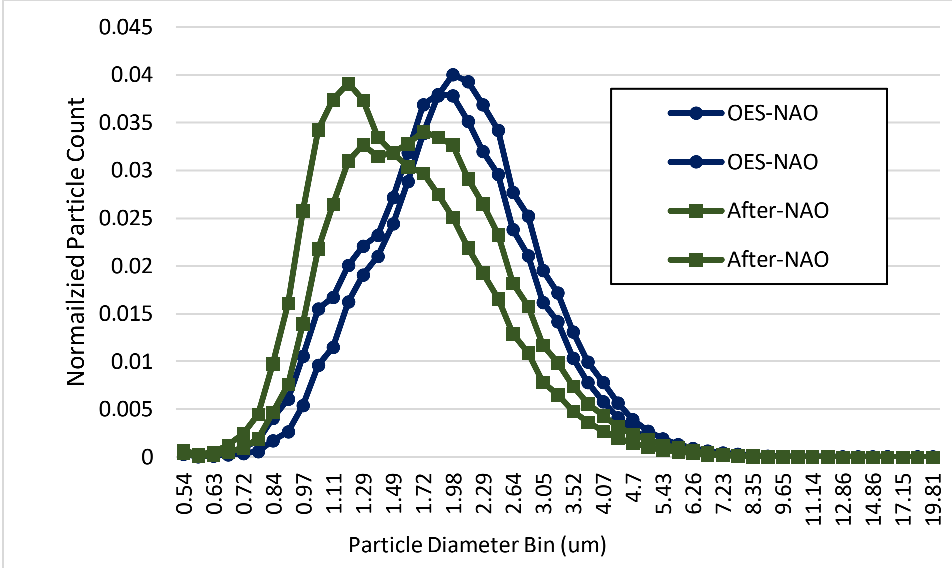

Figure ES-4. Particle size distribution for the Civic Front axle tests, 0.5-18 µm.

ERG also calculated speed correction factors (SCFs) to resolve emission rates by trip average speed. These values were based on the relative emission rates observed from continuous measurements associated with brake events representing vehicle operation at different average speeds. ERG performed this analysis using continuous PM mass measurement data divided into 5 speed bins. The overall correction factors for PM2.5 and PM10 are presented in Figure ES-5. Emission rates were highest for trips with medium average speeds and lowest for trips with high average speeds.

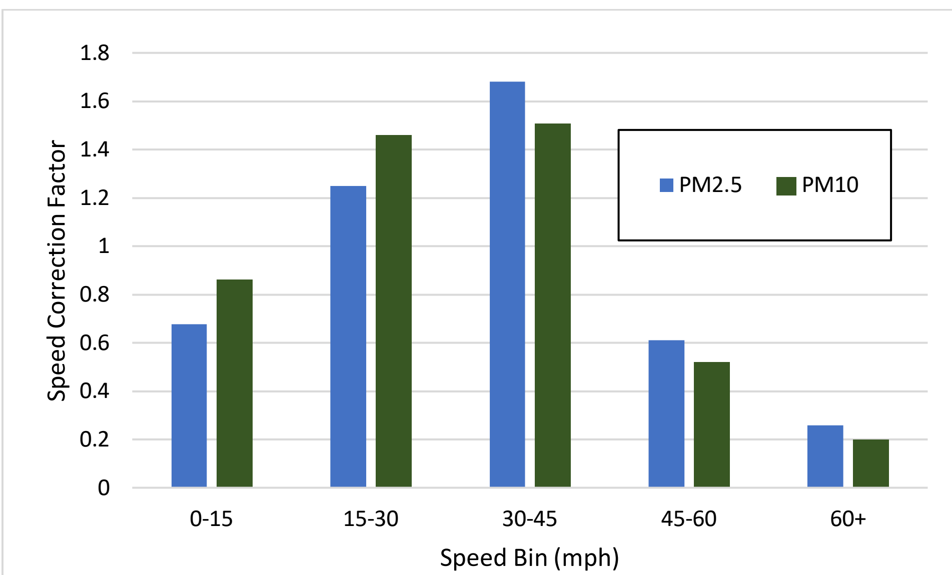

Figure ES-5. Speed correction factors for PM2.5 and PM10.

Correlations were also found between PM emissions and other test parameters. Particle count emissions generally trended with overall mass, however the observed range from the lowest to highest emitter was reduced as compared to the range of measured masses. ERG observed a loose correlation between PM mass emissions and the component mass loss from each pad and rotor.

Conclusions

The test results were sensitive to the various parameters in the test matrix. When in-use pad material rates are accounted for, the estimated vehicle-level PM emission rates vary from 3.3 to 13.6 mg/mi depending on model. Metallic pad materials tended to emit higher PM masses and tended to have larger particles in their emitted size distributions.

Main Report

Introduction

This research project was conducted to measure and analyze particulate matter (PM) emitted during light-duty vehicle braking to allow California Air Resources Board (CARB) to update emission factors in the Emission Factor inventory model (EMFAC). CARB relies on EMFAC to project future emission levels and to test how new regulatory programs can affect community air. As tailpipe emissions of PM from the light-duty fleet have decreased significantly, non-tailpipe PM emissions, such as brake and tire wear have become more relevant and may be significantly impacting air quality near roadways. This research was conducted to inform the relative level of PM emissions from braking in the light-duty fleet, characterize PM emission factors and speed correction factors that could be used for EMFAC, and generally better understand the variables most significant in affecting brake emissions.

Light-Duty Vehicle Braking Systems

Typical light-duty vehicle braking systems rely on hydraulically activated friction between two component surfaces, one that is generally stationary with respect to the vehicle's suspension, and the other that rotates with the vehicle's wheel. During braking, the friction generated between brake components generates heat and abrades the components at their frictional interface resulting in particles being released into the atmosphere.

Most modern vehicles rely on pad and rotor combinations for braking; the rotor rotates with the wheel, and the pads are mounted in a caliper stationary to the suspension. The driver's application of force to the brake pedal provides hydraulic pressure within the caliper to squeeze the pads against opposite sides of the rotor and the resulting frictional torque slows the vehicle. Less common in modern light-duty vehicles are drum brakes, in which a cylindrical drum rotates with the wheel and hydraulic force presses stationary shoes against the inside of the rotating drum to provide deceleration torque. Hybrid and modern electric vehicles also employ a relatively new method of slowing the vehicle, regenerative braking, that operates in parallel with the hydraulic brake system and uses the electric drive motor to slow the vehicle and provide energy back to the vehicle's electric storage. These vehicles use complex blending strategies to manage the amount of braking between the regenerative system and the hydraulic system such that driver perceives the system as operating like a conventional vehicle.

LINK Brake Dynamometer Experience and Capabilities

ERG partnered with LINK at the proposal stage of this project. LINK has been designing, manufacturing, and performing testing with brake dynamometers for decades. Their organization is a part of the Particle Matter Program (PMP) overseen by the EU's Joint Research Centre (JRC). They have been involved in recent years with the development of the state of the art for the measurement of PM emissions from braking. LINK has the capability to:

- conduct particulate matter emissions sampling of different brake configurations using a brake dynamometer and representative drive cycle.
- sample particulate matter emissions between 6 nm and 20 μm in size,
- collect particle characterization measurements of the particles, including particle number, particle mass, and size distribution
- collect continuous particulate matter measurements (g/sec), with the ability to correlate the continuous measurements to gravimetric filter measurements

LINK operates in accordance with all sections of the ISO 17025:2017 standard, titled General Requirements for the Competence of Testing and Calibration Laboratories[1], and management is committed to continually improving the quality of all operations. A familiarity with, implementation of and compliance with the ISO 17025:2017 standard is a mandatory requirement for individuals at all levels of the LINK organization.

Around the time of the initiation of this project, the US Environmental Protection Agency (EPA) provided additional funding to expand the types of measurements conducted during the study. These additions primarily involved the parallel gravimetric measurement of PM emissions using Teflon (PTFE) filters in a manner consistent with the requirements for PM sampling described in 40 CFR 1065. The relevant results from those additional measurements are included in this report.

ERG initiated the program by reviewing two existing test cycles relevant to this work, the EMFAC Unified Cycle (UC) and its associated Speed Correction Cycles (SCCs), as well as the World-Harmonized WLTP-Brake cycle, developed in Europe in cooperation with the JRC.[2] The UC/SCCs were designed for exhaust emissions testing, while the WLTP-Brake was designed specifically for use on brake dynamometers. ERG also reviewed available literature to begin developing a list of vehicle operational parameters most relevant to brake emissions. From this review, and in discussion with CARB, ERG selected the following four parameters as the initial assumption of the operational parameters with the most relevance to brake PM emissions:

- Vehicle speed during braking event
- Deceleration rate
- Brake component temperature
- Brake event duration

---

[1] International Standards Organization "General requirements for the competence of testing and calibration laboratories". https://www.iso.org/standard/66912.html

[2] Mathissen, M. et. al., A novel real-world braking cycle for studying brake wear particle emissions, Wear, Volumes 414–415, 2018

The test program was designed to evaluate the PM emission responses to the above parameters as well as to perform testing over a representative range of values for each.

Materials and Methods

Representative Test Vehicle and Friction Material Selection

The first task that ERG and LINK completed was to determine the list of representative test vehicle models that would be used to develop an understanding of brake thermal regimes during in-use vehicle operation. Brake system components from these vehicle models would then be used during PM emissions tests on the brake dynamometer. The on-track vehicle testing involved operating each vehicle over the WLTP-Brake cycle (adapted for track testing) followed by a heating and cooling matrix cycle of standardized stops and cruises. By measuring brake temperatures during these on track operations, the laboratory testing could be designed to replicate actual vehicle temperatures within reason and provide relevant measurement and characterization of brake emissions. Also, the temperature ranges encountered during track testing informed a new ERG-developed model of operational temperatures of the driving in an in-use vehicle speed dataset. The measurement of brake emissions using repeatable and reproducible systems and isokinetic constant volume sampling will further improve the estimation of emissions inventories for light-duty vehicles in the State of California.

To guide the selection of vehicle models, LINK adapted the concept of the brake wear index (BWI), which is a representation of the total material present in the in-use fleet that can be emitted as particulate. There are several assumptions used to determine a BWI to guide the vehicle selection. First, the ranking assumes proportionality between the number of registered vehicles and the amount of PM becoming airborne during and after braking. Second, the larger the wearable mass of the foundation brakes, the larger the potential for contribution of PM. The wearable mass is assumed to be a direct function of the friction material volume before reaching the service thickness. In addition to the friction material, the wearable mass includes the volume of the mating disc or drum with its volume up to its service thickness. To estimate the mass, the method uses nominal and typical material density for the predominant compositions (non-asbestos organic/ceramic versus semi-metallic or low-metallic for the friction material) with the estimated market share as a function of the vehicle age range. The wearable mass uses grey cast iron for the disc and drums. The third assumption to complete the computation of a BWI, combines the number of registered vehicles with the total wearable mass as well as the replacement rate of the friction material and the disc or drum. The main sources of information used by LINK in this analysis were: a) registration counts by make, model, and year of manufacture provided by CARB for 2016; b) brake dimensions obtained from the yearly publication and the online catalog from the Friction Materials Standards Institute (FMSI®) and from consulting with aftermarket friction manufacturers; c) material densities from consulting with friction materials formulators, and d) replacement rates as the fraction of vehicles that have had brake materials replaced during a given year for vehicles in a given age range.

The selection of six vehicles to characterize brake emissions representative of the light-duty vehicle market in California was completed in multiple steps. The first step was to review the statistics for vehicles registered in California for the year 2017. The top-25 vehicles based on registration counts included 'make' and 'series' of different 'model year' and 'model'. Therefore, LINK prescreened vehicles of different series from the original statistics. The column "Top-25 Reg" in Table 1 illustrates an extract of this pre-screening step. The approach is to treat all models of Toyota Corolla as a single entry in the development of the top-25 vehicles list. The next vehicle with a series different than Corolla is Toyota Camry. Camry was selected as the second vehicle in the top-25 vehicles list. Only the first few vehicles are included here for brevity, but the complete list is presented later in this section.

Table 1. Counts of Make, Series, Model, and Model Year

Entry #	Model Year	Make	Series	Model	Count	Top-25 Reg
1	2016	Toyota	Corolla	L	58637	1
2	2015	Toyota	Corolla	L	55315	1
3	2010	Toyota	Corolla	BASE	54362	1
4	2014	Toyota	Camry	L	53570	2
5	2015	Toyota	Prius		53318	3

Next, the friction material and backing plate identification codes ('FMSI' codes) of front and rear axle friction materials were determined for more than 100 different entries of different model years, make, series, and models. The number of vehicles having the same FMSI codes were then summed together and this new count was taken for each model, grouped together by all series and model years having the same FMSI codes.

The FMSI database and industry surveys were used to determine the dimensions of disc or drum and friction material. These dimensions, along with representative material density values were used to estimate the wearable mass of the brake parts using the following equation. The actual values used during this process for each of the top-25 vehicles are included in Appendix A.

Estimated wearable mass =
(Wearable volume of friction material) · (Density of friction material)
+ (Wearable volume of front axle disc) · (Density of disc)
+ (Wearable volume of rear axle disc/drum) · (Density of disc/drum)

Density of friction material depends on the type of friction material used in the vehicle of interest. For example, density of non-asbestos organic (NAO) material is 2.9 g/cm^3 and density of semi- or low-metallic (LM) material is 3.75 g/cm^3. Thus, a brake lining made of semi-metallic material contains higher wearable mass than an equivalent lining made of NAO material.

Interviews and surveys with technical specialists resulted in percent population of friction material formulations as a factor of vehicle age. Figure 1 illustrates the overall general trend regarding the relative presence of NAO and Semi-metallic/Low-metallic (SM/LM) friction materials for light-duty vehicles in use. Except for special applications, most street service passenger car and light truck Original Equipment Manufacturer (OEM) and Original Equipment Service (OES) pads in North America use NAO friction materials. As vehicles age, SM/LM pads become more common as they tend to cost less than NAO pads and are therefore more likely to be selected as vehicles depreciate.

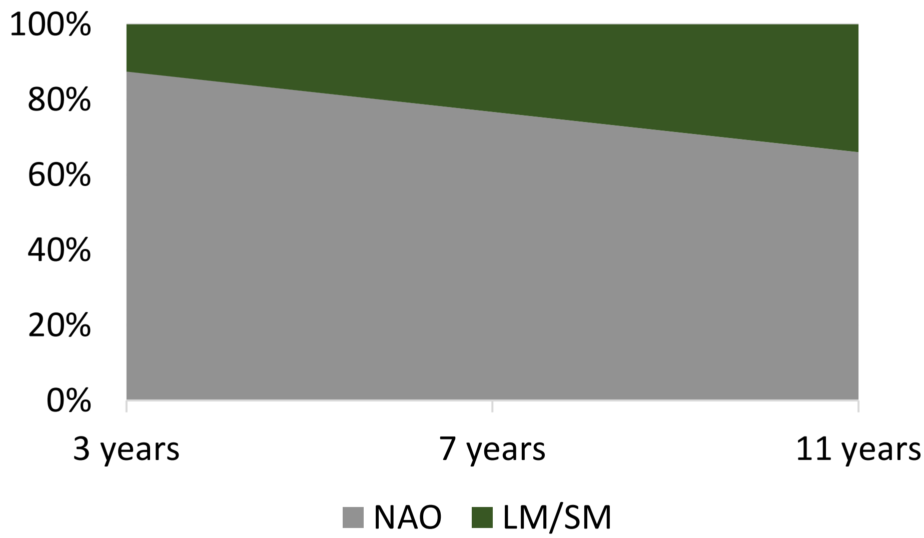

Figure 1. General trend in pad material mix by vehicle age

Using these market statistics based on vehicle age, LINK generated Table 2, which indicates the estimated mix of metallic versus NAO for the six vehicles selected. The wearable mass for the friction material prorates the density of the friction material (NAO v. Semi- or Low-Metallic) and the estimated market share. Note that the estimates presented are based on vehicle age range and general vehicle type only and are not adjusted for specific vehicle characteristics (as that level of detail was not available from industry surveys). For example, the Prius may have a different level of low/semi-metallic market share as a result of its regenerative braking systems.

Table 2. Estimated Pad Material Breakdowns by Combined Models

Make	Model	MY	Production Years	Est. % NAO	Est. % Metallic
HONDA	CIVIC LX	2012-2015	3-6	77%	23%
TOYOTA	PRIUS REGULAR	2010-2016	2-8	82%	18%
NISSAN	ROGUE S	2014-2016	2-4	88%	12%
TOYOTA	CAMRY (BASE, L, LE)	2009-2016	2-9	82%	18%
TOYOTA	SIENNA LE	2011-2015	3-7	77%	23%
FORD	F150 SUPERCREW	2015-2016	2-3	87%	13%

In addition, it is important to note the fact that, in aftermarket supplier parlance, there are three broad commonly-used categories of aftermarket friction materials of "good, better, and best." Good friction materials provide a good performance and relatively quiet braking at a reasonable price in NAO and semi-metallic formulations. Better friction materials are the most extensive line of aftermarket friction materials and also come in NAO and semi-metallic formulations. They are designed to last longer and wear better and perform well at the mid-price range. Better friction materials feature chamfers, slots, and anti-noise shims in many applications, and provide smooth pedal feel and proper fit. Best aftermarket friction materials are the closest to the OEM/OES friction material in terms of dimensional quality, hardware kits, performance, comfort, and product life. Figure 2 illustrates the general mix of friction material quality in relation to the vehicle age. In the chart, the total percentages for NAO and SM sum to 100% within each vehicle age group.

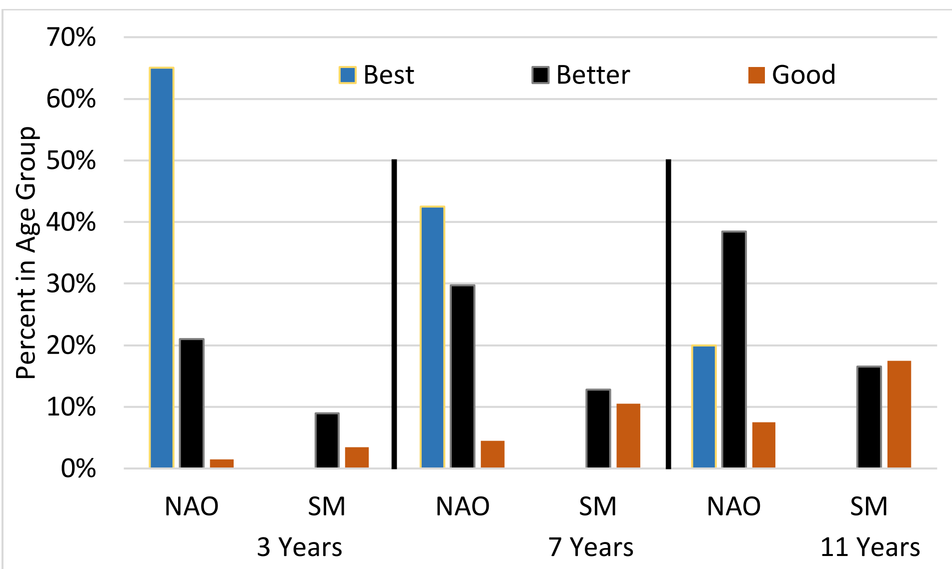

Figure 2. Overall mix of friction material quality by age

When all the above factors are combined in one graph, it becomes apparent how wide the range of friction materials is that can be applied to a given vehicle during a given brake job. Figure 3 illustrates the combined effect of vehicle age on friction material type and formulation equipped on in-use vehicles.

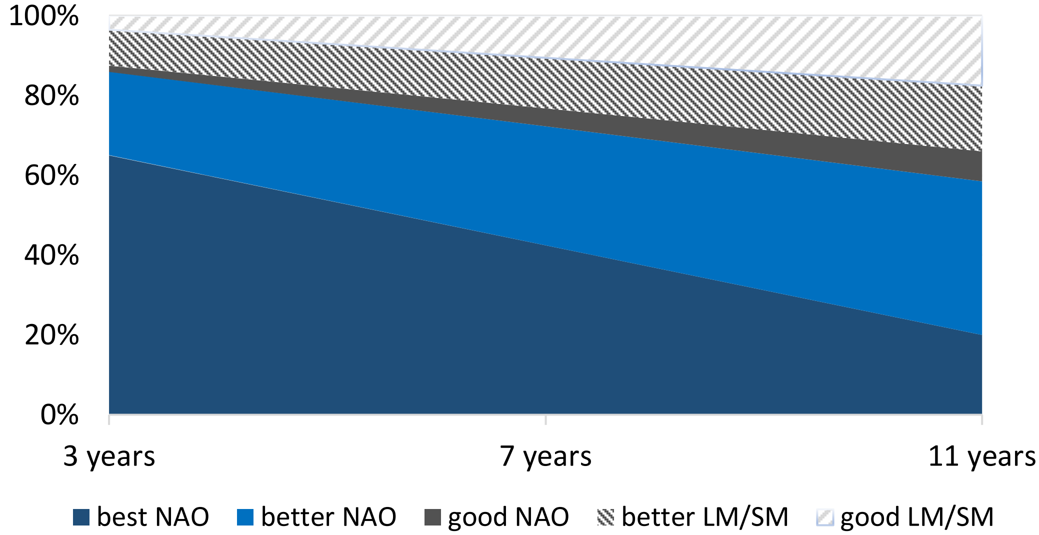

Figure 3. Overall Mix of Friction Materials, Quality Grade, and Vehicle Age

Other factors which influence the ultimate friction material used for the specific vehicle include vehicle aging behavior, demographics, market dynamics among dealers, large retailers, and private branding, etc.

Based on aforementioned steps to determine registration count as well as the wearable mass (including pad material type), a first iteration index, BWI_1 was determined for the top-registered vehicles as follows.

$$BWI_1 = (\text{Registration Count}) \cdot (\text{Wearable mass})$$

To complete the numerical assessment of which vehicles were relevant, representative, and available for rental to conduct the proving ground test track measurements, LINK conducted a technical survey to determine the replacement rates of brakes. The survey provided by the brake suppliers and manufacturers resulted in replacement rates as a function of vehicle age. A second BWI index (BWI_2) was then determined as follows:

$$BWI_2 = (BWI_1) \cdot (\text{Replacement rate by vehicle age})$$

In the end, three levels of ranking were established among the top 25 vehicles. The total registration count of vehicles for a given make, series, and model resulted in the first phase of ranking. The BWI_1, with the total wearable mass resulted in a second phase of ranking. The BWI_2, includes an additional factor (replacement rate), to generate the third phase for the vehicle ranking. The BWI_2 allows the adjustment of the BWI_1 index to reflect the relative wear rate of different vehicles having a similar registration count, and a similar wearable mass. Low replacement rates will demote the total ranking for the vehicle as it wears (releases debris and PM) at a lower rate, compared to another vehicle with similar registration count and wearable mass but with a higher wear rate (reflected indirectly by the replacement rate).

Vehicle models were grouped by all series and model years within a model that had the same FMSI codes. Table 3 lists an excerpt of the top vehicles of various make, series, model year, and models. Shaded rows indicate vehicles that are 10 years old or newer from the publication date of registration statistics. This age range is considered to avoid uncertainties of working condition, availability and procurement of specific vehicles for track testing with older vehicles. The last column in Table 3 'FMSI FRONT AXLE' shows the friction material identifier for brake lining on front axle. The first four digits represent the friction formulation and the digits after the letter represent the geometrical features and dimensions of backing plate. As seen, the same FMSI identifiers apply for various entries (vehicle make, series, model year, and model).

Table 3. Series, Model, Model Year, and FMSI Code for Most Common Vehicles

MAKE	SERIES	MY	MODEL	COUNT	FMSI FRONT AXLE
TOYOTA	COROLLA	2016	LX	58637	8969-D1210
TOYOTA	COROLLA	2015	LX	55315	8969-D1210
TOYOTA	COROLLA	2014	LX	45202	8969-D1210
TOYOTA	COROLLA	2013	BASE	45180	8330-D1210
TOYOTA	COROLLA	2012	BASE	27327	8330-D1210
TOYOTA	COROLLA	2011	BASE	26460	8330-D1210
TOYOTA	COROLLA	2010	BASE	54362	8330-D1210
TOYOTA	COROLLA	2009	BASE	38783	8330-D1210
TOYOTA	COROLLA	2007	CE	36541	7824-D923
TOYOTA	COROLLA	2006	CE	38106	7824-D923
TOYOTA	COROLLA	2005	CE	39963	7824-D923
TOYOTA	COROLLA	2004	CE	30255	7824-D923
TOYOTA	COROLLA	2003	CE	34015	7824-D923
TOYOTA	COROLLA	2001	CE	20481	7611-D741
TOYOTA	COROLLA	1999	VE	20106	7611-D741
TOYOTA	CAMRY	2016	LE	45855	8331-D1293
TOYOTA	CAMRY	2015	LE	46855	8331-D1293
TOYOTA	CAMRY	2014	L	53570	8331-D1293
TOYOTA	CAMRY	2013	L	30383	8331-D1293

Table 4 shows the revised list that shows the combination of all rows in Table 3 with a same FMSI # into a single entry that covers a model year range and all model identifiers.

Table 4. Consolidating Top Series by Model Year and FMSI

MAKE	SERIES	MY	COUNT	AXLE	FMSI FA
TOYOTA	COROLLA	2014-2016	159154	FA	8330-D1210
TOYOTA	COROLLA	2014-2016	159154	RA	1635-S945
TOYOTA	COROLLA	2009-2013	192112	FA	8330-D1210
TOYOTA	COROLLA	2009-2013	192112	RA	1635-S945
TOYOTA	COROLLA	2003-2007	178880	FA	7824-D923
TOYOTA	COROLLA	2003-2007	178880	RA	1515-S801
TOYOTA	COROLLA	1999-2001	40587	FA	7611-D741
TOYOTA	COROLLA	1999-2001	40587	RA	1515-S750
TOYOTA	CAMRY	2009-2016	342992	FA	8331-D1293
TOYOTA	CAMRY	2009-2016	342992	RA	8332-D1212
TOYOTA	CAMRY	2007	50693	FA	8331-D1222
TOYOTA	CAMRY	2007	50693	RA	8332-D1212
TOYOTA	CAMRY	2002-2006	185766	FA	7787-D908
TOYOTA	CAMRY	2005-2006	67612	RA	1617-S911
TOYOTA	CAMRY	2002-2004	118154	FA	7787-D908
TOYOTA	CAMRY	1998-2004	198316	RA	1447-587
TOYOTA	CAMRY	2001	25651	FA	7357-D697

Table 5 lists the top 25 light-duty vehicles registered in the state of California, as grouped according to the above process. It should be noted that the column labeled 'weight class' is defined according to CFR 45, Part 565 VIN (Class A = GVWR less than or equal to 3000 lbs., B for (3001 to 4000) lbs., C for (4001-5000 lbs., etc., up to GVWR of 10 000 lbs.). The top 25 vehicles list includes a mix of a variety of vehicle weight classes spanning from class B thru F. The goal in vehicle selection was to select representative models from a range of vehicle types including compacts, sedans, SUVs, minivans, full-size trucks, as well as at least one vehicle with regenerative braking. These corresponded in some cases to the weight classes, but the priority in diversifying vehicle selection was on vehicle type, not weight. Based on the registration count ranking only, the vehicles selected would have been: Camry, Prius, Corolla, Altima, Civic, and Sentra. These vehicles fall under two vehicle weight classes and one vehicle type (4-door sedan), and alone do not provide enough representation of the vehicle population in California to suit the needs of this program. The top 25 vehicles were selected to ensure multiple models would remain for each of the following desired vehicle groups: compacts, sedans, pickups, minivans, SUVs, and hybrids.

Table 5. Counts of the Top 25 FMSI-Grouped Vehicles in California

MAKE	SERIES/MODEL	MY	WEIGHT CLASS	GVWR	Reg #	RANK BY Reg
			/ A-to-H	/ kg	#	
TOYOTA	CAMRY (BASE, L, LE)	2009-2016	C	2073	342992	1
TOYOTA	PRIUS REGULAR	2010-2016	B	1800	241055	2
TOYOTA	COROLLA L	2014-2016	B	1732	159154	3
NISSAN	ALTIMA (BASE, 2.5)	2012-2016	C	1910	149096	4
HONDA	CIVIC LX	2012-2015	B	1595	140733	5
NISSAN	SENTRA S	2013-2016	B	1687	110629	6
HONDA	ACCORD LX	2014-2016	C	1934	52193	7
TOYOTA	SIENNA LE	2011-2015	D	2715	44921	8
LEXUS	RX 350	2014-2015	D	2527	43306	9
NISSAN	ROGUE S	2014-2016	C	1968	41213	9
HYUNDAI	SONATA (GLS, SE, SPORT)	2013-2015	C	2074	40117	11
HONDA	ACCORD EX	2014-2016	C	1904	39344	12
HONDA	ACCORD SPORT	2014-2015	C	2107	37332	13
TOYOTA	RAV4 XLE	2014-2016	C	2035	36803	14
TOYOTA	TACOMA DOUBLE CAB	2015-2016	D	2540	36052	15
FORD	F150 SUPERCREW	2013-2014	F	3239	33721	16
FORD	F150 SUPERCREW	2015-2016	E	3000	32921	17
HYUNDAI	ELANTRA GLS	2013	B	1720	30566	18
CHEVROLET	SILVERADO 1500	2014-2015	E	3085	27578	19
HONDA	CIVIC LX	2016	B	1695	25782	20
HONDA	ACCORD SPORT	2016	C	1964	22978	21
DODGE	RAM 1500 ST	2004	E	2989	19739	22
CHEVROLET	TAHOE C1500	2007	F	3266	19517	23
LEXUS	RX 350	2016	D	2562	12540	24
HYUNDAI	SONATA SE	2016	C	2074	11363	25

Table 6 shows the revised and re-ordered ranking based on the brake wear index BWI_1. The index BWI_1 is a product of registration count and the total wearable mass of pads/shoes and discs/drums at all four brake corners of a given vehicle. On comparing the registration counts with the BWI_1 rankings, the influence of wearable mass on BWI_1 ranking was more evident for SUVs and trucks such as the Nissan Rogue, Toyota Tacoma, and F150 trucks. Based on the BWI_1 ranking, the vehicles selected would have been: Camry, Corolla, Prius, Civic, Altima, and Tacoma. These vehicles fall under three vehicle weight classes and two vehicle types (4-door sedan and pick-up truck). The selection of the Tacoma would overemphasize this vehicle due to its wearable mass (over two times the average of the other five vehicles selected with the BWI_1 ranking). In addition, this selection limits the selection of vehicle types, makes, and models present in California.

Table 6. Top FMSI-Grouped Series, with BWI_1

Make	Series /model	My	Reg #	Rank by reg	Total wearable mass/ gm	bwi_1 / ton	Rank by bwi_1
Toyota	Camry (base, l, le)	2009-2016	342992	1	2133	732	1
Toyota	Corolla l	2014-2016	159154	3	3028	482	2
Toyota	Prius regular	2010-2016	241055	2	1749	422	3
Honda	Civic lx	2012-2015	140733	5	2322	327	4
Nissan	Altima (base, 2.5)	2012-2016	149096	4	1510	225	5
Toyota	Tacoma double cab	2015-2016	36052	15	5256	189	6
Nissan	Sentra s	2013-2016	110629	6	1436	159	7
Toyota	Sienna le	2011-2015	44921	8	2717	122	8
Lexus	Rx 350	2014-2015	43306	9	2707	117	9
Ford	F150 supercrew	2013-2014	33721	16	2878	97	10
Ford	F150 supercrew	2015-2016	32921	17	2895	95	11
Toyota	Rav4 xle	2014-2016	36803	14	2462	91	12
Honda	Accord lx	2014-2016	52193	7	1598	83	13
Nissan	Rogue s	2014-2016	41213	10	1845	76	14
Hyundai	Sonata (gls, se, sport)	2013-2015	40117	11	1678	67	15
Chevrolet	Silverado 1500	2014-2015	27578	19	2431	67	16
Hyundai	Elantra gls	2013	30566	18	1649	50	17
Chevrolet	Tahoe c1500	2007	19517	23	2521	49	18
Dodge	Ram 1500 st	2004	19739	22	2180	43	19
Honda	Civic lx	2016	25782	20	1666	43	20
Honda	Accord ex	2014-2016	39344	12	993	39	21
Lexus	Rx 350	2016	12540	24	2668	33	22
Honda	Accord sport	2014-2015	37332	13	803	30	23
Hyundai	Sonata se	2016	11363	25	1803	20	24
Honda	Accord sport	2016	22978	21	803	18	25

The total wearable mass may or may not indicate the actual amount of wear debris seen during a typical year of driving activity because different models' brake components do not all wear out after the same amount of driving. The annual estimates of the brake replacement rates were acquired through a business intelligence survey. Table 7 presents the continued analysis by including the replacement rates by vehicle age. A newer vehicle is expected to have low value of replacement rate and vice versa. A value of 16% in the first row of Table 7 implies that 16% of all vehicle population with year of manufacture between 2009 and 2016 are estimated to have had a brake service. The prevailing brake service job at the time of this survey was to replace friction couple i.e. pad and rotor or shoes and drum at any given service. A second wear index is formulated which assumes that a brake service would include replacement of brake parts. The wear index BWI_2 is a product of BWI_1 and the brake replacement rate. Table 7 includes vehicles in the order determined by BWI_2. This ranking still leaves the Sentra, Altima, and Corolla near the top of the list, though they are in the same vehicle class.

Table 7. Top FSMI-Grouped Series, with BWI_2

Make	Series/model	My	Rankby bwi_1	Replacement rate per vehicle age/ %	Bwi_2/ton	Rank by bwi_2
Toyota	Camry (base, l, le)	2009-2016	1	16	117	1
Toyota	Corolla l	2014-2016	2	11	53	2
Honda	Civic lx	2012-2015	4	14	46	3
Nissan	Altima (base, 2.5)	2012-2016	5	14	32	4
Nissan	Sentra s	2013-2016	7	11	17	5
Toyota	Sienna le	2011-2015	8	14	17	6
Ford	F150 supercrew	2013-2014	10	16	16	7
Lexus	Rx 350	2014-2015	9	11	13	8
Chevrolet	Tahoe c1500	2007	18	23	11	9
Ford	F150 supercrew	2015-2016	11	11	10	10
Toyota	Rav4 xle	2014-2016	12	11	10	11
Toyota	Tacoma double cab	2015-2016	6	5	9	12
Honda	Accord lx	2014-2016	13	11	9	13
Dodge	Ram 1500 st	2004	19	21	9	14
Toyota	Prius regular	2010-2016	3	2	8	15
Nissan	Rogue s	2014-2016	14	11	8	16
Hyundai	Elantra gls	2013	17	16	8	17
Hyundai	Sonata (gls, se, sport)	2013-2015	15	11	7	18
Chevrolet	Silverado 1500	2014-2015	16	11	7	19
Honda	Accord ex	2014-2016	21	11	4	20
Honda	Accord sport	2014-2015	23	11	3	21
Honda	Civic lx	2016	20	5	2	22
Lexus	Rx 350	2016	22	5	2	23
Hyundai	Sonata se	2016	24	5	1	24
Honda	Accord sport	2016	25	5	1	25

Table 8 indicates the final vehicle selection after a joint engineering review with CARB, ERG, and LINK. The first update was to include an SUV, and the team selected the Nissan Rogue. Note that the Lexus RX 350 was higher ranked among SUV's than the Nissan Rogue, however the RX 350 was excluded due to it being a luxury vehicle and being likely to have a significantly higher cost for brake components than the Rogue which was not accounted for in the project budget estimate. The second update was to include a pick-up truck, with the F-150 being selected for being the most common pick-up truck in California (and the United States). The model year range for the F-150 was selected to be 2015-2016 (instead of the previous FMSI model year range of 2013-2014) because interviews with industry experts suggested that this year range was a very common benchmarking and development candidate. After confirming the availability for rental and availability of brake parts, the project moved on to its next phase, to prepare the logistics and technical documentation for track testing.

Table 8. The 6 Specific Makes, Series, and Model Years Selected for Testing

Selected Vehicle Model	Reg RANK	BWI_1 RANK	BWI_2 RANK	COMMENTS
2009-2016 Toyota Camry	1	1	1	Top rank by all three metrics
2012-2015 Honda Civic	5	4	3	Rear drum brakes
2011-2015 Toyota Sienna	8	8	6	Top in the list of class 'D' Reg #, Minivan
2015-2016 Ford F-150	17	11	10	Top in the list of class 'E' Reg #, Large Pickup, Very common vehicle for friction material formulation evaluations
2010-2016 Toyota Prius	2	3	15	Regenerative braking
2014-2016 Nissan Rogue	10	14	16	Top in the list of non-luxury SUVs Medium level ranking based on BWI_1 and BWI_2

The processes followed during this phase of the project allowed the evaluation of a significant list of vehicles in terms of make, model, and trim level, with the goal of selecting a subset for track and dynamometer testing. The final list of six vehicles given in Table 8 provides a good cross section of vehicle weight class/type and powertrain systems while representing common light-duty vehicles used for brake development and brake testing. The range of vehicle weights and disc brake dimensions allow the proper characterization of the thermal regimes of a wide variety of light-duty vehicles during the planned measurements of brake emissions on the brake inertia dynamometer. This task also introduced the concept of BWI as a predictor for the total potential contribution of a given vehicle to PM (fallout, airborne, and resuspension). The inclusion of BWI_2 as a metric for evaluation did not significantly alter the vehicle selection as compared to selecting based on registration counts when also accounting for selecting from a variety of vehicle types, however.

At the conclusion of this task, LINK procured one of each of the following vehicle models for track testing. These vehicle models were also used as the basis for acquiring brake assemblies for testing on the brake dynamometer. The selected FMSI numbers are also included.

- **2011 Toyota Camry LE**
  - Front axle FMSI# 8331-D1293
  - Rear axle FMSI# 8332-D1212
- **2013 Honda Civic LX**
  - Front axle FMSI# 8791-D1578
  - Rear axle FMSI# 1618-S913
- **2013 Toyota Sienna LE**
  - Front axle FMSI# 8436-D1324
  - Rear axle FMSI# 8500-D1391
- **2015 Ford F-150 Supercrew**
  - Front axle FMSI# 8528-D1770
  - Rear axle FMSI# 9018-D1790
- **2016 Toyota Prius Two Eco**
  - Front axle FMSI# 8538-D1184
  - Rear axle FMSI# 8463-D1423
- **2016 Nissan Rogue S**
  - Front axle FMSI# 8449-D1737
  - Rear axle FMSI# 8501-D1393

In addition to representing the vehicles registered in California, the listing provides the appropriate representation of vehicle weight classes from 1700 kg to 3200 kg of gross vehicle weight; vehicle types with sedans, pickup trucks, and sport utility vehicles; brake systems with disc brakes all around and with drum brakes on the rear axle; and vehicles with conventional gasoline powertrains and with regenerative braking systems. Note that specific model years are given from the ranges of model years with the same FMSI values provided in previous tables. The model years given above represent the actual model years of test vehicles sourced by LINK for track testing. The final listing was discussed and agreed upon among project staff from CARB, ERG, and LINK.

Track Testing and the Brake Temperature Model

Existing literature regarding PM emissions from braking indicates that brake temperature has a significant effect on emission rates.[3,4] To account for this, ERG selected brake temperature as a parameter for use in cycle development. Because brake temperature was not measured during the Caltrans survey, ERG developed a model of brake temperature based on track testing data. This temperature model was used to determine the distribution of in-use brake temperatures associated with vehicle speed data from the Caltrans household travel study and to estimate the brake temperature profile during operation on the dynamometer for the new test cycle.

ERG and LINK conducted track testing to gather data about operational brake temperatures. LINK acquired the test vehicles and replaced their wearable brake components with new components. Test vehicles were instrumented for temperature measurement of various brake system components and the vehicles were subject to controlled driving in three different phases. A photograph of the type of temperature measurement equipment installed by LINK is presented in Figure 4, which depicts a brake mounted thermocouple installed on the Camry test vehicle. The thermocouple wires are routed through the wheels to a wireless transmitter that rotates with the vehicle's wheel and transmits measured data to a receiver mounted inside the vehicle.

---

[3] Garg, Bhagwan D. et. al. "Brake Wear Particulate Matter Emissions." Environmental Science & Technology 34.21 (2000): 4463–4469

[4] Sanders, Paul G. et. al. "Airborne Brake Wear Debris: Size Distributions, Composition, and a Comparison of Dynamometer and Vehicle Tests." Environmental Science & Technology 37 (2003): 4060–4069

Figure 4. Brake Thermocouples and wireless hub transmitter installed on the Camry test vehicle

After installing the instrumentation, LINK then burnished the new friction materials of each vehicle on-track over five repeats of Trips 2 and 4 of the WLTP-Brake cycle. Then, brake temperatures were logged while driving the complete WLTP-Brake cycle followed by an ERG-defined **Heating and Cooling Matrix**. The Heating and Cooling Matrix consisted of a series of standardized stops and steady-speed cruises to help separately analyze brake heating and cooling patterns. The events making up the Matrix are tabulated in Appendix B. The WLTP-Brake and Heating and Cooling Matrix temperature measurements were used in the development of ERG's brake temperature model. Historgrams of rotor/drum temperatures measured over the WLTP-Brake cycle on the test track are presented in Figure 5. In the figure, the temperature range is presented as the temperature difference above the ambient temperature in the wheel well (which was approximately 25°C during most of the testing.

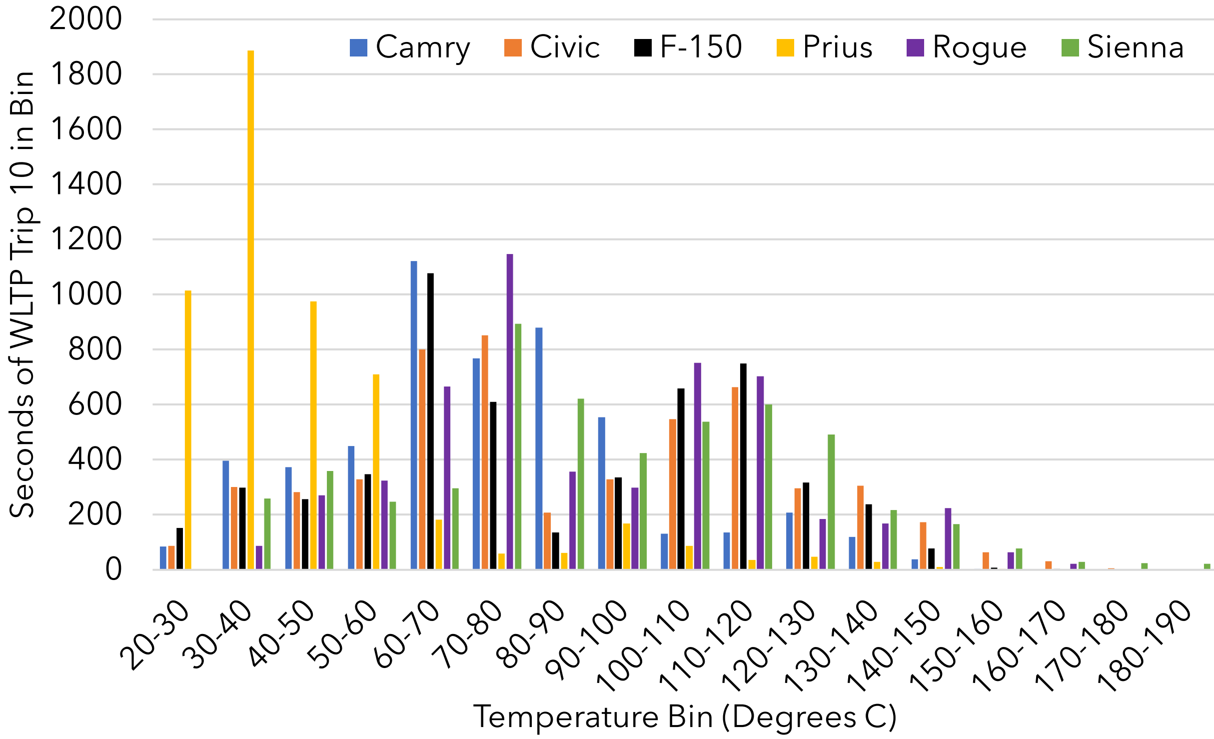

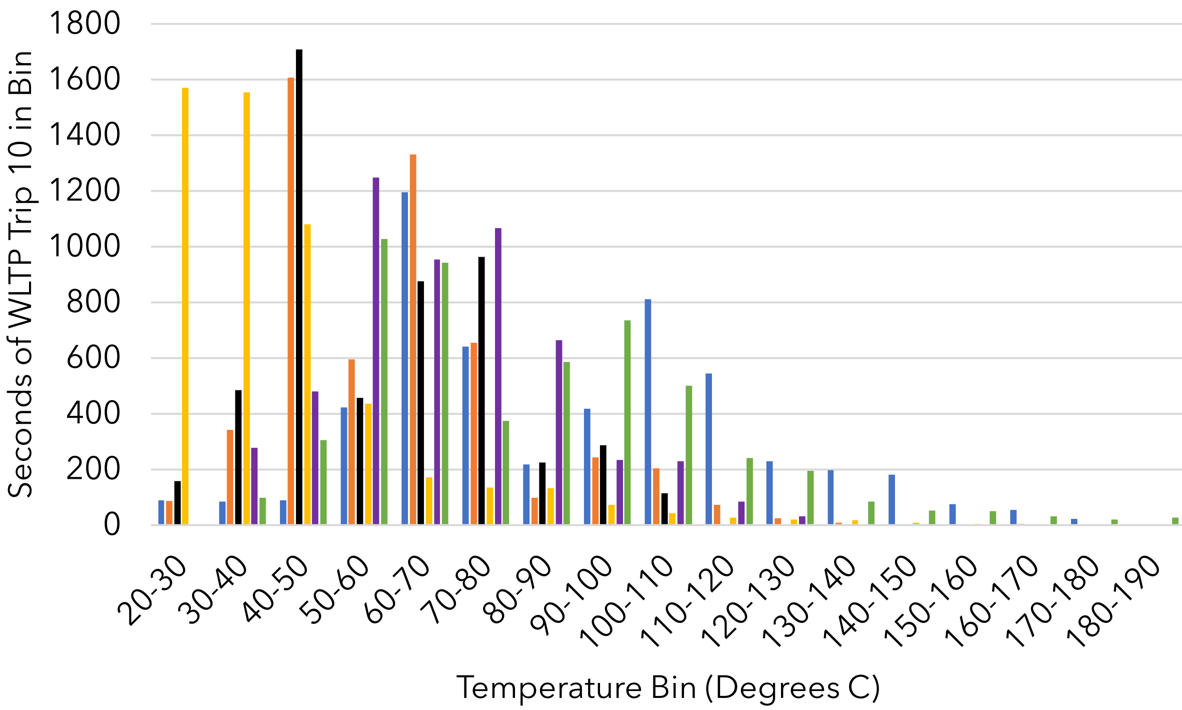

Figure 5. Histograms of temperatures of front rotors (top) and rear rotors/drums (bottom) over the WLTP-Brake cycle operated on the test track.

ERG developed a generalized form of an equation to describe brake heating and cooling rates based on an energy balance of the energy flow into the brakes during deceleration and the energy flow from the brakes due to convective cooling. The equation for change in temperature, ΔT, is of the form:

$$\Delta T = (A + B \cdot V_0 + C \cdot V_0^2) \cdot (T_0 - T_{amb}) \cdot \Delta time + D \cdot (V_0^2 - V_1^2) \cdot \Delta time$$

In the equation, A, B, C, and D are heating/cooling coefficients specific to a given vehicle. V_0 is the vehicle speed (kph) at the prior instant and V_1 is the speed (kph) at the next instant. T_0 is the brake temperature at the given instant (°C), and T_{amb} is the air temperature around the brake system. Track testing was conducted for six vehicles to determine brake temperature trends over the two measured driving cycles, the WLTP-Brake cycle (adapted for track driving) and the Heating and Cooling Matrix consisting of standardized stops of various intensities to determine brake heating rates as well as steady-speed cruises to determine cooling rates. The temperature measurements during track testing were used to determine the coefficients A, B, C, and D for the different vehicles. Note that D is set to zero if braking is not taking place (i.e. the vehicle is not decelerating more rapidly than would occur during a coastdown).

Track data excerpts containing only the cooling periods from the Heating/Cooling matrix were initially extracted to determine cooling coefficients A, B, and C. The cooling periods were extracted first because the cooling is a relatively slow process that follows a readily-modeled exponential decay, and any time delays in the data for this operational regime would not have much effect on measured temperature and thereby confound the modeling. Cooling coefficients were modeled by first using the nonlinear regression procedure (Proc NLIN) in SAS on each of the 13 steady-speed cooling segments of the Heating and Cooling Matrix to fit e^(A+Bv). Then, a polynomial fit to speed was applied to the results of the NLIN procedure for the 13 different segments using Excel. The coefficients of this polynomial model became the cooling coefficients. Using these, ERG then determined the best single heating coefficient by determining the best least-squares fit between the entire modeled and measured temperatures by means of iteration using the already-determined cooling coefficients. For the units given in the previous paragraph, the coefficients for the Toyota Camry are given in Table 9. The Toyota Camry was selected for use in modeling the Caltrans data (and for cycle development) due to its representativeness of the vehicle fleet as well as having a good fit between the modeled and measured temperatures of the test vehicles. ERG determined that the decision to use the results of a single vehicle was acceptable because the temperature model used for the complete Caltrans dataset was the same as that used for cycle-building. The form of the equation is the key aspect, not the specific coefficients; the temperature model was used only as a bridge between the relative amounts of heating energy and cooling time in the in-use dataset and in the new cycle.

Table 9. Temperature Model Coefficients (based on the Toyota Camry)

A, 1/s	B, 1/(s·kph)	C, 1/(s·kph²)	D, °C/(s·kph²)
-0.001264	-0.000053926	0.0000001431	0.0088

The level of agreement between the model and the measured data is presented in Figure 6. Note that there were 10 instances in the following graph in which the test vehicle's braking system was allowed to return to at or near ambient (and in some cases datalogging was stopped during those intervals to allow for driver rest). At these times, the model was also set back to match the measured temperature (which was near ambient at the end of these intervals). The plot presents approximately 8 hours of operation.

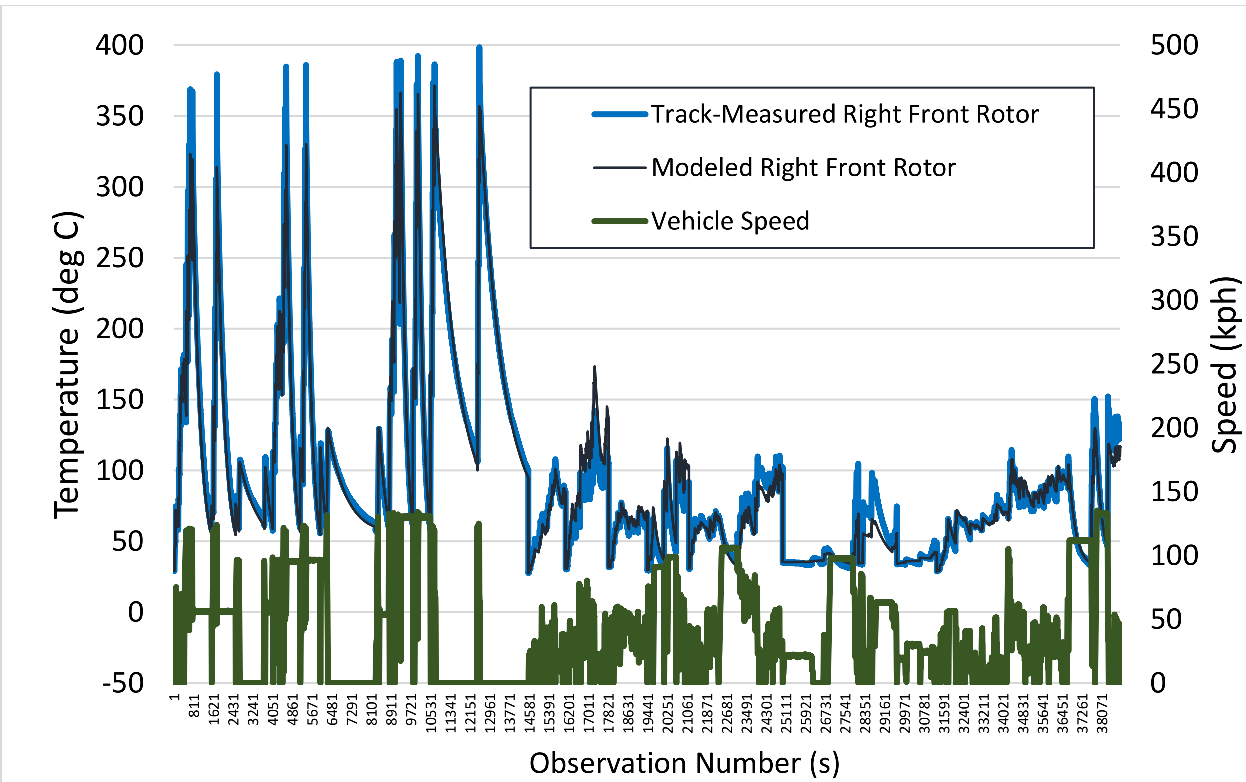

Figure 6. The modeled right front outer rotor temperature and the corresponding track-test measured temperature.

Test Cycle Development

After completing the temperature model, ERG proceeded to the selection of a test cycle to be followed on a brake dynamometer during PM emissions testing. The goal for the project was to utilize a cycle that is representative of California driving and practical for brake dynamometer operation. In this project, ERG developed a completely new cycle as a candidate for use during testing under this project. Consideration was also given to two existing test cycles, the EMFAC UC and its associated SCCs, as well as the World-Harmonized WLTP-Brake cycle, developed in Europe specifically for use on brake dynamometers. The UC was designed for exhaust emissions testing on a chassis dynamometer, so this report will describe its potential application as a braking test. The WLTP-Brake cycle is an "engineered" cycle, meaning it is not intended to be directly based on actual driving traces, but rather consists of engineered braking events at various deceleration thresholds.[5] The engineered aspects were constructed from vehicle activity data from Europe, the US, India, Japan, and South Korea. ERG evaluated all three cycles with various measures of their representativeness of real-world California driving. ERG presented the results of the evaluation to CARB and collaborated to select the cycle that would be used during the PM testing during this program.

Data Sources

This section describes the data sources used in this work including the two existing candidate test cycles that were evaluated. The data sources included in-use on-road vehicle survey data, temperature measurements performed on test vehicles operating on the track, and data from EPA's new vehicle emissions certification results. The existing cycles were either sourced from public information (for the WLTP-Brake cycle and the UC) or provided by CARB (for the EMFAC SCCs). This section also describes the methods that ERG followed to prepare and use these data sources in the selection of the test cycle for use on the brake dynamometer in this project.

The key material gathered for cycle selection was the Caltrans 2010-2012 California Household Survey data. This data includes actual in-use second-by-second operational data (vehicle speed over time is of primary interest for this work) from a variety of vehicle types operating across the state. ERG analyzed logged data from the operation of over 2,000 vehicles including over 14,000 hours of operation. This data served as the basis for evaluating the representativeness of both existing cycles (WLTP-Brake cycle and the EMFAC UC/SCCs) as well as for the creation of a new ERG-developed brake dynamometer test cycle.

---

[5] Marcel Mathissen, Jaroslaw Grochowicz, Christian Schmidt, Rainer Vogt, Ferdinand H. Farwick zum Hagen, Tomasz Grabiec, Heinz Steven and Theodoros Grigoratos, A novel real-world braking cycle for studying brake wear particle emissions, Wear, https://doi.org/10.1016/j.wear.2018.07.020e

Caltrans Survey Data

The Caltrans Survey included instrumentation of vehicles using either On-board Diagnostic (OBD) dataloggers, GPS dataloggers, or both OBD and GPS dataloggers. The survey was designed to be as random as possible and included participants from each county in California making it an excellent data source to represent typical California driving. The quantity of vehicles and logged data for each logger type is presented in Table 10. It can be seen that the vast majority of the data was collected using OBD-only dataloggers.

Table 10. Statistics on data logged with the 3 different logger types in the Caltrans Survey Data

	OBD-Only	OBD+GPS	GPS Only
Number of Vehicles	2130	365	677
Hours of Data	14,001	1,819	3,162
Time gaps of 2s in data	1.6%	0.1%	0.1%

The survey data included over 60 million seconds of data. Because of the large (and, therefore computationally-intensive) amount of data, ERG elected to use only the cleanest subset of data. After reviewing samples of each data type, ERG determined that the OBD-only dataloggers appeared to generate the highest quality data. This decision was based on reviews of the amount of clipping of trip starts and ends, the data resolution, and the steadiness of the zero measurement when vehicles were at idle. ERG also looked for time lags in the data (which would be of particular concern for braking analysis). Calculated mean and median deceleration rates during braking events were higher for the OBD-measured data than for the GPS data. This was consistent with ERG’s previous experience that GPS data tended to have speed lag in time during acceleration or deceleration (which would likely result in a lower reported deceleration rate for a given braking event). For all reasons given, ERG selected only the OBD-only survey data for use in this work.

ERG applied further adjustments/corrections to the relatively clean OBD-only Caltrans data. Most notably, OBD speed data is reported to the nearest whole kph value, with no decimal places given. As a result, the speed traces were digitized, which challenged the ability to discern braking events from cruising events in the speed-trace data on a 1-second basis. This is because, due to digitization, an actual gradual reduction in speed by a vehicle would be represented as a constant value with a single 1 kph/s jump, followed by further constant values. Using a formula to assign braking would assign braking to that one second even though the vehicle was actually coasting for the whole period of time. To address this, ERG numerically smoothed all OBD data using the local weighted regression procedure (Proc LOESS) in Statistical Analysis Software (SAS). This procedure included a feature in which the optimum smoothing parameter can be automatically detected. ERG found the average optimum smoothing parameter for each vehicle and applied the average to all vehicles. The goal in the regression was to address the digitization without over-smoothing and reducing the measured deceleration rates of all braking events. Finally, some vehicles that had various speed discrepancies were dropped from analysis. Less than 5% of the OBD data was dropped for this reason.

When reviewing a vehicle's smoothed speed trace data, the coastdown rate of the vehicle is an important input for use in determining whether and when that vehicle's brakes were applied. Because the specific make and model of each participating vehicle in the Caltrans survey data was not available, ERG used a **Generalized Coastdown Curve** sourced from EPA emissions certification result report data. The road loads and inertia for different vehicles can be found in the EPA Certified Vehicle Test Results Reports published for each model year.[6] These reports include the road load curves used during emissions certification on the chassis dynamometer; these road loads are also relevant to the setup of a brake dynamometer. To determine a general coastdown curve for use in this work, ERG averaged the EPA-published target coastdown curves for the 6 vehicles chosen for testing on the test track. These 6 vehicles covered the range of light-duty vehicle types available and can therefore be used to represent an average or reasonably representative overall vehicle coastdown rate. The derivation of the generalized coastdown curve is described further in Appendix C, which also includes the target road load coefficients for the 6 test vehicles. Note also that specific vehicle coastdown coefficients are an input to brake dynamometer testing. The coastdown coefficients for the vehicle being simulated are entered into the dynamometer control at the start of a test, and these coefficients govern the system's application of brakes over the test cycle using the same type of calculation as was used to determine braking events in the Caltrans set.

ERG then assigned driving modes to the smoothed Caltrans survey data. There were only two important driving modes for this analysis, braking and non-braking. The braking driving mode was assigned any time the vehicle's deceleration rate exceeded that which would be experienced while following the generalized coastdown curve found previously. All remaining times in which the vehicle was not decelerating more rapidly than that coastdown curve were assigned as non-braking. Once the vehicle came to a stop, it was no longer considered to be braking (even through the brakes may have still been applied) because there was no further sliding at the brake friction interface and therefore no appreciable brake heating or PM emission taking place.

Further classifications of the survey data were applied for use in the overall cycle building process. The survey data was divided into **Microtrips**, defined as the period starting the moment a vehicle comes to a stop, through an idle period, acceleration, cruise, deceleration and ending at the next moment that vehicle comes to a stop.

---

[6] https://www.epa.gov/compliance-and-fuel-economy-data/annual-certification-data-vehicles-engines-and-equipment

Each microtrip contains one or more **Braking Events**, defined as the moment the brakes are applied to the moment that either the brakes are released or the vehicle comes to a stop, whichever occurs first. The ERG new dynamometer cycle was constructed based on combining a selected series of braking events that actually occurred in the Caltrans survey data. Information about the microtrip from which each braking event was extracted was retained to associate the braking event with microtrip average speed and distance traveled. This is done because, while some distance is traveled during braking, emission rate results from braking in EMFAC are given on a per-mile basis and these must also appropriately consider vehicle distance traveled between braking events for inventory purposes. An excerpt of a speed trace is presented in Figure 7, with graphical depictions of the start and end of a microtrip and its braking events.

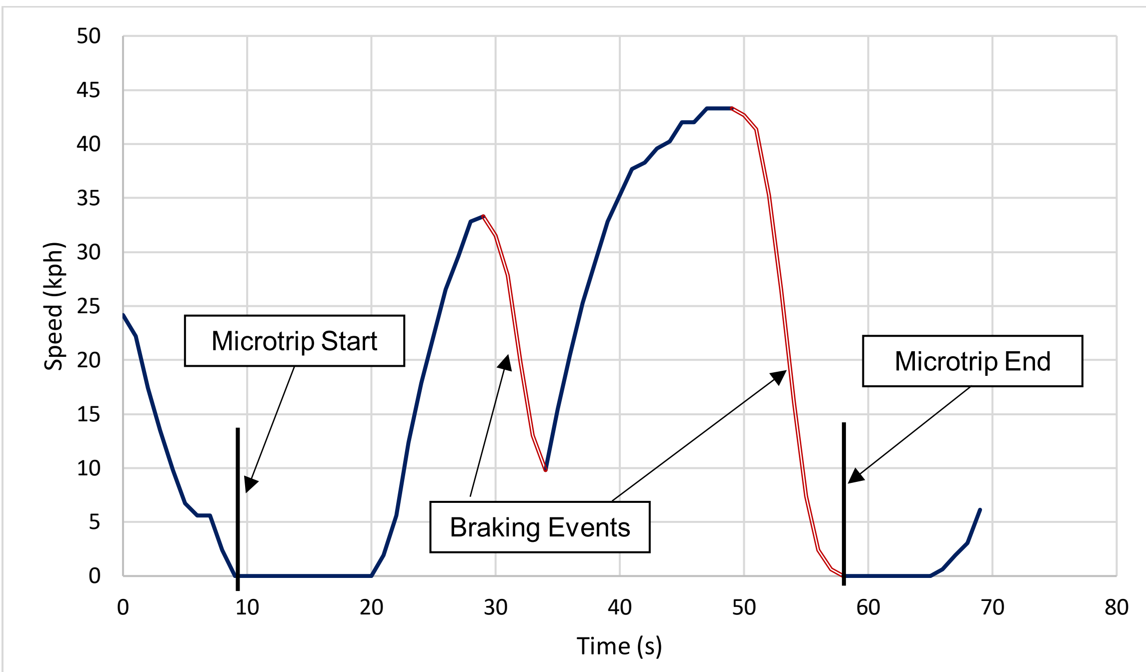

Figure 7. Illustration of microtrips and braking events within a speed trace

New Cycle Development and the Vector Collinearity Method

Over the last 25 years, ERG has developed and refined a method to measure agreement between a candidate test cycle and in-use data. The method is based on the determination of the angle between normalized vectors that represent the distributions of key time-series attributes in the candidate cycle and in the in-use data. An angle of zero degrees represents collinear vectors, that is, the key attributes of the candidate cycle and the in-use data times series would be the same (and normalized distributions of those attributes would be identical). Thus, the candidate cycle whose vector has the smallest angle with the vector of the in-use time series data is the best test cycle. Appendix D contains further information regarding the vector collinearity method including an excerpt from a previous ERG report in which the method was described in detail.

ERG used the vector collinearity approach to build the new brake dynamometer cycle from the Caltrans survey data. Put simply, the method involved sequentially selecting actual braking events from the Caltrans data so that the joint distribution of the key variables of the built-up cycle on the dynamometer best matched the same distribution of the braking events in the Caltrans data. Brake events continued to be selected in this manner until the built-up cycle reached a target overall duration or distance. The key variables used in this work were:

- Vehicle speed (distribution)
- Modeled brake temperature (distribution)
- Deceleration (distribution)
- Braking event duration (single value for each event)

Three of the variables allow for a distribution of second-by-second values within any braking event, but the event duration is just a single value for each event. Each of the four parameters were weighted equally as there was no reason to justify prioritizing one of the parameters over the others. The resulting distributions of the parameters show that all matched the target reasonably well, so it wasn't necessary to weight the matching of one at the expense of any other (i.e. weighting them differently would not have significantly affected the outcome).

The vector collinearity method was applied to create a series of braking events whose distributions of speed, modeled temperature, deceleration, and event durations best matched those in the entire Caltrans set. It should be noted that this selection method results in selecting the group of braking events that best match the target, but the procedure does not result in any particular order for the events (meaning they need to be ordered later).

The evaluation of the distributions of the four different parameters of braking events on the millions of braking events present in the Caltrans survey data was extremely computationally intensive. To keep computation time reasonable, ERG randomly selected a pool of 1000 Caltrans survey braking events to choose from during the vector method. The target vector was created from the entire Caltrans dataset; however, the new cycle could be built up from only selections from the 1000 randomly-selected microtrips.

Matching the braking events' distribution for temperature created a new challenge for the cycle development process. During brake dynamometer testing, the test brake system cools according to how quickly it is rotating over time. However, applying the brakes is the only way to heat the brake system. Because of this, the method could select different braking events whose associated temperatures could result in temperature gaps between the different selected braking events, meaning one or more of the higher temperature events could not be reached by the temperature increases available from any of the other chosen events. As a result, ERG developed rules regarding temperature for selected events to allow for the testing to be as realistic in temperature as possible while also reaching all specified modeled temperatures.

To eliminate temperature gaps, in which one or more selected braking events had an initial temperature that couldn't be reached based on the heating of any of the others, ERG implemented rules regarding temperature selection. To be eligible for selection by the vector collinearity method, brake events had to have an initial temperature less than the maximum ending temperature of any of the events that had been previously selected. For the initial selection, any event with a starting temperature of less than 2°C above ambient was eligible. While necessary to eliminate temperature gaps in which the highest temperatures could not be reached, this rule created a downward bias in temperature, as throughout the early stages of event selections only relatively low-temperature events were eligible for selection. To compensate for this, the selection pool of 1000 microtrips was adjusted to include 800 events selected at random, and 200 events selected at random from only those events with initial temperatures between 140°C and 190°C. As a result, ERG was able to develop a test cycle that could have completely reachable temperatures on the dynamometer as well as be representative of the distribution of modeled temperatures reached during on-road driving. The representativeness of the actual temperatures can be verified in histograms of operating temperature of the cycle and the target (included in the following sections).

After the microtrips were selected, they next needed to be ordered. Because of the rule that microtrips could only be selected if their initial temperature was less than the maximum temperature previously reached, they could, by definition, be ordered to increase without gaps (but there may be only one order that could reach the maximum without gaps). Braking events were ordered to achieve the maximum temperature relatively early in the cycle; those events that were needed to reach high temperatures were used to move rapidly up to the maximum. Otherwise, they could end up being "wasted" or lost by being followed by a cooler brake event leaving a temperature gap later in the cycle. So, the resulting trend of this process is a prompt rise to the maximum temperature followed by an oscillating and slowly decreasing temperature trend for the rest of the cycle. During cooling, brake events were ordered by always prioritizing the use of the highest starting temperature event that was accessible from the previous ending temperature. Sometimes, the time required by the dynamometer for speed changes after the point of highest temperature did result in a small number of temperature gaps. After the maximum-selected temperature had been reached, any further brake events with gaps were dropped from consideration. Dropping these events (after the maximum selected temperature had been reached) did not affect the resulting temperature distribution significantly. This is because there were generally few gaps at this point of ordering and they generally occurred across the entire temperature range such that their removal did not skew the resulting temperature distribution appreciably.

After each braking event was selected and ordered, the different events needed to be connected by a continuous speed trace that could be followed on the dynamometer. ERG added “engineered” segments between each braking event to allow the dynamometer speed and brake temperature to arrive at the initial speed and temperature of the next braking event. They included ramping to the next event’s speed as well as allowing time to pass at constant speed if further cooling was necessary to match the starting temperature associated with the next selected event. Cooling was assumed to take place as a function of speed (simulated by dyno RPM) according to the temperature model. The dynamometer positive acceleration ramp rate was limited to a maximum of 8 kph/s to stay within typical brake dynamometer capability. Some brake events had initial speeds less than the ending speed of the previous brake event. The negative deceleration level was specified at -3 kph/s. If a large amount of cooling was needed to get to the next event’s temperature, the speed was kept at the higher of either the previous event’s end speed or the next event’s initial speed to maximize the cooling rate. For those segments in which the speed was held at the previous event end speed, deceleration took place at -3 kph/s near the end of the segment in order to arrive at the next event speed at the correct target temperature.

After the cycle was completely selected, ordered, and the engineered segments added, it was taken from that point as only a speed trace. The modeled temperatures are no longer a part of the trace, they were used in its creation only. The speed trace is the cycle and is independent of temperature now that it has been created. This means that testing of different brake assemblies will follow the same speed trace but will be allowed to run at completely different temperatures depending on the vehicle/brake assembly characteristics and modeled vehicle mass.

While some vehicle distance is traveled during the braking events selected in the cycle, each braking event actually represents a much greater distance traveled in the Caltrans set. Because the braking events were extracted from microtrips, the distance of the source microtrip must be accounted for to generate a representative on-road emission rate in g/mi. To do this, information on the microtrip source of each braking event was retained to associate braking events with a total distance traveled (which is greater than the distance traveled just during braking). For microtrips that contained multiple braking events, the braking energy for each event was used to proportionally assign the total microtrip distance traveled to that represented by each braking event. Dynamometer distance is also traveled during the engineered segments of the cycle; however, these segments only exist to set the dynamometer speed and the amount of brake cooling. The dynamometer operation during the engineered segments has no actual basis in vehicle distance traveled, which also contributes to why the dynamometer cycle distance traveled is not useful for g/mi calculations. The ERG cycle will specifically advise a **represented distance** to be used in all g/mi calculations and it will not be the same as the integrated distance traveled by the rotational assembly on the dynamometer. Figure 8 illustrates an example microtrip from which one braking event was selected and inserted into the test cycle. The speed trace of the braking event is identical, however the rest of the microtrip is excluded.

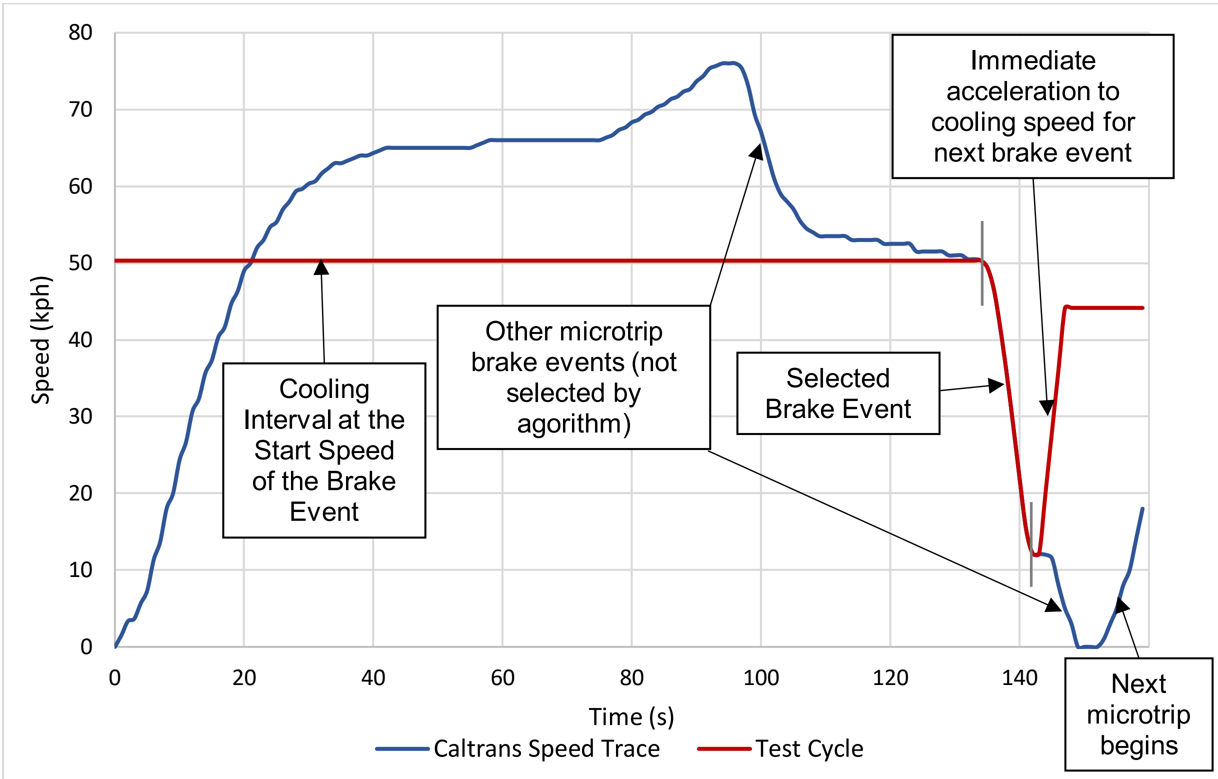

Figure 8. Illustration of a braking event, extracted from the original microtrip speed trace (blue), and inserted into the test cycle between engineered segments (red)

In addition to representativeness of California driving, the test cycle also needs to have the ability to resolve emission factors by speed. The ERG cycle is divided into three **speed segments** representing different average speed ranges. ERG selected three speed ranges based on trends in the average speed of all microtrips in the Caltrans data. Figure 9 depicts a histogram of the number of microtrips with each average speed. The histogram represents all microtrips in the Caltrans set, weighted by the duration of each microtrip (i.e. longer microtrips have higher weighting to reflect the greater duration and distance of driving that they represent). The average speed ranges for the segments of the new cycle were selected as 0-21 kph, 21-69 kph, and 69 kph and above. ERG used the cycle building approach to develop a brake dynamometer cycle for each average speed range. Each phase would contain braking events taken only from microtrips falling within its respective microtrip average speed range.

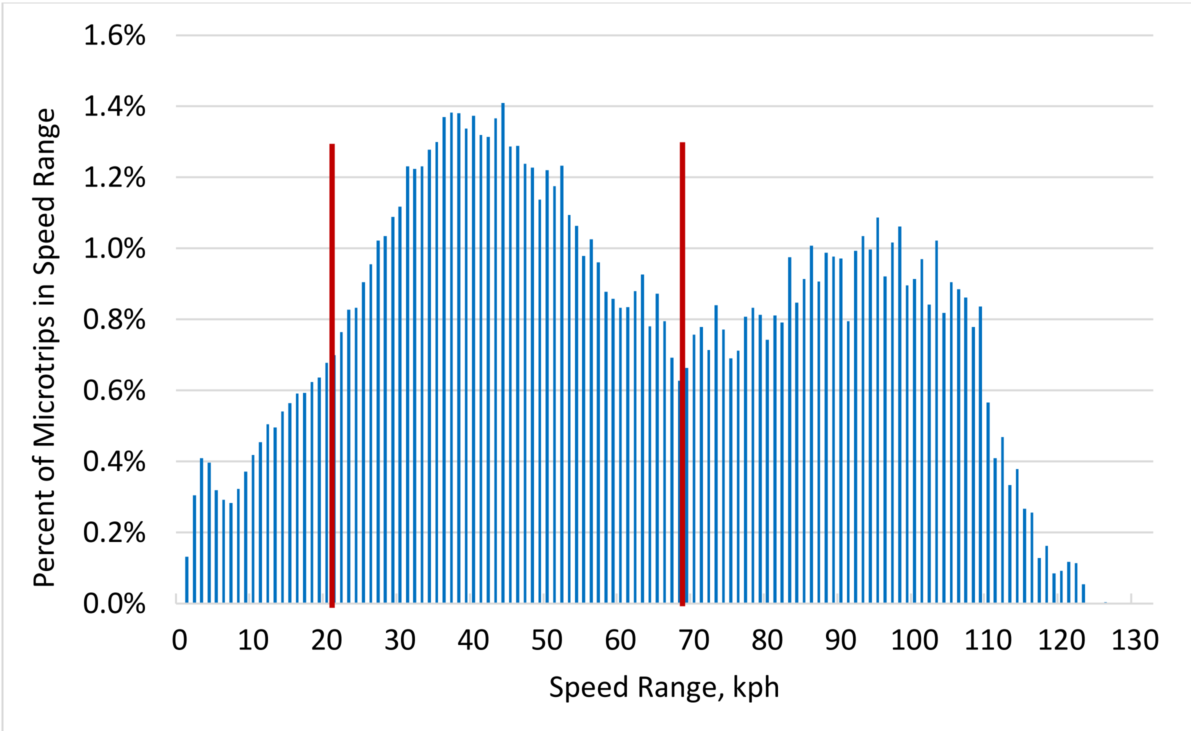

Figure 9. The percentage of the number of microtrips within each bin of average speed

ERG used the vector method described previously to construct each of the three speed segment. For a given speed segment, the selection pool of 1000 brake events were chosen from only those microtrips with an average speed within the segment's speed range. The target vector from Caltrans used for each speed segment was taken to be that made up of the braking events from all microtrips with an average speed in that range. The overall cycle is made up of the three speed segments run in succession. The representative distances of each was also taken to represent the relative distances traveled in the Caltrans survey by all microtrips falling within each speed range. This results in the overall per-distance emission rate being representative of overall brake emission rates in California. Because the speed segments are specified to run in succession, the speed-based emission factors could be based on either continuous or batch (i.e. filter-based) PM measurements.

ERG used a specific method to determine the overall duration/represented distance of the speed segments as well as how the distances were apportioned within each of the three speed segments. The following procedure was followed:

1. Use the vector collinearity method to build up 200 braking events for each of the three microtrip speed ranges
2. Determine the total distance represented by each range's 200 events
3. Determine the total distance traveled in the Caltrans dataset by microtrips in each of the 3 speed ranges and find the percentage for each

4. Correct the two speed segments that over-represent distance by removing trips at random, but do not remove trips that would cause a temperature gap in the cycle

After determining the relative distances of each cycle, ERG inserted engineered portions between each speed cycle to allow the brakes time to cool to a near-ambient starting temperature. The percentages of distance traveled in the overall Caltrans dataset of microtrips in each of the three speed ranges are presented in Table 11 along with the resulting represented distances and times for the new cycle.

Table 11. The percentage of Caltrans-survey and new test cycle total distance traveled by microtrips within each average speed range

Microtrip Avg. Speed Range	Percent of Total Caltrans Distance traveled	New Cycle Represented Distance (km)	New Cycle Represented Distance %	New Cycle Duration (s)
0 – 21 kph	3.96 %	6.163	4.7 %	2,741
21 – 69 kph	38.34 %	47.309	36.0 %	8,339
69+ kph	57.7 %	77.775	59.3 %	3,853
Total	100 %	131.247	100 %	14,933

Figure 10 presents a speed trace of the new ERG-developed braking cycle for this program.

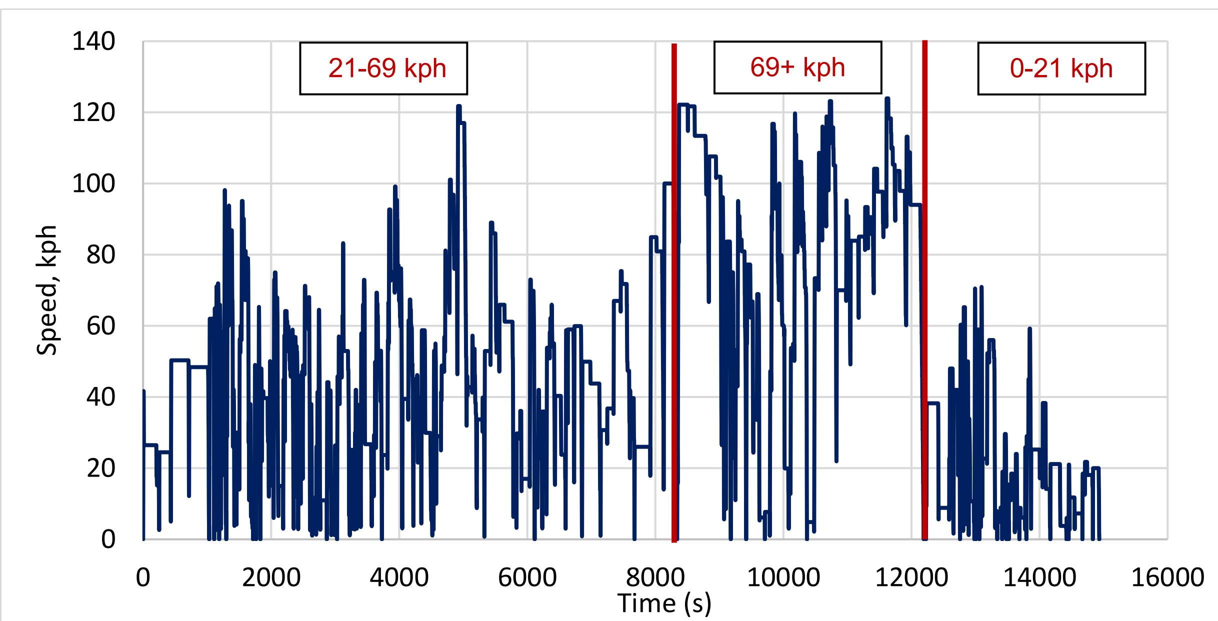

Figure 10. Speed trace of the braking cycle developed for this work

The new cycle developed from the vector collinearity method was evaluated against the two existing cycles, the EMFAC cycles and the WLTP-Brake. For each of these cycles, the same general coastdown curve was used to isolate braking events from the speed traces. The same temperature model was applied to these cycles to develop temperature distributions of each. To evaluate the EMFAC UC and SCCs, ERG created a single cycle from starting with the UC and appending all the SCCs to it. Modeled temperature was reset to ambient between each of the UC and SCCs. To develop distributions for the WLTP, the temperature was set to 10°C over ambient between each of the 10 trips to reflect the cooling soaks to 30°C between trips as specified in the WLTP-Brake test procedure.

In this report, findings and comparisons for the EMFAC UC/SCCs are included, however these cycles may not be able to be repeatably run on the brake dynamometer. These cycles have a range of brake event durations that includes events down to 1s and 2s in duration. The LINK brake dynamometer cannot repeatably test braking events of this short of duration. This cycle could not be chosen for this project for this reason; however, the EMFAC cycles are left in the analyses in this section. Correspondingly, the ERG cycle development algorithm described previously was modified to only select braking events of 3s duration or longer to meet the dynamometer requirements for repeatable operation. Speed traces of the WLTP-Brake and the concatenated UC/SCCs are presented for reference in Figure 11.

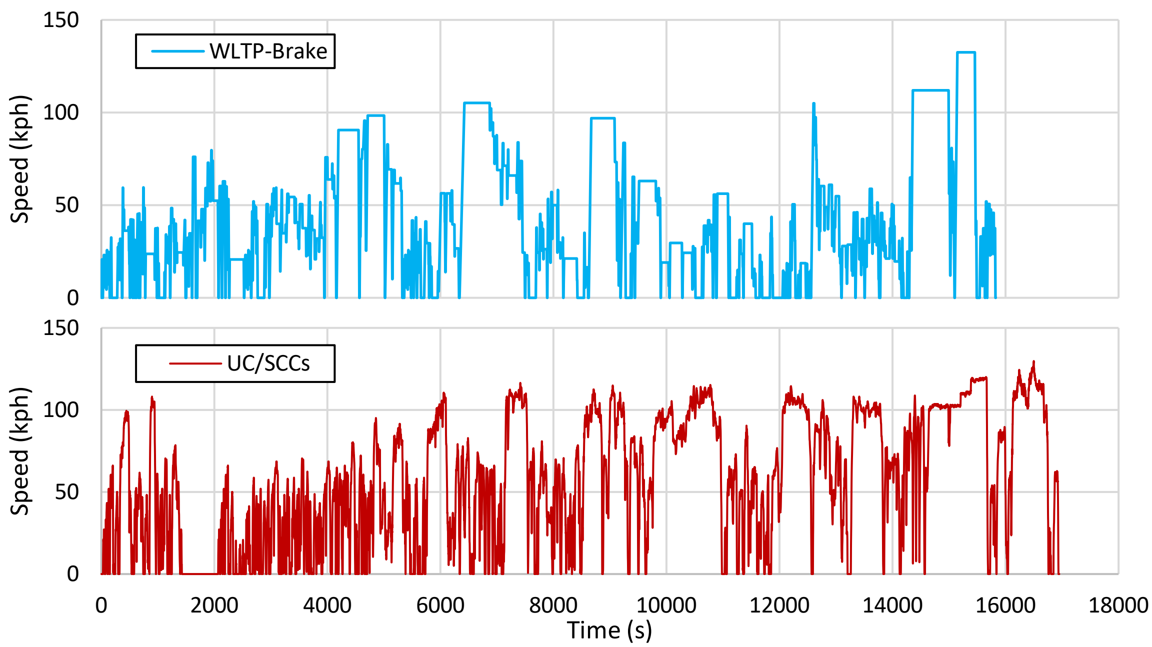

Figure 11. The Speed traces for the WTLP-Brake and the concatenated UC/SCC

Comparisons across the three cycles are presented in two ways. First, Table 12 describes some of the relevant properties of the three cycles. Later in this section, distributions of various parameters of interest are presented for the three cycles.

Table 12. Relevant parameters of the three candidate brake test cycles

	Duration (s)	Number of Braking Events	Distance (km)	Brake Events/ Distance (#/km)	Average Speed (kph)	Max. Speed (kph)
ERG Vector Method (Overall)	14,933	347	131	2.65	50.3[1]/30.3[2]	123.9
0-21 kph speed segment	2,741	65	6.16	10.55	21.7[1]/8.0[2]	70.9
21-69 kph speed segments	8,339	198	47.31	4.19	45.7[1]/19.4[2]	121.8
69+ kph speed segment	3,853	84	77.76	1.08	80.6[1]/69.8[2]	123.9
WLTP-Brake	15,826	303	192	1.58	43.7	132.5
EMFAC UC/SCCs	16,952	1,015	272	3.73	57.7	129.8

[1] – Calculated based on the actual number of dynamometer revolutions

[2] - Indicates the represented distance for inventory (accounting for brake cooling and elimination of unnecessary cruises – this is the value relevant for EMFAC)

It is important to note some specifics regarding the values in the table as follows:

- **Duration:** Duration is a count of the number of cycle-specified seconds only. The WLTP also includes cooling between most of the 10 Trips and so will take longer to complete. The time listed for the ERG method includes all required cooling.
- **Distance:** As described previously, the overall ERG cycle spins the dynamometer further than 131 km due to the engineered segments. The 131 km listed specifically describes the distance represented by those events for the purposes of g/mi calculations. The distance listed for the other two cycles describes the distance traveled by the dynamometer. The dynamometer spins a longer distance over the ERG cycle to allow the necessary amount of cooling.
- **Average Speed:** Because the ERG cycle spins the dynamometer farther than the on-road distance represented, the average speed is presented two different ways. For the ERG cycle and its constituent cycles, average speeds denoted with a “1” indicate the average speed of the **rotation on the dynamometer** including the cooling intervals. The average speeds denoted with a “2” indicate the average speed based on the distance represented by the cycle for the **purposes of inventory modeling**.

The following section includes distributions of various parameters of interest for the 3 cycles. The Caltrans survey data is shown as the target for representation of real California driving. In all plots, the distributions reflect the parameters from only the time during brake events; the values during periods of time with accelerations and cruises are not included in the distributions. Braking events are defined by decelerations that exceed the generalized coastdown curve used in this work. Temperature distributions are estimated using the temperature model developed for the Camry test vehicle. Additional detail is presented in Appendix E, which contains similar distributions further broken down by each of the three speed segments that make up the new cycle.

The distributions of brake event durations are presented in Figure 12. Note that the ERG New Cycle does not have any brake events shorter than 3 seconds. This is intentional due to a limitation of the brake dynamometer used for testing and would otherwise be likely to result in the UC/SCCs not being repeatably testable as they have many 1s and 2s events. The number of events in the 3-second bin of the ERG cycle are higher as a result because the vector collinearity method was targeting the Caltrans distribution which contains a large number of 1s and 2s events.

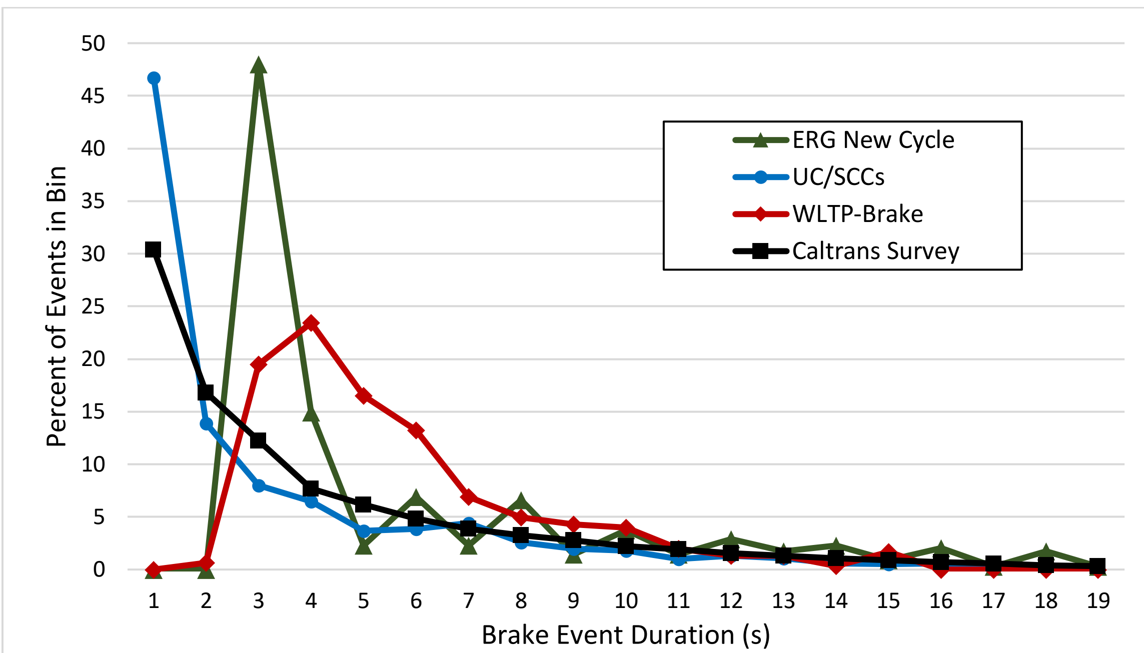

Figure 12. Distribution of brake event durations for the candidate cycles and the Caltrans data

The distributions of speeds encountered during braking events are presented in Figure 13. The distribution of (negative) acceleration rates during braking is presented in Figure 14.

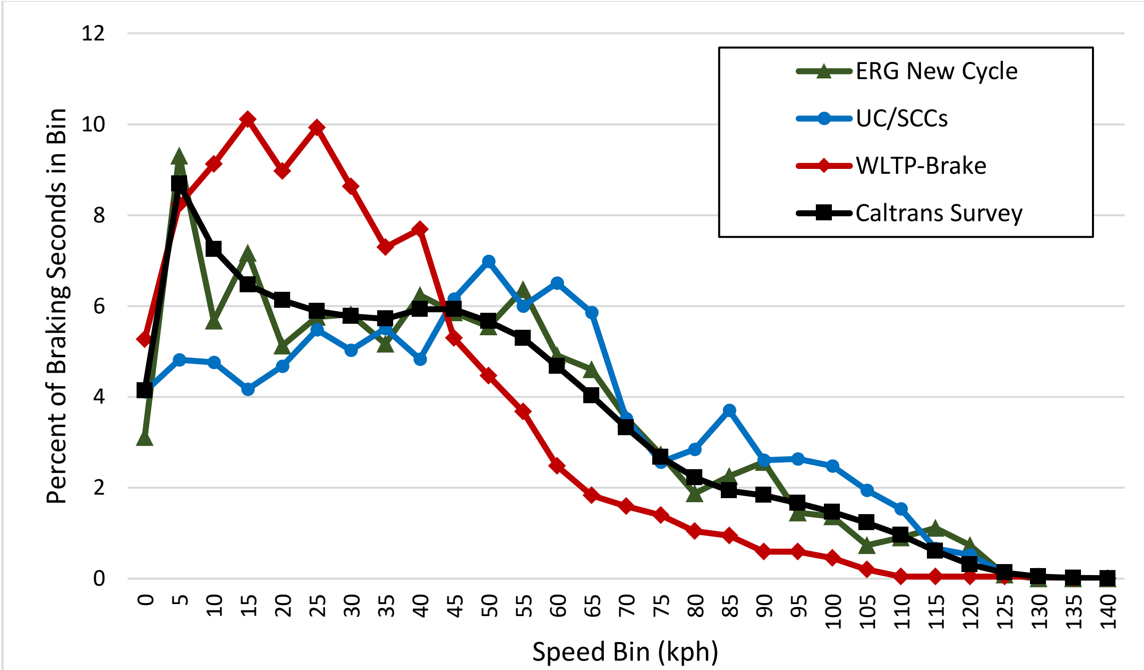

Figure 13. Distribution of vehicle speeds for the candidate cycles and the Caltrans data

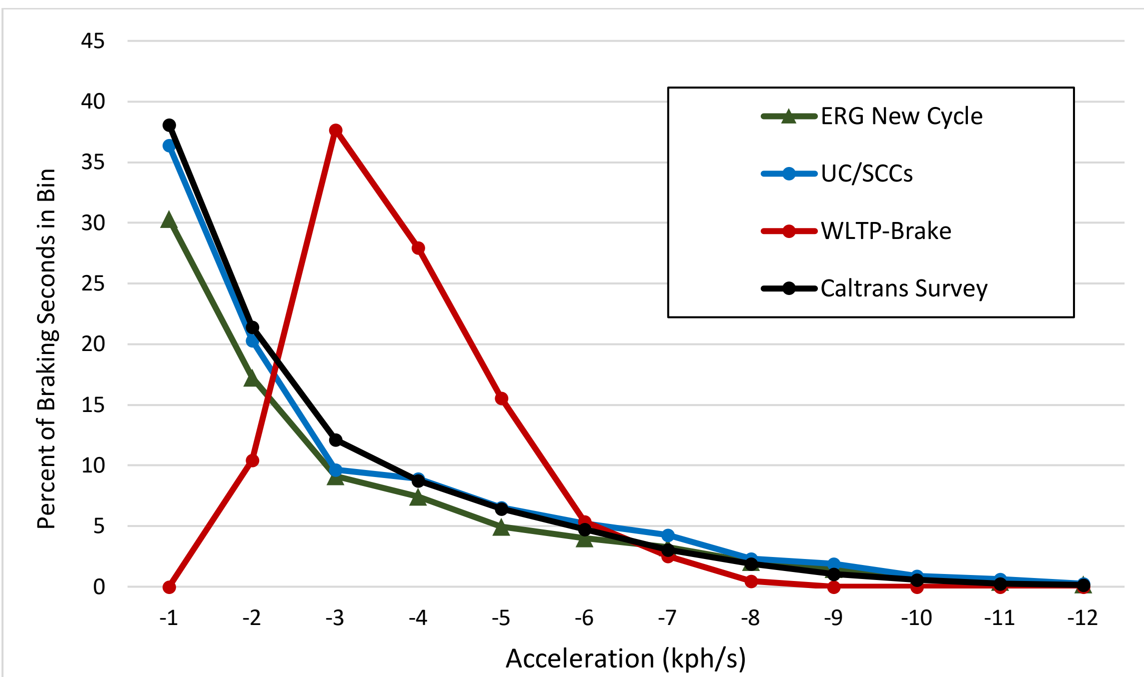

Figure 14. Distribution of braking event (negative) acceleration rates for the candidate cycles and the Caltrans data

The distributions of modeled brake temperatures for each cycle are presented in Figure 15. The same temperature model was used to estimate temperatures for the three candidate cycles as well as the Caltrans survey data.

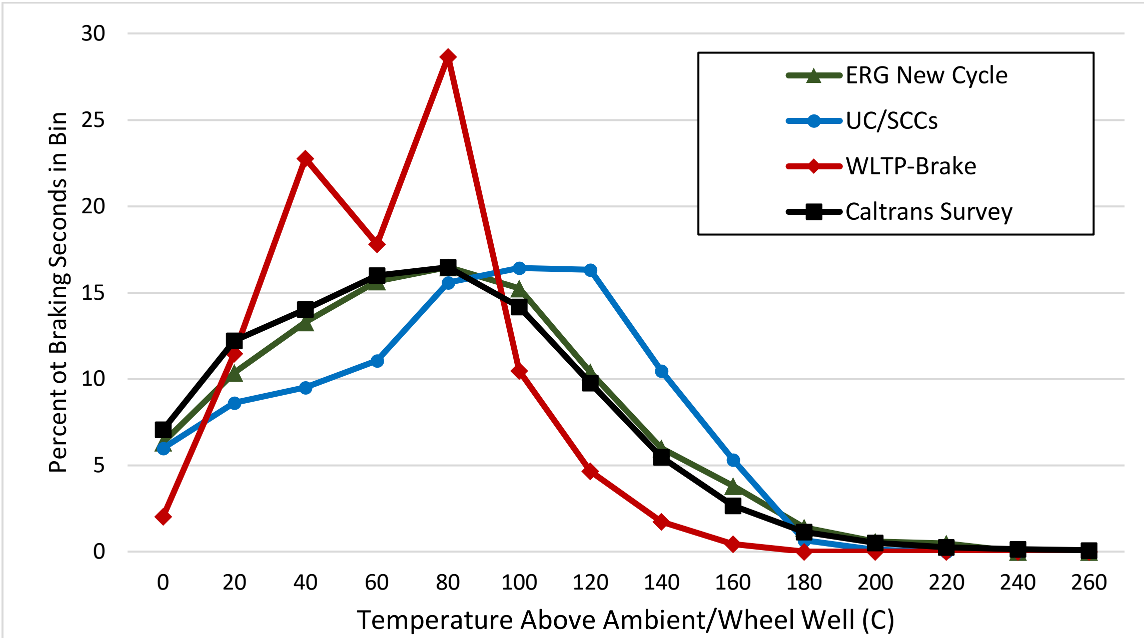

Figure 15. Distribution of modeled brake temperatures for the candidate cycles and the Caltrans data

The distribution of relative power per brake event is presented in Figure 16. In this plot, relative power is defined as the change in speed squared (accounting for the coastdown-rate of energy loss) divided by the duration for the entire brake event in seconds, with units of kph^2/s. Relative power was not one of the parameters used during cycle building, but is presented here for completeness.

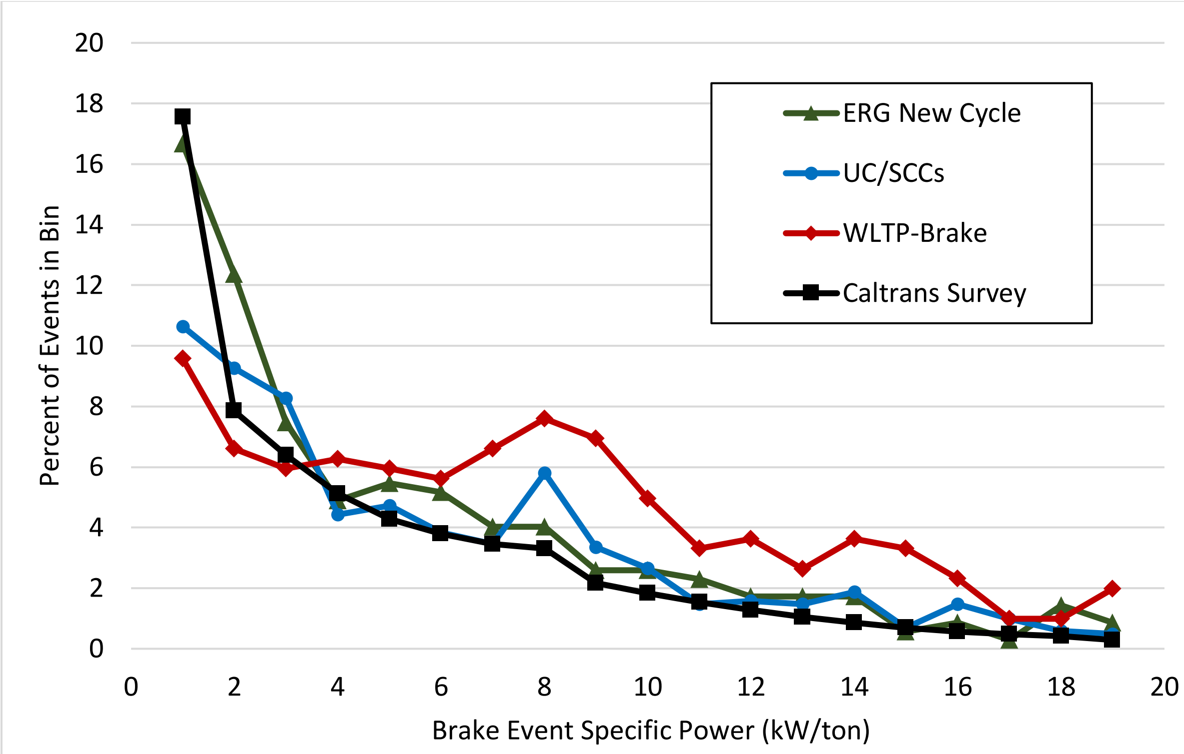

Figure 16. Distribution of brake event relative power for the candidate cycles and the Caltrans data

Each candidate cycle has advantages and disadvantages. The following summaries for each cycle were presented to CARB staff during the evaluation and selection of the cycle to be used during dynamometer testing.

ERG Vector Method Cycle. The distributions on the parameters of interest for this cycle match very well with the Caltrans survey results because it was designed to result in a match on the four main parameters. It allows directly for determination of speed-based emission factors using its three constituent speed segments. However, it is an unproven cycle with no reputation across the research community. Some members of the community may not agree with the approach to have a represented distance for g/mi calculations (for the purposes of inventory modeling) that is separate from the actual dynamometer distance traveled. ERG planned to have a separately-specified represented distance from the start of this project as it ensures that g/mi calculations are appropriate for representing California driving.

WLTP-Brake. The WLTP-Brake is an engineered cycle designed for use on a brake dynamometer. As a result, it contains brake event durations appropriate for dynamometer testing. However, of the three candidate cycles, its distributions on the parameters of interest have the least similarity to the Caltrans survey results. Also, it was not designed to have the distance traveled over the cycle be on the same basis as PM emissions from California driving, resulting in potential error in g/mi calculations. The WLTP-Brake cycle also does not necessarily lend itself to the measurement of speed-based emission factors. With this cycle, speed-based factors would only have been able to be generated from extracting different brake event segments from the continuous PM measurement traces. An advantage of the WLTP-Brake cycle is commonality and comparability with European brake testing which will heavily utilize the WLTP-Brake.

UC/SCCs. The analysis of braking events showed that the EMFAC cycles matched the Caltrans survey results reasonably well for the parameters of interest. The key limiting factor of these cycles will be that they contain a significant number of short duration (1-2s) brake events that cannot be repeatably simulated on the brake dynamometer. It is not possible to remove these short duration events without significantly reworking these cycles. For this reason, it would have been inadvisable to utilize these cycles for this program despite EMFAC being designed around them such that test results would be readily adapted into EMFAC emission factors including those that are speed based.

Cycle Selection. The three cycles were evaluated for how well they represented the driving logged during the Caltrans survey. The EMFAC UC and SCCs represented the Caltrans data fairly well and could be readily adapted to speed-based emission factors because the speed correction cycles already exist. However, the EMFAC cycle consisted of many 1s and 2s duration brake events, which cannot be repeatably simulated on the brake dynamometer. For this reason, the UC/SCCs could not be used in this work. The WLTP-Brake cycle is designed specifically for brake dynamometer testing but was not specifically designed to represent California (or US) driving as it was developed from data from multiple nations. The WLTP-Brake is also not designed to directly determine speed-based emission factors. The ERG vector-based method generated a cycle that both represented different speed ranges of operation and was very similar to the Caltrans travel survey data on the four important parameters of interest, so CARB and ERG staff agreed that ERG's newly-developed cycle would be used during the dynamometer testing in this work. From this point forward, it will be known as the **California Brake Dynamometer Cycle (CBDC)** for light-duty vehicles. A spreadsheet file containing the CBDC second-by-second speed trace is included with this report submission as Appendix N.

Brake Burnish Cycle. Newly installed brake friction materials go through a process of "bedding in," in which the friction couple equilibrates and a layer of pad material becomes adhered to the disc or drum. Particulate emission rates may not be stable during this time. Also, brand new materials may have a protective coating to prevent oxidation prior to installation. After installation, this coating is worn off in the early stages of use but may result in particulate emissions that are not representative of emissions during the remaining life of the components. For this reason, a burnish procedure was performed after the installation of new components but prior to testing.

ERG developed a new brake burnish cycle with the goal of being as short as possible (to allow for a 24 hour test turnaround) while still resulting in a stable friction couple at completion. The PMP was developing a standardized burnish cycle concurrently with this project, and industry experts participating in the process indicated that a minimum of 5 repeats of the WLTP-Brake would be necessary for a stable burnish. ERG used this as the source of the development of a new burnish cycle for this work. ERG developed a new burnishing cycle by using the following method:

- Calculate the total braking energy in 5 WLTP-Brake cycles
- Select a relatively high energy segment of the newly developed CBDC brake cycle that has a similar start and end temperature (starting at 707s, proceeding to 1740s)
- The burnish cycle starts from the beginning of the CBDC and runs through the end of the selected high-energy segment. Then, that segment is appended repeatedly until the total braking energy of 5-WLTP-Brake cycles is reached
- An engineered high-speed cruise is added to cool the brake assembly to near ambient temperature
- Finally, to cool down and equilibrate the friction couple so that it doesn't end during high intensity operation, a single, low speed segment is appended to the end of the burnish (the complete 0-21 kph speed segment).

The resulting burnish cycle has a duration of approximately 11 hrs 30 mins (as compared to approximately 30 hrs for 5 WLTP-Brake cycles when including the specified cooling between trips). A speed and temperature trace of the resulting burnish cycle (used for all tests in this program) is presented in Figure 17. The repetitive nature of the cycle facilitates the determination of whether PM emissions reach steady state.

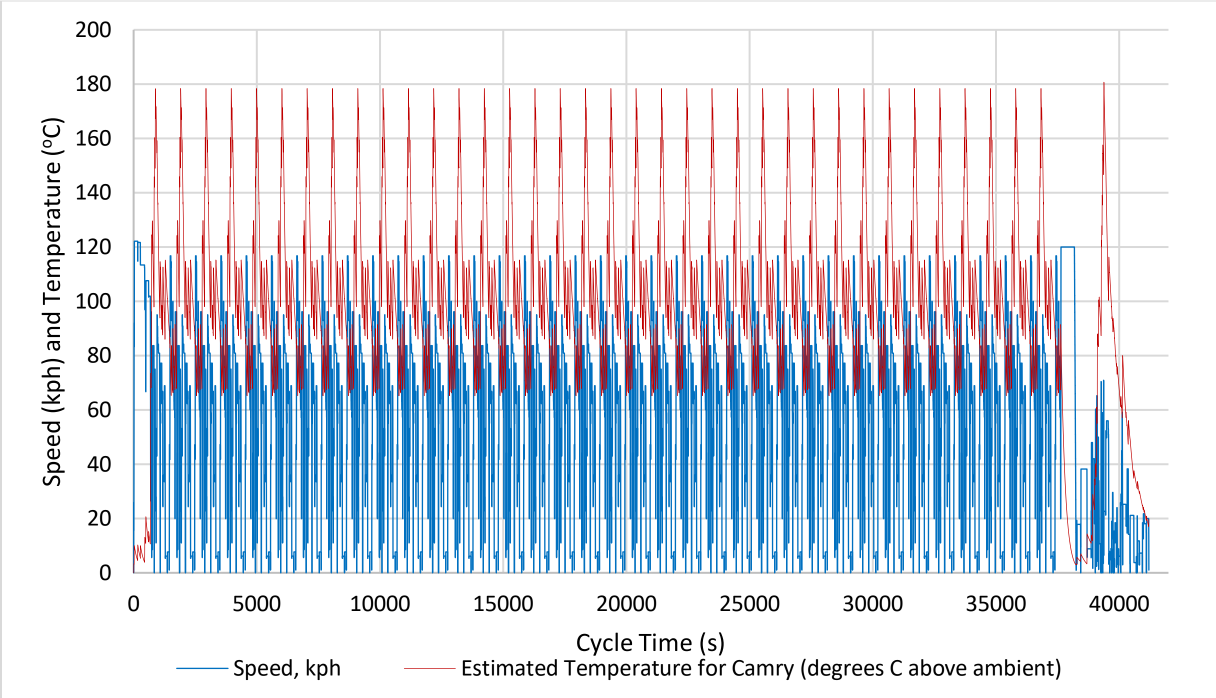

Figure 17. Dynamometer speed and estimated Camry front rotor temperature traces for the CBDC burnish cycle

Test Matrix

After the test cycle was developed, ERG and LINK then began the development of a test matrix that would describe the various tests that would be conducted during the dynamometer testing phase of the project. The first step in the development of a test matrix was to consider the parameters of interest to be tested. This section lists those parameters, the different options or values to test within each parameter, and their relative importance. The options and selections within many parameters were based on the market research findings presented in the Representative Test Vehicle and Friction Material Selection section. The parameters that were considered are:

Vehicle make and model. The initial parameter that was considered was the vehicle make and model of each brake assembly. The selection of the test vehicles was described previously in the Representative Test Vehicle and Friction Material Selection section, in which the selection of the following 6 vehicles was documented:

- 2011 Toyota Camry LE
- 2013 Honda Civic LX
- 2013 Toyota Sienna LE
- 2015 Ford F-150 Supercrew
- 2016 Toyota Prius Two Eco
- 2016 Nissan Rogue S

These vehicles are all equipped with front and rear disc brake systems except for the Honda Civic, which utilizes front brake discs and rear brake drums. The Toyota Prius is a hybrid vehicle and is equipped with regenerative braking. The operation of the regenerative braking system was simulated by the brake dynamometer for this vehicle's assemblies only. These are the same vehicle make, model, and model year as those that were track tested during the development of the brake temperature model.

Vehicle front/rear brake assembly. The brake dynamometer tests the brake system components of a single vehicle wheel/hub assembly at a time. Because of weight distribution and weight transfer during braking, front and rear brake assemblies are designed differently. Front brakes typically receive a larger proportion of braking energy than do rear systems, and for this reason, their design is different from rear assemblies and the components typically have a greater mass and greater surface area for heat rejection. However, because they are generally lighter and less vented, rear brakes tend to operate within approximately the same temperature as front brakes. To estimate total PM emissions from braking, this project involved testing both front and rear assemblies to better understand the relative and total emission rates from these components.

Brake pad material. Modern brake pad materials fall into the categories of low metallic (LM) or NAO. A given vehicle may be fitted with different brake pad materials at different points in its life as aftermarket options may differ from original equipment components. Not all brake assemblies have the same brake lining materials available. Thus, brake lining materials were selected based on the individual vehicle assemblies tested. At a minimum, for each test vehicle the OES friction material was chosen for one of the pad material options (which was NAO for all models). Testing of each vehicle then included one or two aftermarket options, either one or both of a common NAO aftermarket pad and/or a common metallic aftermarket pad depending on availability.

The test plan included matching the rotor selection (or drums in the case of the Civic) to the selected pad type where possible. OES pads were tested with OES rotors. For aftermarket pads, LINK used business intelligence and existing brake supplier relationships to determine the most likely/representative aftermarket rotor to be matched with each pad material during a real-world aftermarket purchase. This allowed for the friction couple between the pad and rotor to be more likely to be representative of real-world operation.

The selection of brake friction materials also included consideration of the copper content in each material formulation. California legislation in SB 346 specifies a phase-out of copper (as well as selected other metals[7]) in commercial brake pad formulations due to environmental harm associated with these compounds being carried into waterways by roadway runoff. Other states have also adopted the legislation and it is likely that, to simplify supply chains, eventually most or all brake manufacturers will produce only friction materials that meet SB 346 requirements nationwide. Under SB 346, copper must be reduced to 5% or less of total material content by weight by 2021, and to 0.5% or less by 2025. Friction material manufactured prior to the January 1, 2021 with <5.0% copper by weight may be sold until January 1, 2031. The Brake Manufacturer's Council has developed the LeafMark letter labeling design to indicate to consumers which of the above thresholds that a given pad meets. The LeafMark letter labels and their respective thresholds are defined as follows:

- A – formulation contains more than 5% copper by weight
- B – formulation contains between 0.5% and 5% copper by weight
- N – formulation contains less than 0.5% copper by weight.

In this work, LINK had limited control over which formulations were associated with the different brake assemblies that were tested. OES materials were tested in whichever formulation was used by the OES component. For aftermarket, in which a project goal is to test high-selling, representative components, one of two options existed:

- Only one LeafMark is associated with the best or second-best selling component. In this case, that LeafMark was selected.
- The LeafMark is not yet specified for a given aftermarket component. This situation exists for those components for which current inventory exists under multiple LeafMarks. In this case, the desired component was ordered and whichever LeafMark was delivered was tested (as there is no way to order these components based on the LeafMark).

Based on LINK business intelligence, there were no instances in which the top two selling components each had a different, specified LeafMark. So, there was no assembly for which ERG and LINK had to select one LeafMark over another. The two vehicles for which metallic pads will be tested are most likely to carry the A label. The test matrix contains the LeafMark that was planned for testing if it was known for a given friction material.

Simulated vehicle weight/load. To decelerate at a given rate, more braking energy is required by a more heavily laden vehicle. To better understand the effect of this, additional tests of some vehicles will be performed at a higher weight than the normal test weight for each vehicle. The normal test weight simulated for each vehicle

[7] SB 346 also limits the presence of cadmium, chromium salts, lead, mercury and asbestiform fibers in brake friction materials sold in California during or after 2014. (https://leginfo.legislature.ca.gov/faces/billNavClient.xhtml?bill_id=200920100SB346)

will be calculated as given for passenger cars in 40 CFR 86.129-00. The nominal equivalent test weight (ETW) for each vehicle will be the curb weight plus 300 lbs.

ERG selected the three vehicles with the largest cargo-carrying capacity for additional testing representing higher-laden weight operation. For these vehicles a heavily-laden weight (HLW) was defined as an additional two thirds of the capacity added between the curb weight and the gross vehicle weight (GVW). HLW was calculated as:

$$HLW = Curb\ Weight + \frac{2}{3} \cdot (GVW - \ Curb\ Weight)$$

Test cycle. For the majority of tests, ERG used the cycle that was developed and selected for use in this program. This cycle was developed based on actual in-use vehicle survey data from California. The new CBDC test cycle has a duration of approximately 4.3 hours and represents a total of about 81.55 miles of driving. It contains 347 braking events. The cycle consists of three different segments representing slow, medium, and high average speed driving. The three segments are proportioned in distance similarly to the actual in-use California distances driven in those average speed ranges based on the Caltrans survey data.

For comparison with outside brake PM research, a small number of tests with a subset of the test vehicles was conducted using the World Harmonized Brake Dynamometer Cycle (WLTP-Brake). The WLTP-Brake cycle has a duration of approximately 4.4 hours (plus cooling intervals) and represents approximately 119.3 miles of driving. It is divided into 10 trips containing a total of 303 braking events.

Test replicates and references. Conducting replicates helps determine the repeatability of the testing procedure. The selection of the quantity of replicates was optimized in terms of the number of replicates given that the total number of tests was limited. The number of replicates was decided prior to testing and was not adjusted during testing. Given that testing had not yet been conducted at the time of test matrix development, ERG had limited data from which to estimate the number of replicate tests required to determine statistical significance. Based on the total number of different brake materials and vehicles in the study, ERG decided to do two replicate tests for almost all test matrix combinations. Replicate tests were conducted using new components of the same specification (or part number) for each test. So, test repeatability could be influenced by both the test setup and the differences from using separate sets of friction materials manufactured to the same specification.

Additionally, one vehicle/assembly/material combination was selected to serve as a reference test. The single reference combination was repeated in the test matrix at regular intervals throughout the project. The reference test can help to better understand and track any measurement drift in the laboratory setup over time. ERG selected the F-150 front brake with OES pads (which are NAO) to serve as the reference. This was selected due to this vehicle being the most popular of the six test vehicles for brake component benchmarking based on LINK market research and business intelligence.

Additional considerations. In addition to the parameters that define the dimensions of the matrix, there were some additional considerations and line items in the matrix that were added to enhance the test plan. These include the types of filter blank measurements to be conducted, a planned testing pause, and additional notes regarding expected EPA and CARB chemical analyses to be conducted after the post-test weighing processes.

LINK conducted two types of filter blanks during the program, zero blanks and tunnel/background blanks. Zero blanks are intended to identify the level of contamination that may occur during the handling of the filter between weighings but outside of the actual test cycle. Zero blanks are not specifically listed in the matrix but were performed approximately once every two weeks during the testing program. Zero blanks were performed as follows:

1. Pre-weigh filter
2. Transport filter from weigh room to the test site and install normally
3. Pause and do not turn on sample pump or expose filter to any sample flow
4. Remove filter, transport back to weigh room and allow to stabilize
5. Post-weigh filter

Tunnel/background blanks required a more rigorous procedure and attempt to quantify not only the handling effects but also any contamination that exists within the complete sampling tunnel. Tunnel/background blanks are listed in the test matrix and were conducted as follows:

1. Pre-weigh filter
2. Transport filter from weigh room to the test site and install normally. Operate and/or log data with all measurement equipment.
3. Install the F-150 rotor, fixture, and caliper, but do not install brake pads. Run the tunnel dilution air pump as well as the relevant sample pump and cooling airflow for the test duration, however do not open the hydraulic brake line valve. Allow the installed rotor to rotate and follow the speed trace (as closely as possible given that no braking will take place). Run the cooling airflow at the flow rate used for the front assembly of the F-150 during tunnel blank measurements. The brake pads will not be present to eliminate any PM that could be generated from them lightly rubbing on the brake rotor.
4. Remove filter, transport back to weigh room and allow to stabilize
5. Post-weigh filter

As described in the original proposal, ERG and LINK planned a testing pause early in the program. This allowed time for an initial data review to determine if any problems exist with sampling plan or execution of testing. The pause allowed for specifically delineated time for any necessary changes to be made prior to conducting the bulk of the testing plan. The test matrix included the expected point for the testing pause.

In addition to the work conducted by LINK and ERG for this project, both CARB and EPA will be contributing work in performing chemical speciation of some samples. This chemical speciation/characterization was outside the scope of this project and was planned to be performed separately by EPA and CARB for the different respective samples. For planning purposes, the labs that will perform different filter analyses are also presented in the matrix. Primarily this included the two different workflows to take place for the Teflon filters. One subset of them originated at CARB, were shipped to LINK for weighing and testing, and then were shipped back to CARB for XRF and/or ICP-MS analysis. A different subset originated at EPA's National Vehicle, Fuel, and Emissions Laboratory (NVFEL) and were used in a filter-weighing "round-robin" in which the pre-test and post-test weighings took place both at LINK and at EPA NVFEL in series. The test matrix includes the tests that were assigned for each of those two workflows.

The different parameters to be tested for each vehicle are presented in the following table. The total number of planned tests was 85.

Table 13. Brake Dynamometer Test Matrix Parameter Summary

Test Vehicle	Front/ Rear	Pad Material	Wheel load	# Replicates	Reference repeats	Test Cycle	Total Tests
Camry	Front Rear	OES After-Met. After-NAO	ETW	2 each	NA	CBDC, WLTP-Brake	14
Civic	Front Rear	OES After-NAO	ETW	2 each	NA	CBDC	8
F-150	Front Rear	OES After-Met. After-NAO	ETW HLW	2 each	5 of a single condition	CBDC WLTP-Brake	25
Sienna	Front Rear	OES After-NAO	ETW HLW	2 each	NA	CBDC	16
Prius	Front Rear	OES After-NAO	ETW	2 each	NA	CBDC	8
Rogue	Front Rear	OES After-NAO	ETW HLW	2 each	NA	CBDC	12
Tunnel Blanks				2 total			

The list of parameter options presented previously must then be ordered based on the relative quantities to be tested for each parameter. It was preferable to test as many different assemblies as possible prior to the pause, but it was also preferable to test at least one replicate prior to the pause to get an initial indication of the level of variability between two tests.

Where possible, the order was then randomized and mixed to reduce the likelihood of external factors biasing the measurements. So, most of the different assemblies were tested prior to the pause, but after the pause the testing order was assigned in groups in random order. Tests were conducted in blocks for each vehicle's front or rear brake assembly to reduce the turnaround time between testing where possible. The first replicates for each pad material were grouped together, but the order of these groups was then selected at random. For example, the "A" replicates of a given vehicle's front or rear assemblies for the OES, aftermarket NAO, and the aftermarket metallic friction materials make up a group to all be tested consecutively. These groups were then ordered, generally at random, to minimize the effects of any time-based biases that could be encountered during the test program. One exception to the complete randomization was that a few changes in order were made in order to reduce the turnaround time from switching between different assemblies. The LINK dynamometer system uses combinations of large and small inertia discs to simulate vehicle inertia. Where possible, assemblies using the same number of large inertia discs were grouped together to reduce the longer amount of time required to change these large discs. However, "A" and "B" replicates for a given vehicle were still kept separate in the matrix, and the vehicle order was not "sorted" by inertia (i.e. vehicles may be grouped together with a common number of required large discs, but the vehicles weren't ordered by ascending or descending number of discs).

The reference tests (of the F-150) were interspersed regularly throughout the testing program. One tunnel blank was conducted at the start of the program, and the other was conducted around two thirds of the way through the program. The complete test matrix, along with the dates of each test, is presented in Appendix F.

Procurement of Test Components

LINK began procuring brake parts once the test matrix was finalized. LINK procured OES components from local dealerships. Aftermarket components were prioritized based on sales levels and availability for non-asbestos organic (NAO) and low-metallic (LM) friction materials. The aftermarket components included several products acquired from Bosch, Wagner, Autozone, and RockAuto.

LINK Test Laboratory Setup

The LINK test laboratory that was used for this project is built around a constant volume (i.e. air velocity) sampling system that operates in a closed-airflow circuit. The cooling and airflow rates are fixed for a given test. The airflow through the test enclosure provides the sampling medium for emitted PM as well as the cooling flow for the brake assembly. The sampling airflow is filtered using HEPA filters after passing through the climate control unit and before entering the brake system enclosure. Figure 18 contains a schematic of the LINK laboratory layout that was used for this test program.

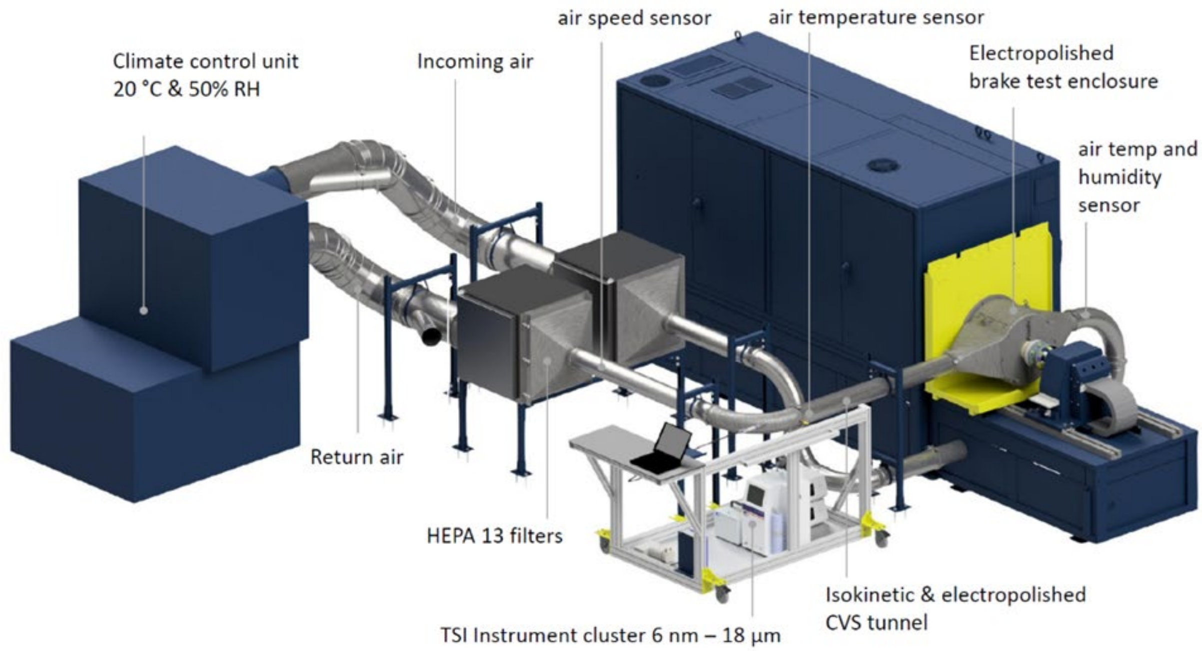

Figure 18. Schematic of LINK Laboratory Setup

The cooling air was controlled to stable temperature (within ± 5°C) and held to a relative humidity of 50 ± 10%; this helps ensure a stable set of conditions when the particles enter the sampling train (between the aspiration position and the point of sampling). The LINK system allows for adjusting the airflow rate prior to each test to reflect the cooling rates established during the project for each brake assembly.

The airflow circulating layout involves the use of round ducting in stainless steel, with internal electropolished finish, with minimal constrictions and at least 8 diameters without disturbances between the brake assembly enclosure and the point of sampling. The sample duct is oriented horizontally, and samples are taken at the point of entry of flow into the 90° elbow downstream of the brake enclosure. Sampling is performed using four separate sampling lines, each originating from an isokinetic sample nozzle arranged in parallel at the upstream end of the sampling elbow. The sampling lines and instrumentation are described later in this document.

From the brake assembly enclosure to the sampling instrumentation, the layout is designed to minimize aerodynamic losses with minimal bends and constrictions. These design characteristics are intended to minimize turbophoretic losses, gravitational deposition, diffusion, and aspiration at the nozzle. Sampling is performed isokinetically (0.95 to 1.15 isokinetic according to ISO 9096) to avoid skewing the particle size distribution data. A transport time of less than 5 seconds from brake assembly to instrument is specified (with a target transport time of 2 seconds) to minimize potential changes in size distribution due to coagulation. In addition, the short transport time will allow the particle size distribution to be closer to the actual distribution as-generated by the friction surface. A photograph of a brake rotor installed in the test enclosure is presented in Figure 19.

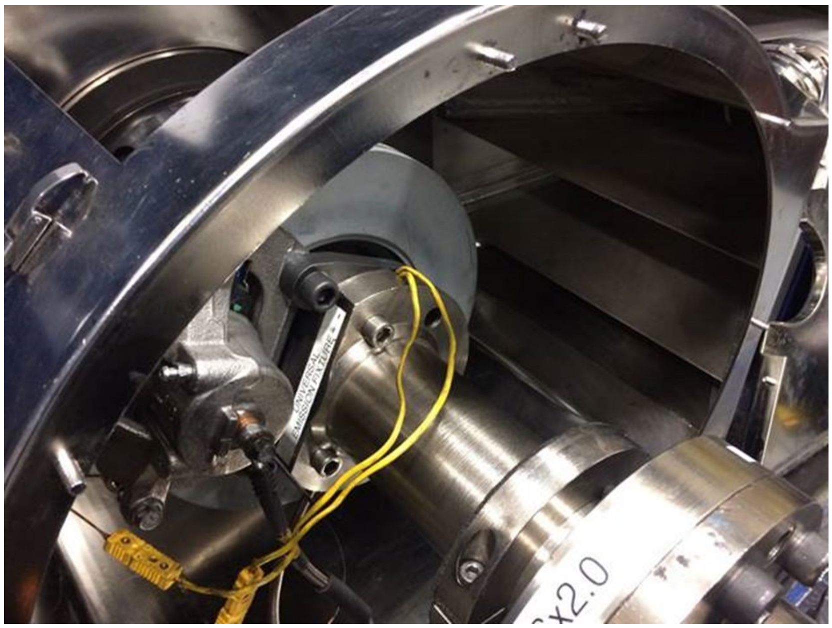

Figure 19. A brake rotor installed in the LINK test enclosure.

CVS Loop Cooling Airflow Setting

The air flow rate through the sampling chamber was set at different rates for the front and rear assemblies of each different test vehicle. The air flow rate was set in an attempt to best match the cooling that takes place in real-world operation, given that the flow rate must stay constant during a test to allow for constant volume PM sampling. During track testing, LINK logged temperature data for the front and rear assemblies of each of the six test vehicles when operating over the WLTP-Brake cycle driven on a test track. This data was used to determine the dyno cooling air flowrate for testing over the new CBDC.

Because all test vehicles were operated over the WLTP-Brake cycle on the test track with temperatures logged, this data was used as a source for flowrate setting. ERG and LINK selected a subset of the 10 WLTP-Brake trips that was most representative of the characteristics of the CBDC, and these were used to set the flowrate to best match the track temperature over the same subset when operating on the dynamometer. To select the WLTP trip or combination of trips to use for setting flow rate, ERG analyzed each WLTP trip in terms of distributions of the same parameters used during test cycle selection: deceleration rates, speed, brake event duration, temperature, and braking energy. From this, ERG determined that WLTP trips 1, 2, 5, and 10 were most similar in the above five parameters to the CBDC test cycle. As an example of the type of distribution that ERG reviewed, Figure 20 presents a cumulative distribution of modeled brake temperature for the Camry over the braking events of the CBDC and the 10 different trips of the WLTP-Brake.

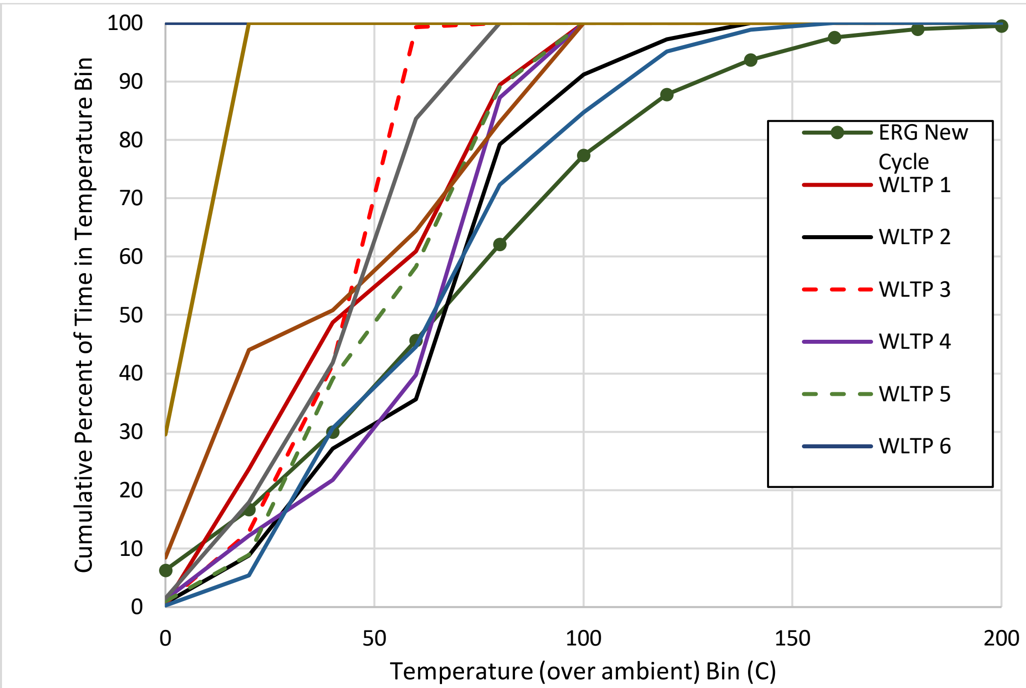

Figure 20. Cumulative distribution of brake temperature over ERG's New CBDC (Modeled) and the 10 trips of the WLTP-Brake (on track)

ERG then investigated the same distributions for various combinations of the four best-matching trips (1, 2, 5, and 10). This was done by comparing the sum of squares differences between the different trip combinations and the CBDC for the five parameters of interest. ERG determined that trip 10 was the best fit, and the addition of any other trip did not necessarily improve the representativeness. For this reason, LINK used only WLTP-Brake trip 10 for air flow rate setting for each different assembly.

LINK ran Trip 10 on the dynamometer for each brake assembly at three equally spaced flow rate settings. LINK then fit a curve to the average braking temperature at each flow rate and calculated the flow rate that best matched the track test temperatures for each brake assembly. Table 14 presents the flow rate used for all tests of each given assembly over the CBDC test cycle. These values represent the air flow speeds through the sampling duct that LINK found would allow the assembly temperatures to best match the temperatures measured on the test track. The cooling airstream speed was measured 8 diameters downstream of the sampling elbow, complying with the requirement defined in EPA Method 1A (the ducting has the same diameter over this entire length). Temperature plots comparing the measured dynamometer temperatures to the test track temperatures are presented for the front and rear assemblies of each vehicle in Appendix G.

Table 14. The CVS cooling/sample flow settings for each vehicle/axle combination

	Front Axle Flow Speed (kph)	Rear Axle Flow Speed (kph)
Camry	7.5	7.5
Civic	7.5	7.5
Sienna	7.5	7.5
F-150	51	7.5
Prius	28	28
Rogue	7.5	7.5

The different sample flow settings do affect the PM residence time between the brake enclosure and points of mass measurement (either the TSI 100S4 or 47mm filter). Overall nominal residence time varies from approximately 0.7s to 1.2s depending on the CVS flow rate.

Dynamometer Operation

The LINK brake dynamometer simulates the rotation and braking functions for a single brake assembly. The unit can simulate front or rear brakes depending on the brake-fixture assembly and the inertia. The system uses both an electric servo motor and the line pressure of the hydraulic brakes to follow a set speed trace over time. The dynamometer controller balances these two sets of torques based on the programmed vehicle road load and inertia. The inertia is the simulated wheel load at the tested brake corner, and the road load describes the force curve representing the drag on the vehicle across a range of speeds when traveling along a level road. During this work, the EPA-published coefficients from the annual certification reports for each model and model year were used to simulate road load for each test vehicle during brake dynamometer testing.

One significant difference in the operation of the brake dynamometer and a chassis dynamometer is the need to split the braking force between the front and rear brakes. Because vehicle weight is transferred forward during braking, the front brakes are designed to absorb and convert a larger amount of energy than rear brakes. The Society of Automotive Engineers (SAE) standard J2789, *Inertia Calculation for Single-Ended Inertia-Dynamometer Testing*, specifies how this energy split can be simulated.[8] Table 15 depicts the standard percentage torque splits for various vehicle categories for two levels of deceleration and two levels of vehicle loading, gross

[8] https://www.sae.org/standards/content/j2789_201008/

vehicle weight (i.e. fully laden) and lightly loaded vehicle weight (LLVW). Where possible, LINK followed J2789 for the proportioning of brake torque between front and rear assemblies in this work. All braking in the braking test cycles evaluated in this work consist of braking events falling within Low deceleration (< 0.65 g-force) as referenced in the table. One exception to the use of J2789 was made for vehicle types in which, during cooling flow setting, a temperature mismatch was observed between front and rear assemblies for a given vehicle compared to track test data. For example, if using J2789 resulted in the front assembly for a given vehicle running hotter than the track data and the rear assembly running cooler than track data, LINK adjusted the inertia split until the brake temperatures matched the track trends (this was the case for the F-150).

Table 15. Brake Torque Split Percentages Based on SAE Standard J2789

Percent of brake force done by each axle (X and Y values)								
Vehicle type	Fixed Proportioning							
	Low deceleration < 0.65 g				High deceleration > 0.65 g			
	GVWR		LLVW		GVWR		LLVW	
	Front X	Rear Y	Front X	Rear Y	Front X	Rear Y	Front X	Rear Y
Passenger car - FWD	78	28	78	28	80	25	80	25
Passenger car - RWD	78	28	78	28	75	30	75	30
Minivan and crossover	78	28	78	28	75	30	75	30
Pick-up trucks	68	38	63	45	80	25	80	25
SUV-RWD	73	33	73	33	75	30	75	30

Appendix C includes the road load coefficients for each model as well as the by-axle inertia settings programmed into the dynamometer for each vehicle, axle, and test weight combination.

Simulation of Regenerative Braking

The Toyota Prius test vehicle is equipped with regenerative braking, in which some amount of braking energy is converted to charge the vehicle's powertrain batteries instead of converting all energy to waste heat as is the case for the other test vehicles equipped with only the hydraulic brakes. LINK conducted the brake emissions testing for Toyota Prius using their 'DutyCycleRegen' control program. This control program is a combination of two operating principles: Duty cycle simulation to simulate a given drive cycle (ProLINK DutyCycle Program), and the addition of regenerative braking functions.

LINK analyzed the operational accuracy of the 'DutyCycle' program on a ProLINK-controlled inertia dynamometer using the SAE J2951 procedure, *Drive Quality*

Evaluation for Chassis Dynamometer Testing[9]. Table 16 presents the results of this analysis for the three segments of the CBDC for two vehicle assemblies.
The table presents the percent of time the parameter exceeded the control limits as well as the root mean squared speed error (RMSSE) for each segment of the test cycle and each assembly. RMSSE is the actual error as a percent of the maximum allowable error. At the initiation of this program, the PMP inter-laboratory round robin had begun the process of defining thresholds of acceptability for these two error metrics. At that time, PMP members indicated that approximately 10% violation time is acceptable for maximum violation time. The threshold for RMSSE was not yet completely defined, but was expected to be at or below 200%.

The overall error levels for both metrics were acceptable based on the threshold of the PMP inter-laboratory round robin (which assigned a threshold of 100% on RMSSE).

Table 16. Results of SAE J2951 Analysis of the Sienna Front Assembly Operating over the CBDC Test Cycle

		F150 Front			Sienna Front		
CBDC Segment	Duration (s)	Violation Time (s)	% Violation	RMSSE	Violation Time (s)	% Violation	RMSSE
1	8,767	308	4%	77%	578	7%	92%
2	4,011	109	3%	67%	207	5%	85%
3	2,784	77	3%	70%	290	10%	118%
Overall	15,562	494	3%	74%	1,075	7%	96%

The duty cycle program primarily included the following features:

- A dedicated section for burnish, the actual test cycle, and any intermediary cooldown phases
- Import of vehicle speed profiles into the control program using '.csv' file format
- User input window to enter the number of repeats of the test cycle (e.g. number of repeats of the ERG-CARB mini-trips for burnish or the WLTP-brake cycle)
- User input window to enter the vehicle coastdown coefficients to account for vehicle running resistance
- User-interface to enter the regenerative brake system specifications

The regenerative braking activity of the selected Toyota Prius vehicle was simulated using mainly four regenerative brake parameters of the electric motors:

- **Regensim_power**: This is the maximum power that the vehicle electric motors can convert to electrical energy
- **Regensim_Trq_Limit**: This is the maximum torque that the regenerative system can compensate for without any payload on the friction brakes.

[9] https://www.sae.org/standards/content/j2951_201111/

- **Regensim_On_Above**: This is the minimum speed above which the regenerative system can operate at full capacity
- **Regensim_Off_Below**: This is the maximum speed below which the regenerative system cannot provide any braking support and all braking energy is handled by friction brakes.

The following scenario is an example of the function of the regenerative braking control feature. Consider a vehicle with regenerative system parameters shown in the screen capture presented in Figure 21. In addition to the four parameters specific for a vehicle, the program includes a generic parameter Regen_Brk_Trq_Min for additional control on brake actuation times. If set to 0, the friction brake torque may take some time to build as the brake is filled. This causes a delay and / or torque overshoot when the brake finally clamps down onto the rotor.

RegenSim | Safeties | Script | Service Brake | Servo Tuning

Vari	Desc (5 items)	Unit	Value
10080	Regensim_Power	kWatt	5
10081	Regensim_Trq_Limit	lb·ft	368.7816
10082	Regensim_On_Above	mph	6.21402
10083	Regensim_Off_Below	mph	1.2428
10084	Regensim_Brk_Trq_Min	lb·ft	0

Figure 21. ProLINK screen capture of regenerative braking parameters

If a brake application from 50 km/h to 0 km/h requires 200 N·m (368.78 lb·ft) of retarding torque, the graph in Figure 22 shows how the torque would be split between the regen system and the friction brakes at different stages of braking.

- **Stage A**: Power is speed· torque and thus for the first 5 seconds, the regenerative brake torque gradually ramps up as the speed comes down with a regenerative peak power of 5 kW.
- **Stage B**: Regenerative system provides all braking needed from 25 km/h (=5000 W/200 N·m) to 10 km/h (6.2 mph).
- **Stage C:** Once the vehicle speed is below the Regensim_On_Above value of 10 km/h (6.2 mph), the friction brake kicks in and ramps up. At the same time, the regenerative torque ramps down at the same rate. This is called “brake blending”.
- Below the Regensim_Off_Below speed, friction brakes absorb all torque.

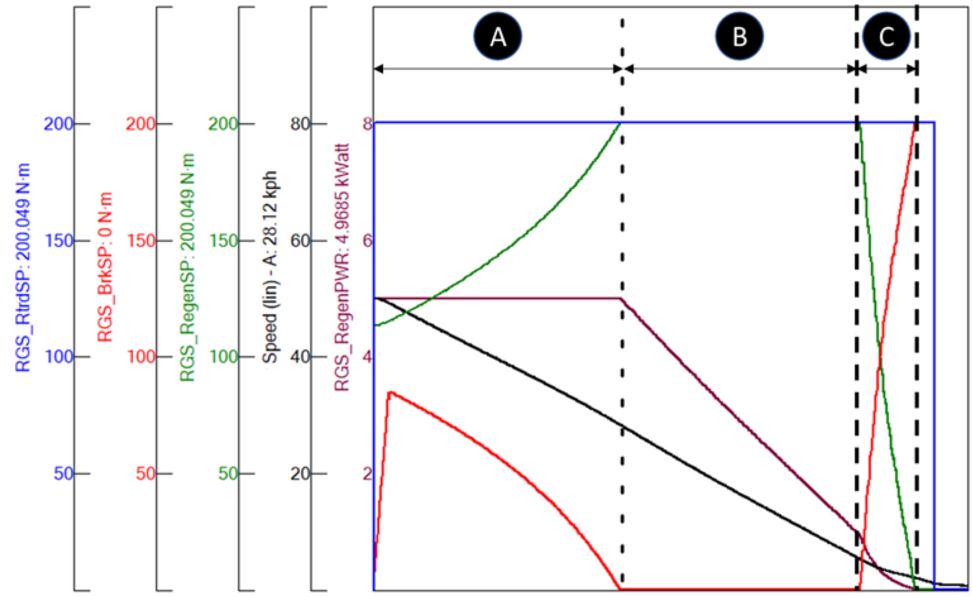

Figure 22. Plot of retarding torque (blue), friction brake torque (red), regenerative torque (green), wheel speed (black), and regenerative power (purple) during a regenerative-equipped braking event.

The original specifications for the Prius regenerative brake system were not available due to non-disclosure policies of the manufacturer so LINK developed preliminary estimates of the regenerative system parameters for the 2016 Toyota Prius Two-Eco vehicle based on previous experience of conducting dynamometer tests for a customer's Prius brake evaluation.

Figure 23 presents vehicle-to-dynamometer comparison plots of brake pressure and total retardation torque for two brake events. These brake events were run on the test track for a range of 0.1g-0.4g deceleration levels. Retardation torque is the combined torque of resistance provided by the friction brake as well as the regenerative motor. Torque was not measured during the track testing as torque wheels were not installed at the time. Instead, the vehicle torque 'Veh Trq' shown here correspond to the values calculated using the deceleration, tire rolling radius, and the wheel load front-to-rear split percent (according to SAE J2789).

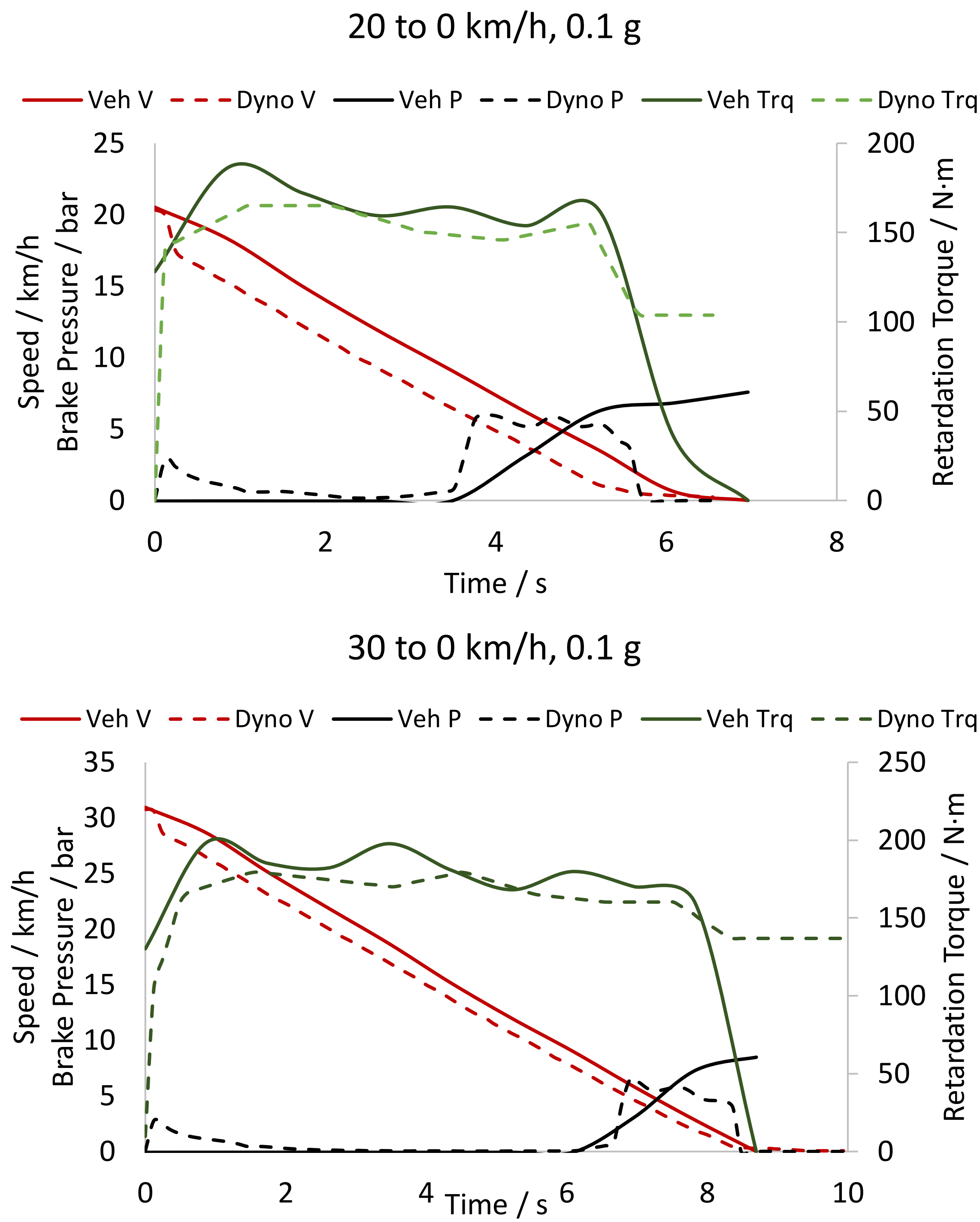

Figure 23. Dynamometer-to-track comparison of velocity, brake pressure, and wheel torque for example regenerative braking events

Torque measured on the dynamometer for a 0.1g deceleration level was within 10% of track-tested calculation. Actuation times of the friction brakes during the dynamometer test match well with the vehicle brake pressure. The Dyno brake pressure (P) was slightly lower than the Vehicle P. A brake event with the duty cycle program starts in a pressure-based control mode (more common in regular brake testing) and then switches to torque mode. This is the reason behind a small spike in brake pressure at the start of brake application on the dynamometer. This spike currently offsets the dyno speed profile with respect to the vehicle speed profile.

LINK refined their regeneration simulation parameters for the dynamometer simulation in the weeks leading up to testing based on continued review of the track test data. This included creating a separate value for one parameter for tests of the front and rear axle assemblies of the Prius. Even though the Prius' regenerative system only acts on the front wheels of the vehicle, the system does affect the demand on the foundation brakes of both the front and rear axles. LINK used the parameters and values in Table 17 for the simulation of the Prius regeneration capacities and speed ranges during all tests of that model's components.

Table 17. Updated parameters used for the simulation of the Prius regenerative braking system on the dynamometer

Parameter	**Front Axle Simulation**	**Rear Axle Simulation**
Maximum Power	2.5 kW	2.5 kW
Maximum Torque	90 Nm	60 Nm
Speed above which 100% regeneration is available	8 kph	8 kph
Speed below which no regeneration is available	3 kph	3 kph

Measurement Instruments

LINK equipped its test laboratory with a variety of TSI instruments for the measurement of PM mass, count, and size distribution. This section describes the capabilities of the various instruments that were used during this program.

TSI 100S4. The TSI 100S4 is the central instrumentation for this project. It has 4 different particle size classifications for the measurement of PM mass. The 100-S4 has an 18 μm inlet stage (i.e. sampling is 18 μm and smaller), which is followed by cut-point stages of 10, 2.5, and 1 μm. The instrument has Micro-Orifice Uniform Deposition Impactors (MOUDI) for the collection of mass at each of these cutpoints. The impactors are followed by a final filter to collect particles smaller than 1 μm. In the 100S4, LINK used coated aluminum impactors, with a glass fiber final filter.

Figure 24. TSI 100S4 MOUDI

TSI QCM MOUDI 140. The Model 140 Quartz Crystal Microbalance (QCM) MOUDI is designed to perform continuous, real-time size-segregated mass concentration measurements of particles smaller than 2.5 µm. The system uses six cutpoint stages at 960, 510, 305, 156, 74 and 45 nm and operates at a 10 L/min inlet flow rate.

Figure 25. TSI QCM MOUDI

TSI CPC. The 3790A Condensation Particle Counter (CPC) is a full-flow design PM particle counter that has a particle size lower detection limit of 23 nm. The unit is designed to linearly respond to particle concentrations from 1 to 10,000 particles/cm^3 and can operate continuously taking 10Hz measurements. TSI indicates a counting accuracy of ± 10%. The PMP has specified the use of this unit as the baseline for brake particle counting without the use of a catalytic stripper or other volatile particle removal (VPR) device. No VPR device was used in this program.

Figure 26. TSI CPC

TSI APS. The 3321 Aerodynamic Particle Sizer (APS) measures the aerodynamic size of particles between 0.5 – 20 µm. The system operates using time-of-flight aerodynamic sizing to determine the particle's behavior while airborne and is unaffected by index of refraction or Mie scattering. The unit also measures light-scattering intensity in the equivalent optical size range of 0.37 to 20 µm. The system offers continuous sampling at 1 Hz.

Figure 27. TSI APS

TSI EEPS. The 3090 Engine Exhaust Particle Sizer (EEPS) is a spectrometer that measures the size distribution of particle emissions from 5.6 to 560 nm continuously at up to 10 Hz. The EEPS provides outputs of size distribution in the above range as well as particle number concentrations down to 200 particles/cm^3.

Figure 28. TSI EEPS

Additional sampling was performed on behalf of EPA through their participation in this project. EPA directed ERG and LINK to perform gravimetric sampling of brake PM during all tests planned in the test matrix in a manner consistent with 40 CFR 1065. Under this direction, LINK conducted parallel sampling of PM captured on 47 mm filters during the tests that were already planned for this work. On behalf of EPA, LINK also collected additional sample on Transmission Electron Microscope (TEM) grids using a Partector device during a large number of tests. When used, this device only sampled for a part of each test cycle (automatically stopping when loaded completely) at a relatively low flow rate compared to the other instruments. These TEM grids were provided to EPA for analysis.

The sampling lines and instruments are arranged as shown in Figure 29. Flow splitters were used to separate the samples in Lines 2-4 into multiple instruments or components. Lines 1-3 provided sample to the TSI equipment described for use for CARB. Sample Line 4 provided sample to the filter equipment installed on behalf of EPA. The four probes were arranged in an equally spaced fashion in a single plane of the sampling elbow. All 4 sample lines were present and operational in all tests in this program.

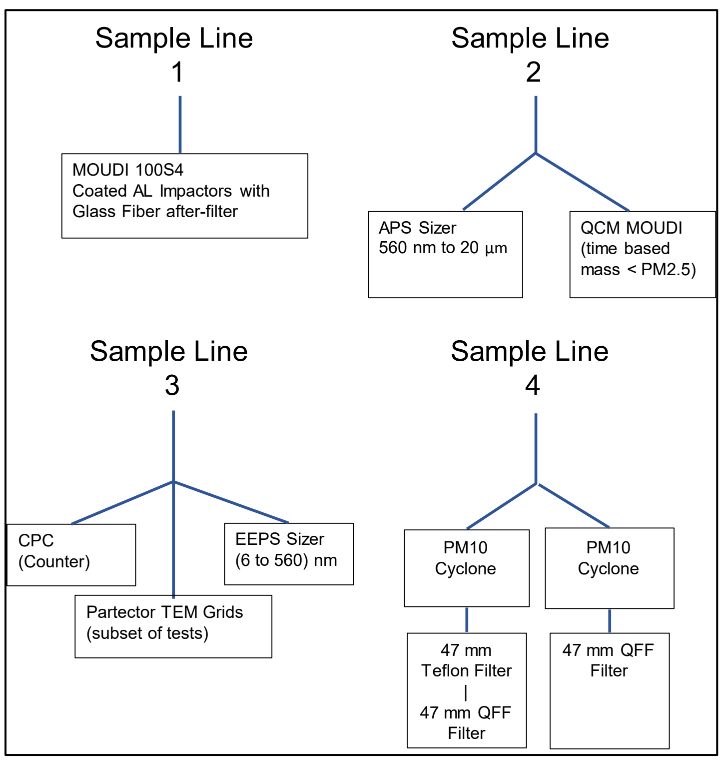

Figure 29. Sample line schematic for this program

Sample line 4 included the measurements added on behalf of EPA. This sample ran through a splitter into two PM10 cyclones. One leg of the splitter fed a 47 mm Teflon filter followed by a 47 mm Quartz fiber filter (QFF). The other leg of the splitter fed only a single 47 mm QFF. To equalize the pressures and flowrates, LINK installed a 47 mm Teflon filter after the lone QFF; however, this filter was not used for any analyses. A schematic of the layout of Sample Line 4 is presented in Figure 30.

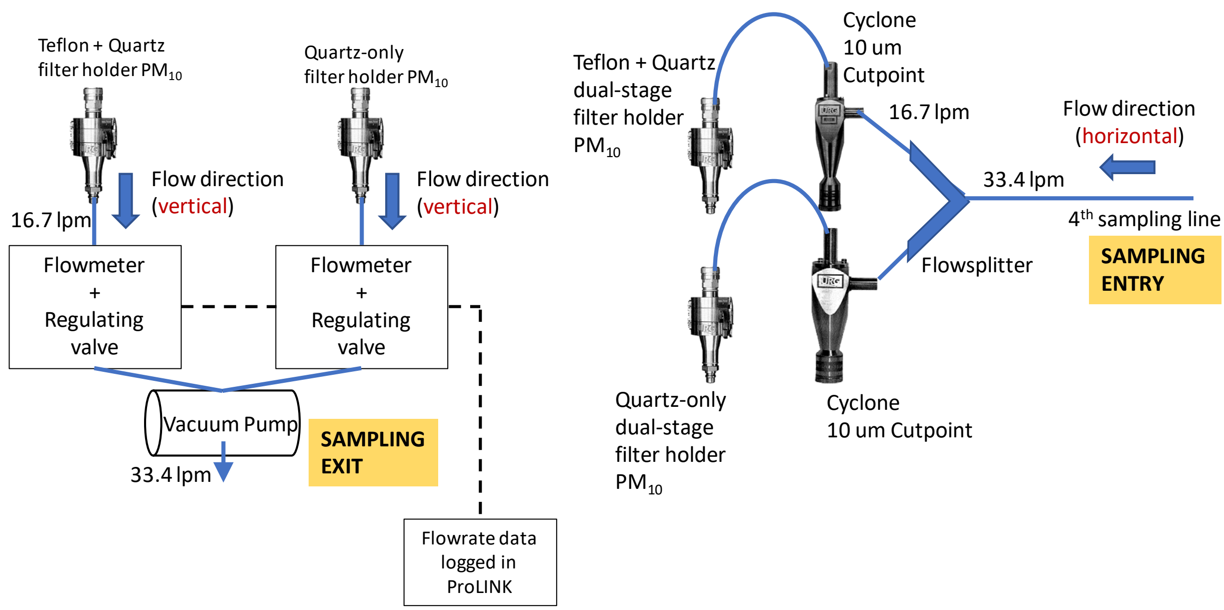

Figure 30. Detail schematic of Sample Line 4

The purpose of each of the three specified filters, along with potential analyses options that could be performed on the TSI equipment media or 47mm filters, is described in Table 18.

Table 18. The various filter media types and the respective analyses for each

Filter Material	Analysis Options
Teflon	• Gravimetric Mass • XRF elemental • ICP-MS
Quartz Fiber (QFF) – Following Teflon	• Volatile Organics that pass through Teflon (artifact collection)
Quartz Fiber (QFF) – Lone	• Particle Phase Organic Molecular Weight Distribution (on initial filters to inform further test types)
Coated AL Impactor	• Gravimetric mass
Glass Fiber	• Gravimetric Mass • Possibly ICP, TBD • No further chemical analysis recommended

In preparation for testing, LINK acquired the Teflon filters for use in gravimetric testing from two sources. Approximately half of the filters were provided by CARB, and half were sourced from EPA NVFEL in Ann Arbor, MI. After the program, each Teflon filter was returned to the organization that provided it for further chemical analysis of the sampled material. EPA also provided all quartz fiber filters (QFFs) for use in capturing sample for later speciation analysis. Details of each filter type are presented in Table 19.

Table 19. The particulate filter types used during testing

Brand/Model	Diameter	Pore Size	Source	Material
Whatman 7592-104	47mm	2µm	CARB	Teflon
MTL PT47DMCAN	47mm	2µm	EPA	Teflon
PALL 2500QAO-UP	47mm	-	EPA	Quartz Fiber

For the TSI 100S4, LINK sourced impactor part number 0100-47-AF, and used silicone spray from MSP, Part #07041. LINK sourced two dual-stage stainless steel filter holders from URG, model URG 2000-30FVT, to collect PM samples on PTFE and QFF 47mm filters. A picture of this filter holder type is shown in Figure 31.
.

Figure 31. Dual-stage stainless steel filter holder for PM10 sampling

Arizona Dust Experiment

Prior to the commencement of testing, LINK evaluated the PM sampling system using Arizona dust as the particulate medium. Evaluations included the particle transport efficiency and system responses to different airflows, brake speed, brake rotation direction, and particle sampling setup. Arizona dust (per ISO 12103-1:2016) was used for these evaluations. The dust was injected at the brake enclosure, travelled through the sampling system, and collected on the 100S4 gravimetric filter. These experiments were conducted prior to the installation of the 47mm filter system, so only the 100S4 was used. Multiple experiments were conducted to determine the recovery efficiency, the repeatability, and the level of detection of the system.

Dust was emitted using a TSI 3410U dust aerosol generator. The generator's feed rate (i.e. dosing speed) was set to 5% and injector pressure was 1.2 bar. Different airflows were evaluated to represent the possibility of covering various axles and vehicle combinations. A brake rotational speed of 45 km/h was chosen to match closely to average speed of WLTP cycle (and later for the CBDC), and a brake speed of 115 km/h was selected as the upper range value as it is equivalent to a typical highway speed. Brake rotation direction is designated viewing from the perspective opposite the dynamometer drive shaft, and both clockwise (CW, airflow opposed to particle exit direction from caliper) and counterclockwise (CCW, airflow parallel to particle exit from caliper)) rotation directions were evaluated. The dust injection duration was 3 minutes for each experiment. Table 20 presents the values that were tested during the Arizona dust evaluation.

Table 20. LINK Arizona Dust Test Parameters

Airflow (m^3/h)	500, 900
Brake speed (km/h)	45, 115
Brake rotation	CW, CCW
Sampling elbow	3-nozzle, 4-nozzle

Figure 32 shows the test setup for the dust injection experiments. Brake pads were not installed inside the caliper to avoid possible emission of particles from brake drag (rotor and pad surface interaction).

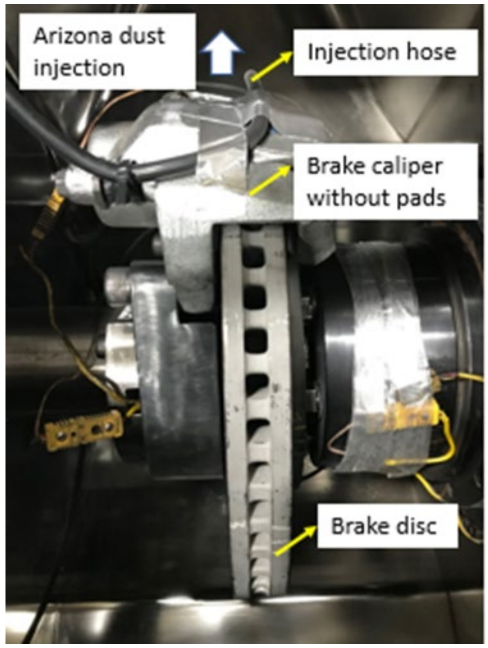

Figure 32. Brake assembly for PM system evaluation with Arizona dust

LINK utilized the 100S4 and APS to evaluate the test results. Figure 33 presents the mass collection results of two replicate tests (Test #67 and #68) for 500 m^3/h airflow, 45 kph brake speed, and CCW brake rotation. The PM system exhibits a collection efficiency (i.e. mass recovered / mass injected) of about 90% with Arizona dust.

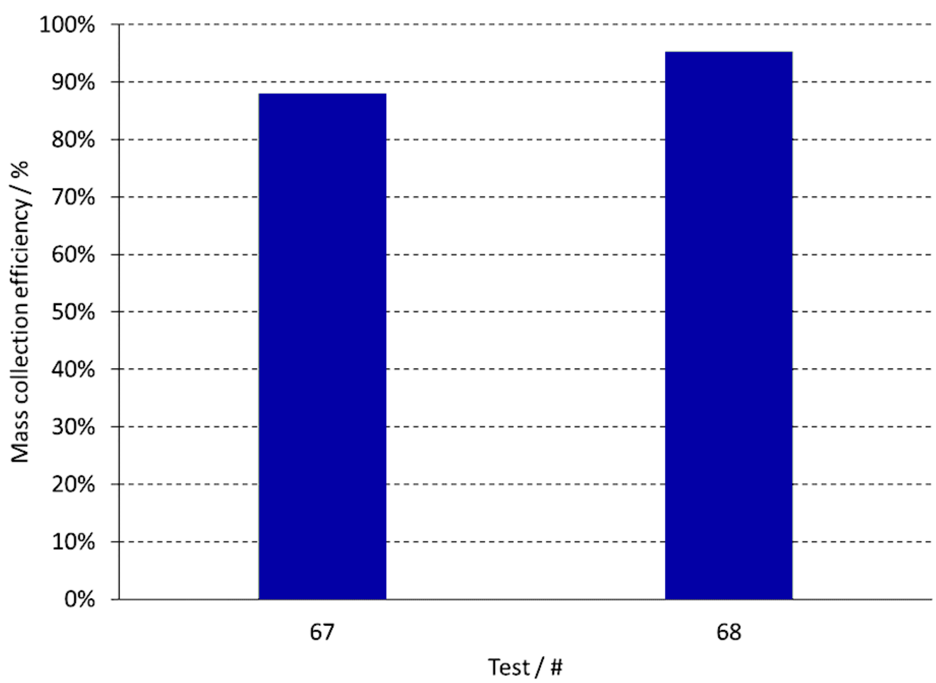

Figure 33. Mass collection efficiency results of two tests of the Arizona dust experiment as measured by the 100S4

Figure 34 compares the particle size distributions (by count) of these replicates, measured using APS, with the values calculated from computational fluid dynamics (CFD) simulations for various particle sizes. These CFD simulations were supervised by LINK staff and included a simulation of particle-laden airflow inside the brake enclosure and the sampling system. Details of this study can be found in the technical paper SAE 2019-01-2139, *Design of Experiments for Effects and Interactions during Brake Emissions Testing Using High-Fidelity Computational Fluid Dynamics* [10]. Probed locations for particle count in the CFD study are at the enclosure exit (inception), nozzle upstream (8D Duct), and inside the nozzles. Predicted particle counts (based on the Arizona dust size distribution) match well with the measured profiles. Also, particle count profile is seen to be very similar in nozzles 1, 2, and 3. This latter result indicates that the PN measurements are independent of sampling nozzle location radially along the duct cross section.

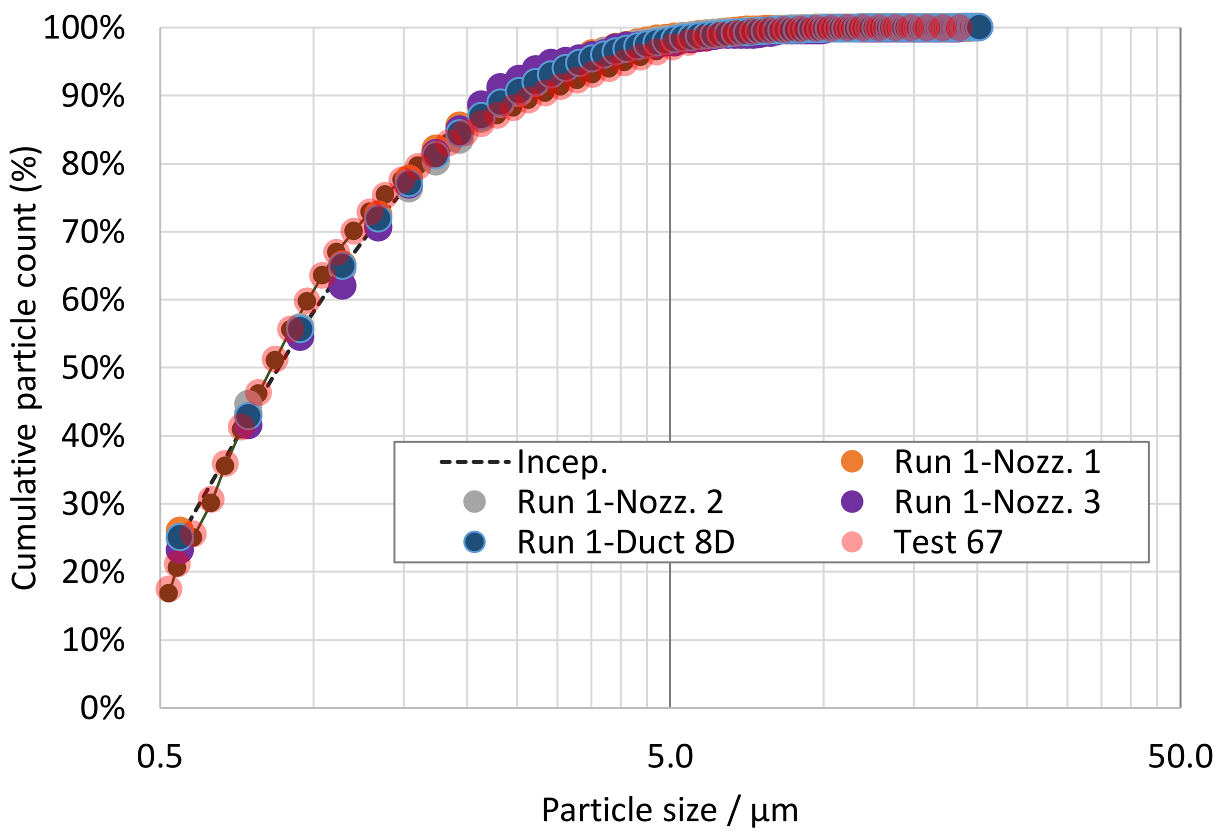

Figure 34. Simulated and measured cumulative particle count at different locations of PM sampling system

[10] Agudelo et. al., "Design of Experiments for Effects and Interactions during Brake Emissions Testing Using High-Fidelity Computational Fluid Dynamics," SAE Technical Paper 2019-01-2139, 2019, https://doi.org/10.4271/2019-01-2139.

Figure 35 presents a graphical representation of the main effects for PM mass emission rate after correcting for duct airflow (duct-to-sampling flow correction) in the Arizona dust experiment. Brake rotation direction showed significant variation in PM mass rate, with high values with counterclockwise (CCW) direction. Sampling setup, airflow, and brake speed did not have noticeable effect on the PM mass rate. LINK conducted all brake emissions tests using the CCW direction for brake rotation as default because that direction resulted in higher measured PM mass (i.e. a higher collection efficiency) during the Arizona dust evaluation.

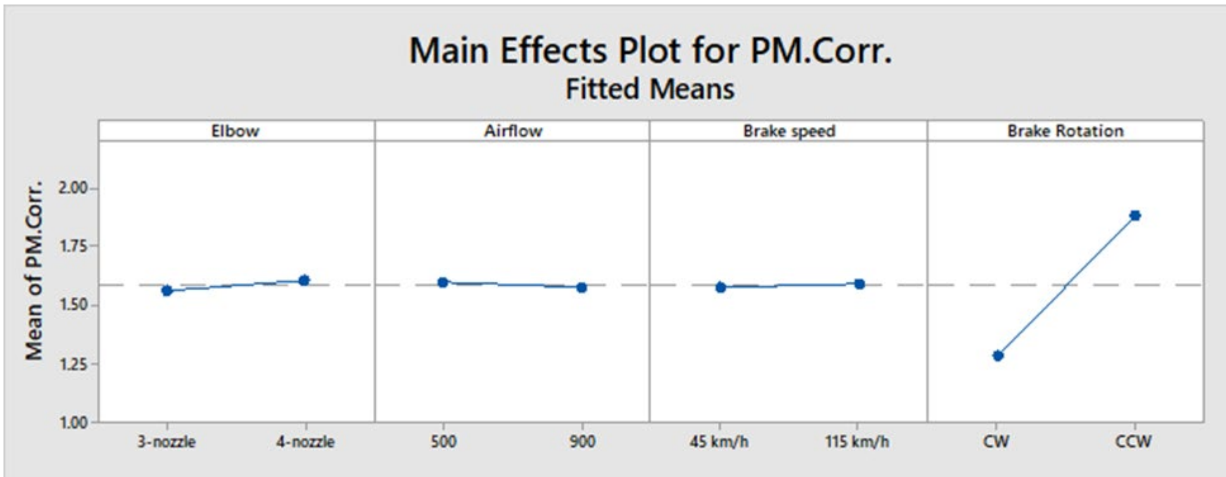

Figure 35. Graphical plot of the PM response to the parameters of the number of sampling nozzles, airflow rate, brake rotational speed, and brake rotational direction during the Arizona dust evaluation

Test Procedures and Quality Assurance Processes

Test Day Steps. One project goal was to be able to complete each test and turnaround in less than 24 hours. The following is a summary of the steps that were taken during each test day along with the estimated time required for those requiring a significant duration:

- Take the dimensions, weights, and pictures of the brake components before the test (15 min)
- After the removal of the previously-tested components, project staff clean the mounting hub as well as any debris that was deposited on the base or walls of the sampling enclosures. (15 min)
- The next test components are installed. On some days, the same caliper and adapter was used from the previous day. During all other days, the complete adapter and caliper was removed and replaced with the components used for the next test. After installation, the hydraulic system is bled of air. (30 min – 1.5 hrs)
- Install the correct isokinetic nozzles for the cooling airflow rate corresponding to the tested brake components

- Record pre-test background air data and then start the CBDC (California Light-Duty vehicle) burnish cycle to bed the friction materials together (approximately 11.5 hrs)
- Monitor the dynamometer and emission data recordings. PM mass was not measured during burnish. To protect from excessive amounts of brake dust noticed in some cases, CPC was turned off during burnish for one of the two replicates of the test matrix
- Record post-burnish background air data. Review burnish data after the cycle is complete.
- Clean the inlet cyclones of EEPS and CPC (whenever used during burnish)
- Take the QFF from freezer to the weighing room for 1 hr stabilization
- Weigh the pre-conditioned coated aluminum, glass fiber, and PTFE filters. PM Weighing is done only if the room temperature is within (22±1) °C and the dew point is within (9.5±1) °C.
- Turn on the QCM unit and install the sampling filters/media in the 100S4 stacks and 47mm particulate mass sampler (PMS) filter holders
- Connect 100S4 and PMS to the dynamometer system
- Run the CBDC brake emissions cycle (4.5 hrs)
- Upon test completion, perform data quality assurance test to check for any defects as defined in the Quality Assurance Project Plan (QAPP for EPA Work Assignment 1-04)
- Remove filters and media and return to weighing room for stabilization
- Remove brake assembly after the data passed the quality test (15 mins)
- Take the dimensions, weights, and pictures of the brake components after the test (15 mins)
- Weigh the post-tested coated aluminums, glass fiber, and PTFE filters.
- Store the QFFs and PTFEs at -20 °C in the freezer

The above schedule required approximately 18-19 hours if no issues were encountered. This allowed a reasonable margin of time to address any problems and with LINK staff working in shifts, the project was generally able to stay on a 1 test per day schedule.

Quality Assurance (QA) of Test Data

Both LINK and ERG staff performed a QA review of the results of each test. LINK completed their internal review first, then data was provided to ERG for further external review.

LINK developed a methodology to check the quality of data for various variables at the completion of each test. These variables include shaft speed (km/h), rotor temperature, cooling air settings, digital emission instruments, and the PM_{10} mass sampler. LINK staff:

- used the GTR15 drive quality regulation to assess the accuracy of the control program in simulating the CBDC test cycle on the dynamometer;
- checked the rotor temperature to ensure there were no loose-wires or defective thermocouples;
- checked that the cooling airflow settings i.e. temperature, relative humidity and air speed, were within the PMP (Particulate Measurement Programme) recommended limits;
- applied certain thresholds for specific channels of APS, CPC, and EEPS, to validate that the data recorded was well above background levels;
- evaluated the PMS flowmeter stability using certain criteria specified based on preliminary runs.

Figure 36 illustrates an example of the software tracking of LINK's quality assurance review for a selected test. It indicates the tolerance range for each parameter and provides a color-coded output indicating the status of the actual value.

Speed Conformity	**Condition**	**%Violation**		**RMSSE**		**PASS/FAIL**
Speed Profile	% Violation ≤ 10% and RMSSE ≤ 100%	0%		25%		Pass
Temperature Metrics	**Condition**	**Min Temp**		**Max Temp**		**PASS/FAIL**
Rotor Temperature	Must be > 15 °C and < 400°C	31 °C		273 °C		Pass
Cooling Air Check	**Condition**	**Trip Avg.**		**%Violation**		**PASS/FAIL**
Cooling Air Temperature	Trip Average within (20 ± 2) % Violation ≤ 15%	21.0		14%		Pass
Cooling Air Speed	% Violation ≤ 15%	7.5		0%		Pass
Cooling Air Humidity	Trip Average within (50 ± 5) %RH % Violation ≤ 15%	50.1		0%		Pass
Instrumentation Conditions	**Condition**	**Engineer Check**				**PASS/FAIL**
CPC	Blob 3 --- Col 3 from 40,000 to 50,000 sec average must be > 50	P				Pass
APS	Blob 2 from 40,000 to 50,000 sec averages --- Col 3 > 20 / Col 25 > 1	P				Pass
QCM	Blob 4 --- Col 7, 9, 11, 13, 15, 17 from 35,000 sec positive trend	P				Pass
PMS	**Condition**	**Min**	**Max**	**Avg**	**ineer Ch**	**PASS/FAIL**
PMS Flowmeter 1 (QFF)	Must be less than 15% fluctuation (14.195 ≤ X ≤ 19.205)	16.1	17.8	16.9	P	Pass
PMS Flowmeter 2 (PTFE)	Must be less than 5% fluctuation (15.865 ≤ X ≤ 17.535)	15.5	18.09	16.2	P	Pass

Figure 36. LINK software example quality review parameters and pass/fail indication

After test data passed the LINK review, datafiles were provided to ERG staff who then took the following steps:

- Cross reference of the test setup parameters as compared to those in the test matrix
- Review of select traces of second-by second data, both during the burnish and during testing
- Review for outliers in various parameters compared to the measurements of other tests. ERG developed a running tracking spreadsheet that would automatically color code outliers in any parameter that differed from other tests by more than two standard deviations- this tool facilitated the data review. In this review, ERG considered particulate mass measured by Teflon filter and by 100S4, particle count, average and peak temperatures, average brake pressure and measured torque, test distance traveled and duration, as well as selected other parameters as applicable.

- ERG reviewed the size distributions from both the aerodynamic particle sizer (APS) and the engine exhaust particle sizer (EEPS) and tracked the peak values for all tests to help track variation in the distributions
- ERG discussed any discrepancies with LINK to determine if any further investigation, explanation, or re-tests were needed

Results

This section presents the results of the brake dynamometer testing that took place during this program. Brake assemblies were tested using a brake dynamometer and CVS system for the measurement of PM. The air flow through the system provided cooling to the tested brake assembly during the test and also served as the medium to carry particulate to the point of sampling. PM mass was measured gravimetrically in batch and continuously. Particulate size and count were also measured continuously throughout each test. Assemblies from six light-duty vehicles equipped with various OES and aftermarket friction materials were tested between September 30, 2019, and January 29, 2020. Eighty-five valid tests (including 2 tunnel blanks) were conducted during this time, including a one-week pause to review the preliminary data after the first two weeks of testing. Appendix F includes the dates that each test in the matrix was conducted.

Where possible, testing was conducted according to the order in the test matrix. In some cases, certain external factors forced LINK to re-order the testing. For example, some of the aftermarket parts that were ordered did not arrive in time to be ready when their test was scheduled to take place. In these cases, the test order was re-arranged, and these tests were inserted into the test schedule once the parts arrived.

The following sections present various test results from this work in graphical and tabular form. Appendix H contains a table of numerical results of all direct measurements for all tests. The table includes the test parameters, gravimetric mass results, condensation particle counter (CPC) results, and some selected operational measurements such as temperatures and brake line pressures. For brevity, some plots or analyses refer broadly to the pads and rotor as the only components; in analyses that include the Civic rear axle these terms are intended to also include that vehicle's brake shoes and drum, respectively.

Operational Parameter Results

This section presents a brief overview of relevant parameters measured over each test day. Test-level averages of three main parameters will be presented, average brake rotor temperature, maximum rotor temperature, and the average brake fixture torque. These values are averaged for each model, axle, and test weight in each of the following figures. Figure 37 presents the average rotor temperature during each test for each model, axle, and test weight combinations. Error bars present the 95% Confidence interval of the mean of all tests of each combination. Similarly, Figure 38 presents the peak rotor temperatures in each test, averaged by model, axle, and test weight.

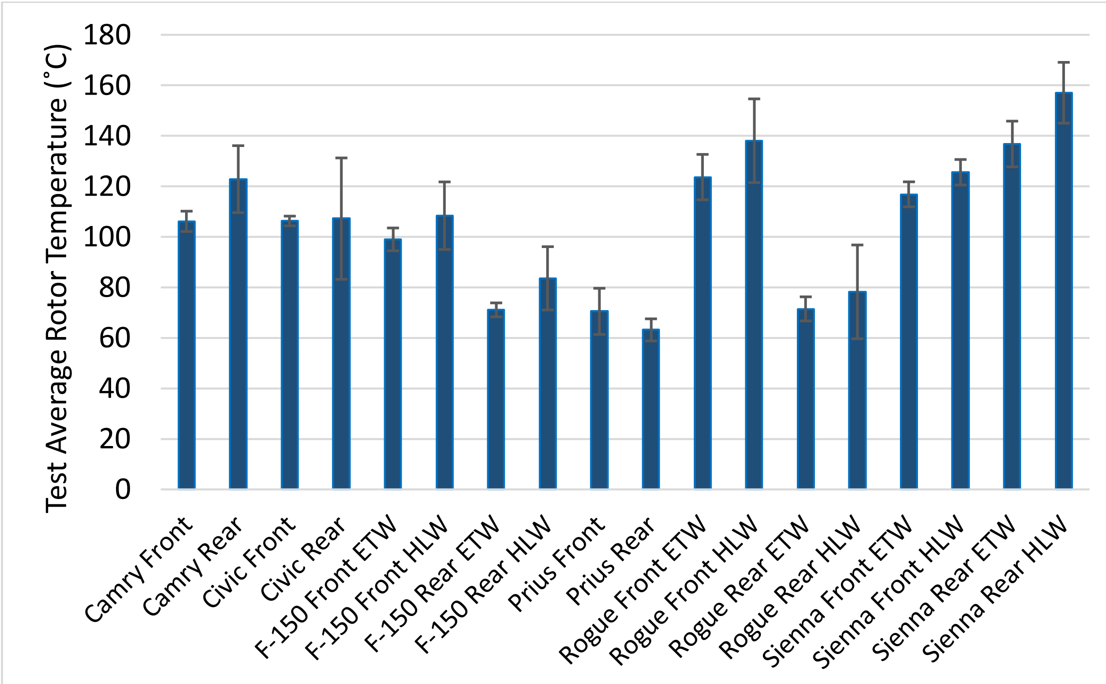

Figure 37. The average rotor temperature over the CBDC, averaged by model, axle and test weight. Error bars represent the 95% confidence interval of the mean of tests

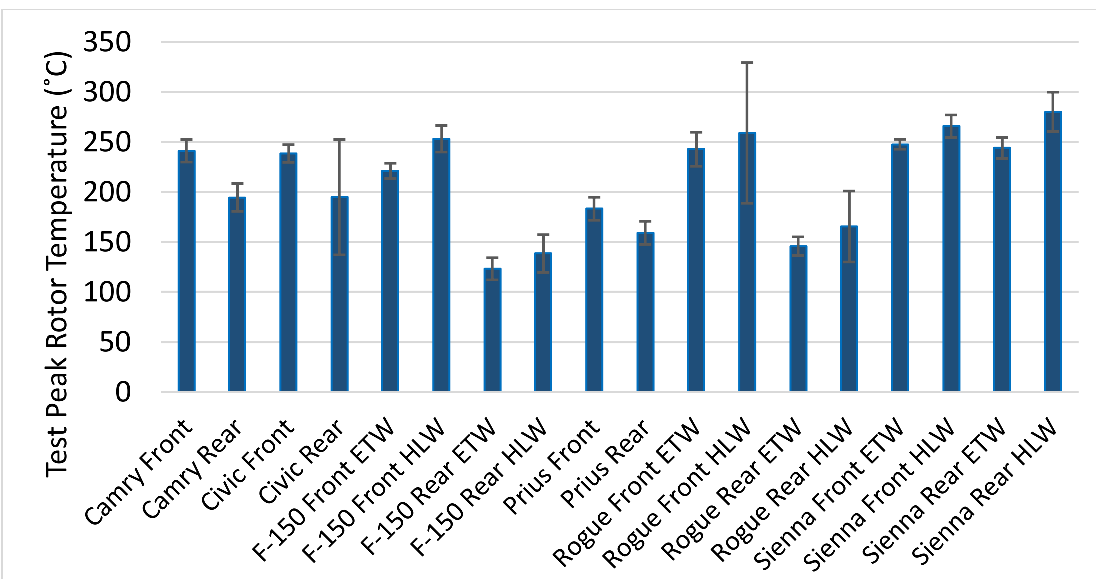

Figure 38. The peak rotor temperature during the CBDC, averaged across tests by model, axle and test weight. Error bars show the 95% confidence interval of the mean of tests

Figure 39 presents the average brake torque measured over each test, and then averaged across all combinations of model, axle, and test weight. The figures in this section are presented to provide some context to the subsequent PM analyses. For example, in terms of brake torque, the F-150 front axle tests exhibited the highest level of braking torque, and the Prius test resulted in the lowest braking torque due to the simulation of that vehicle's regeneration function.

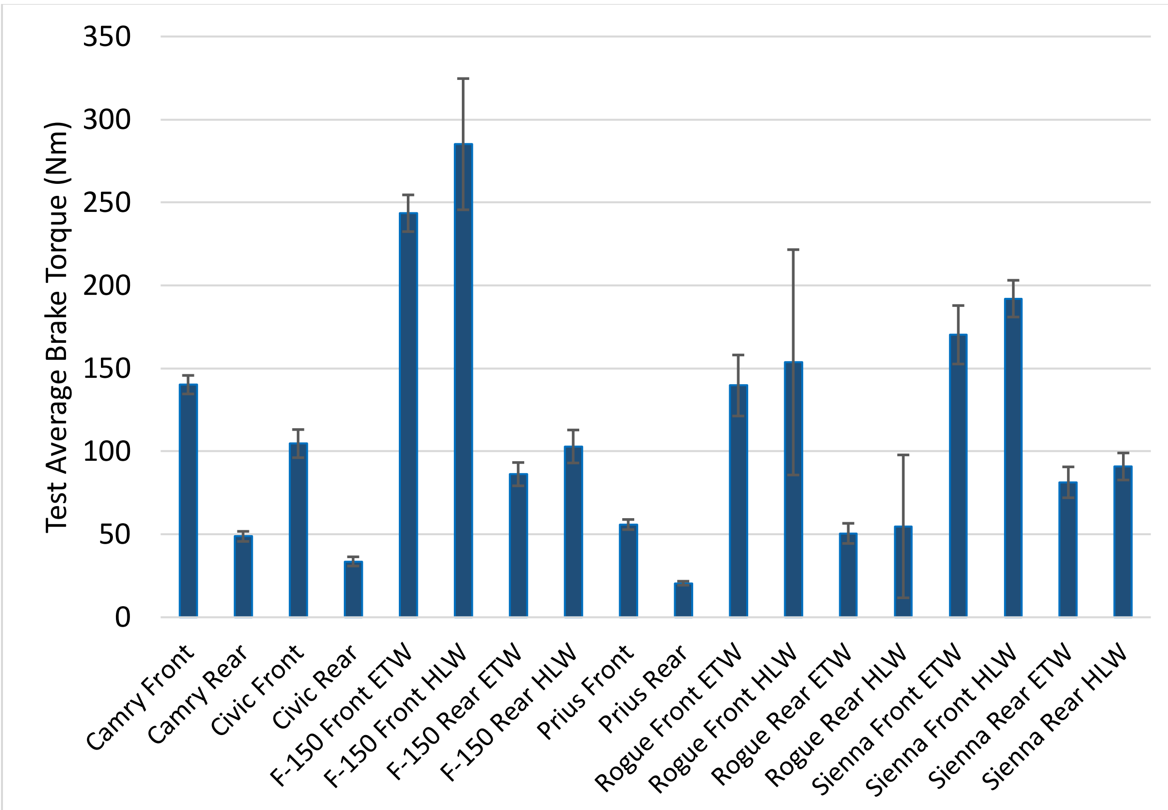

Figure 39. Average brake torque measured during the CBDC, averaged over all tests of each model, axle, and test weight combination.

Batch Gravimetric Results

The highest priority measurements during this project were the various gravimetric PM mass emissions, collected in batch for each test. This section presents those mass measurements, on a by-distance basis, for all tests. Results are shown in bar charts by test vehicle for single-wheel emission rates from front and rear axle assemblies as indicated. The 100S4 stages are shown in the blue bars (the left bar of each test pair) consisting of the three size cutpoints up to PM10. The Teflon filter system sampled PM10 mass and is shown in the green bars (the right bar of each pair). Tests are labeled with the vehicle model and the pad material. All tests can be assumed to be at vehicle mass of ETW tests unless specifically labeled as an HLW test. Each figure depicts front axle results at left, and rear axle results at right.

Figure 40 presents the mass emission measurements for each test of the Camry. Three different pad materials were tested both front and rear. It can be seen that the low metallic pad materials resulted in the highest measured emissions. Figure 41 presents the mass emissions results for the Civic. Both the OES and aftermarket materials tested for the Civic are NAO formulations. Note that the Civic rear brake assembly is a drum; the drum brake geometry is likely the cause of the particularly low emission rate for that assembly, especially for the OES material.

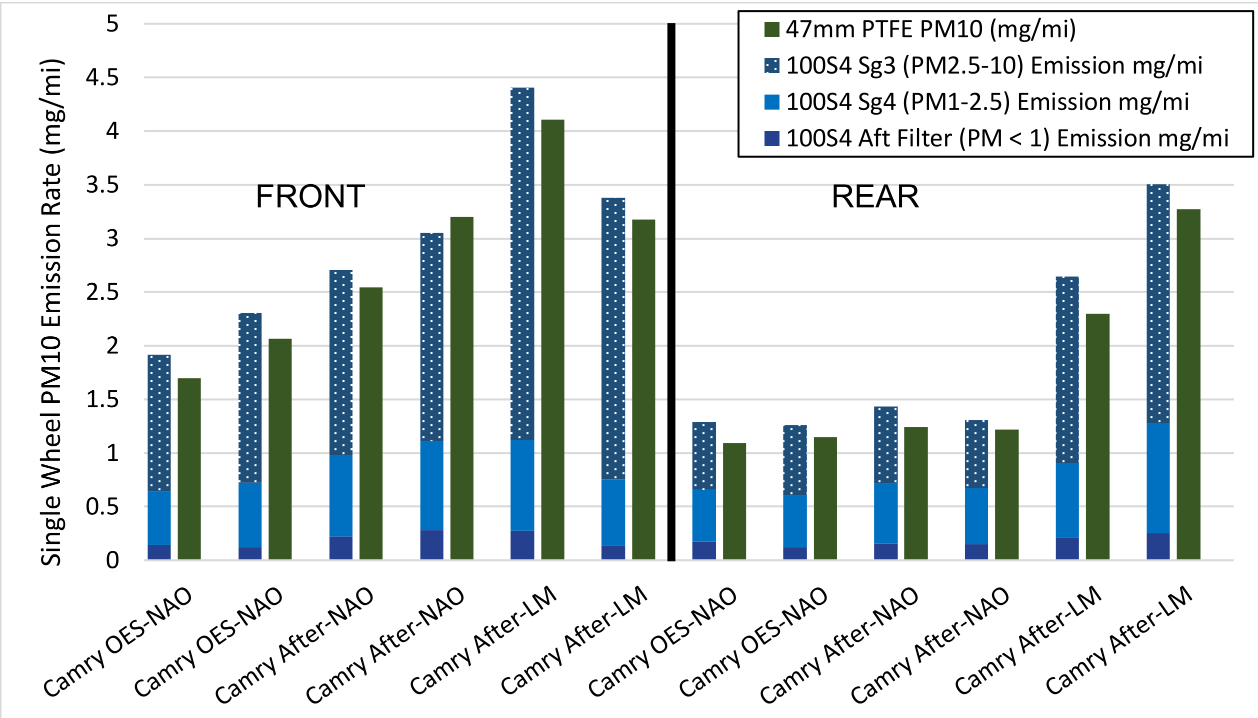

Figure 40. Single-wheel PM Mass Emission Rates for Camry as measured by 100S4 (Blue) and 47mm Teflon filter (Green)

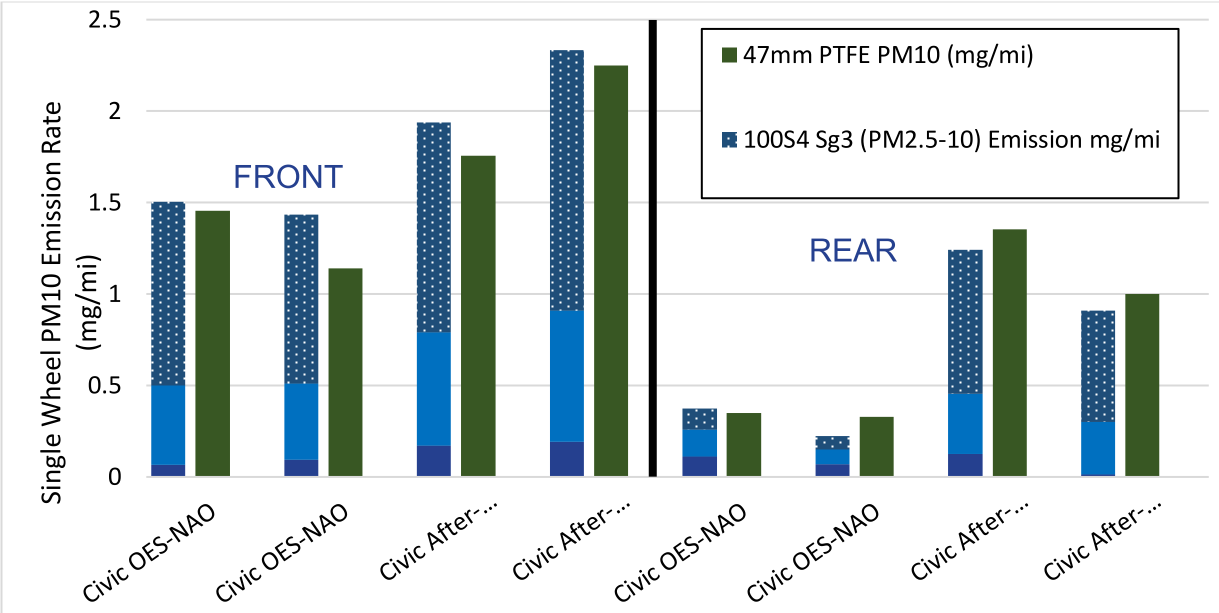

Figure 41. Single-wheel PM Mass Emission Rates for Civic as measured by 100S4 (Blue) and 47mm Teflon filter (Green). Note the Civic rear brake is a drum system

Figure 42 presents the mass emissions results for the F-150. This vehicle was represented in the greatest number of tests because it served as the reference vehicle, was tested with three different friction materials, and was tested at both test weight levels. The PM emissions of the low metallic material was measured at many factors higher than the NAO materials for the front axle assemblies. The various test matrix parameters tested for this vehicle model resulted in the widest range of resulting PM emissions of any model in this program.

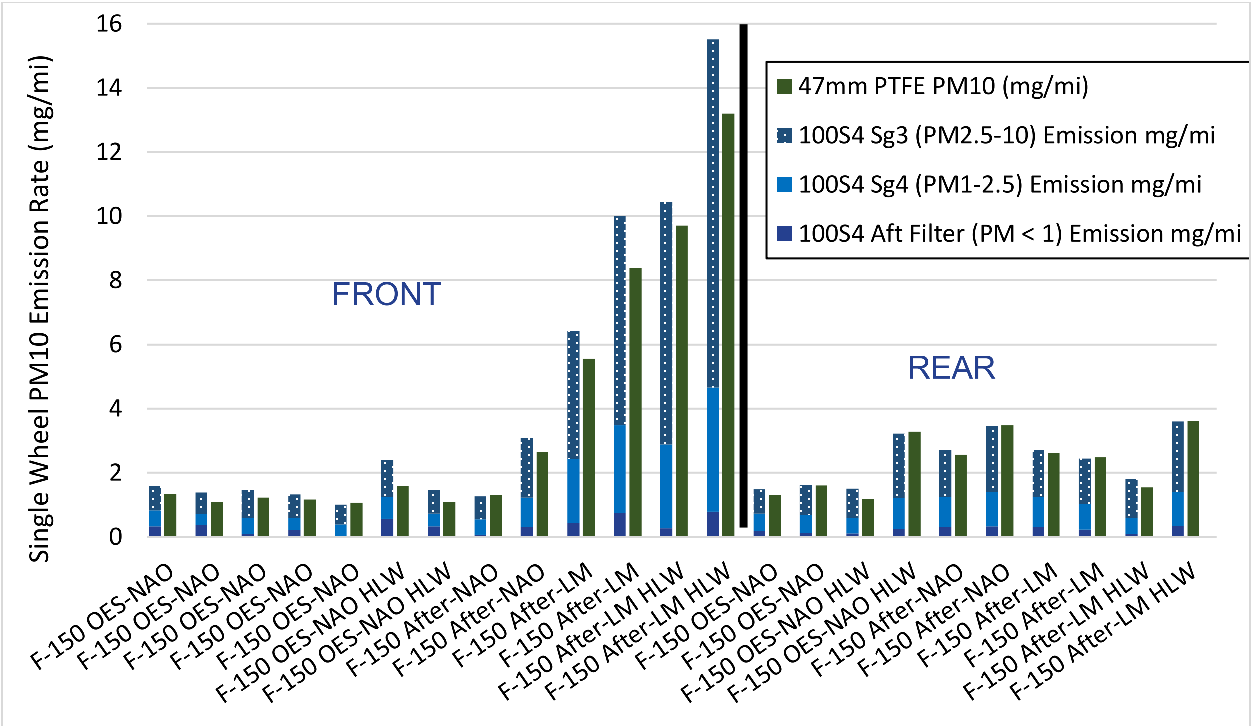

Figure 42. Single-wheel PM Mass Emission Rates for F-150 as measured by 100S4 (Blue) and 47mm Teflon filter (Green).

Figure 43 presents the mass emission rates for the Prius, which was tested with both OES and aftermarket NAO materials. While the Prius has a similar mass to the Camry, the mass emission rate tended to be approximately 50% lower for both the Prius front and rear axles. This is likely to be due to the reduction in demand on the hydraulic foundation brakes caused by the regenerative braking system function.

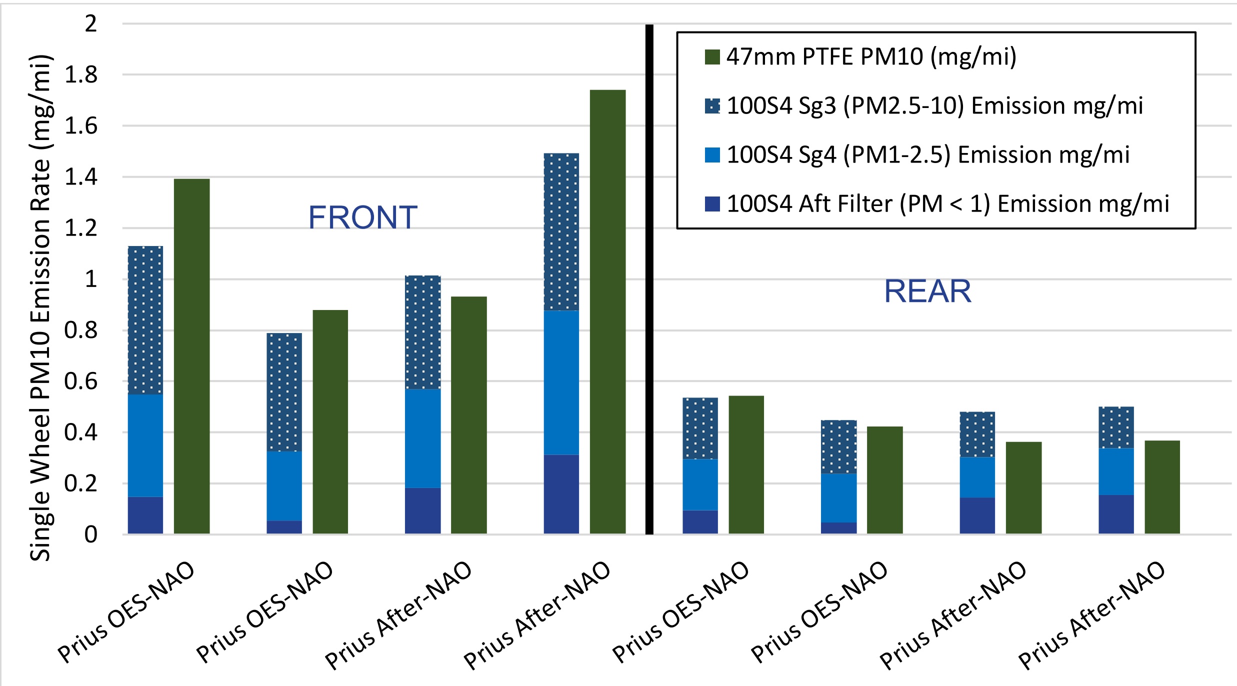

Figure 43. Single-wheel PM Mass Emission Rates for Prius as measured by 100S4 (Blue) and 47mm Teflon filter (Green).

Figure 44 displays the mass emission results for the Rogue, and Figure 45 presents the results for the Sienna. Both vehicles show elevated front-axle emission masses for the HLW tests. For the rear axle, the HLW tests did not result in appreciably higher emission masses, however the Sienna HLW test did result in a higher emission rate than the ETW tests.

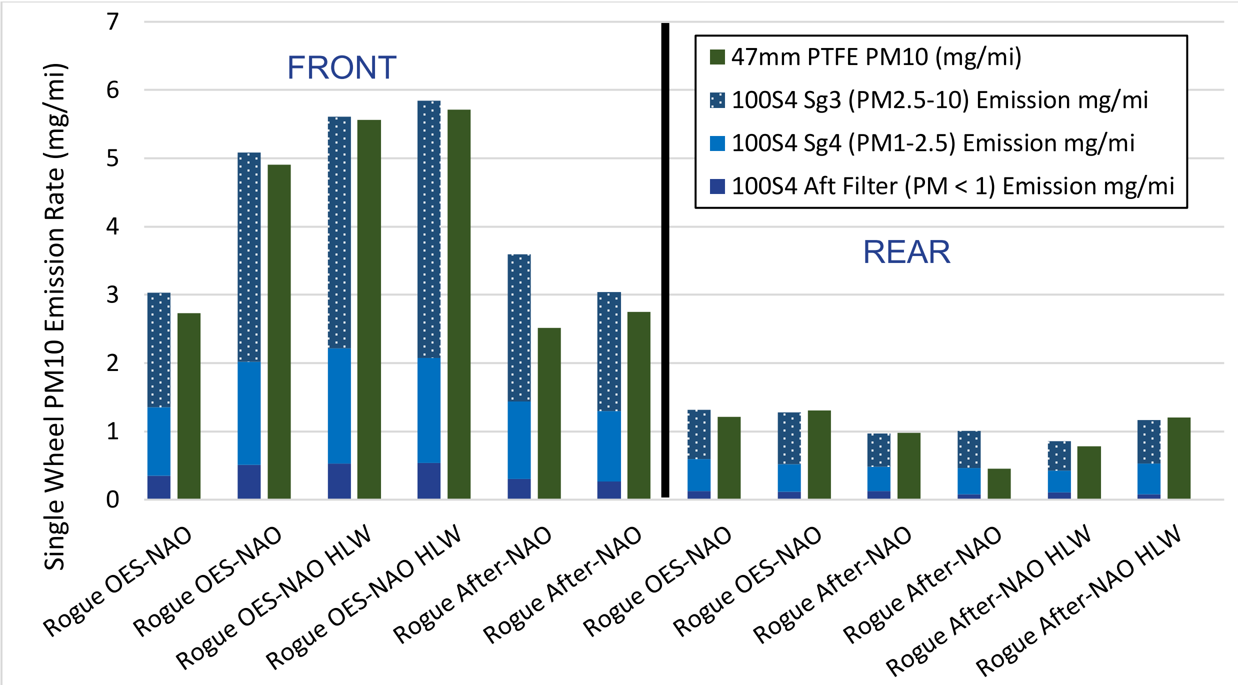

Figure 44. Single-wheel PM Mass Emission Rates for Rogue as measured by 100S4 (Blue) and 47mm Teflon filter (Green).

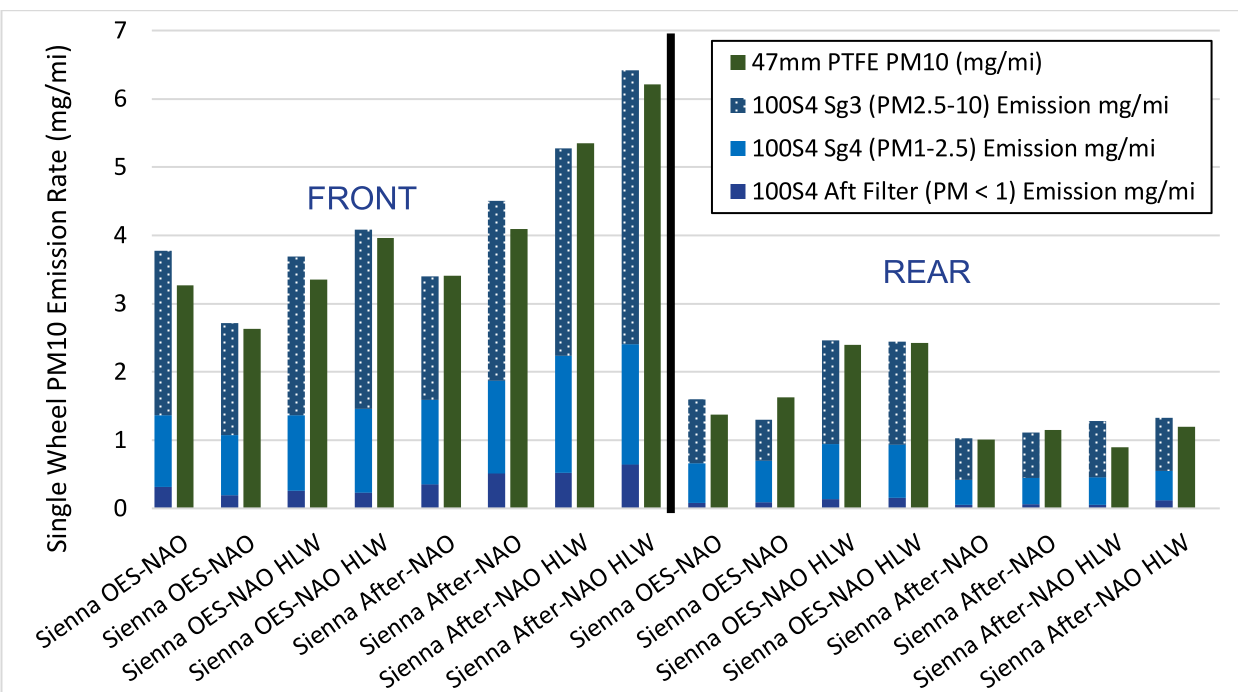

Figure 45. Single-wheel PM Mass Emission Rates for Sienna as measured by 100S4 (Blue) and 47mm Teflon filter (Green).

The previous plots in this section show that the PM2.5 fraction of PM10 tends to range between 0.25 and 0.6. Figure 46 presents the PM2.5 mass emission rates against the PM10 mass emission rate by test as measured by the 100S4. The linear trendline's function is shown on the plot and has a positive intercept; if this intercept is set to zero, the slope is 0.35.

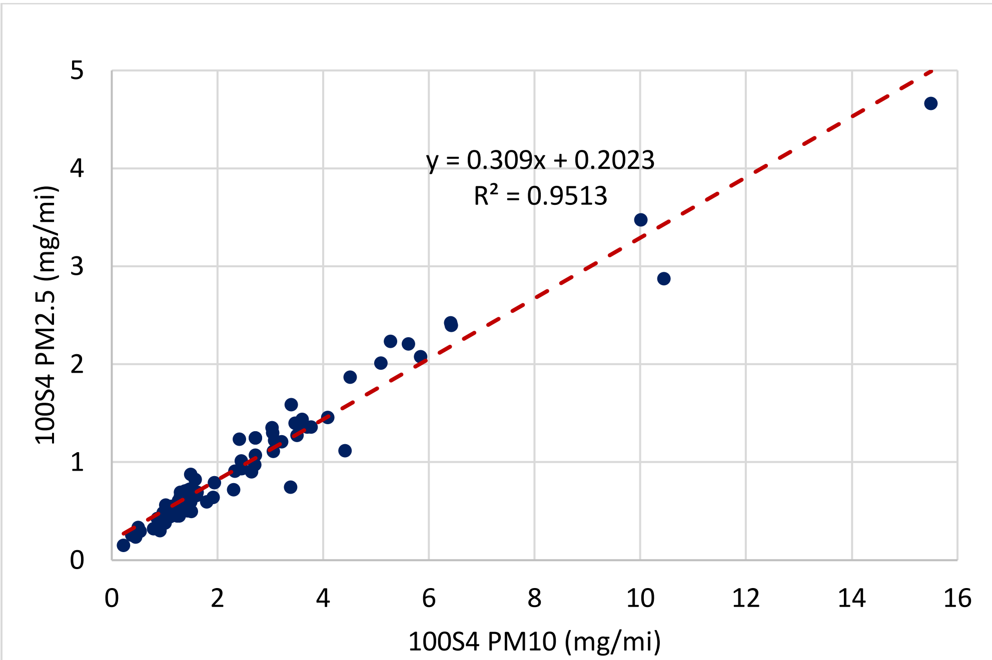

Figure 46. PM2.5 mass emission rate vs. PM10 mass emission rate with linear trendline as measured by 100S4.

As presented in Table 19, two different Teflon filter types were used during testing (generally alternating across each test matrix replicate pair). Appendix I presents the initial and final weights of each filter along with the buoyancy-corrected weight gain. LINK performed buoyancy correction based on the laboratory ambient conditions as per the procedure outlined in 40 CFR 1065.690.

ERG also reviewed the test results against the as-delivered BMC Leafmarks for each pad material. The delivered LM pads all were assigned the letter "A" (the highest copper level). The overall material type appeared to have a larger effect on PM emission mass than the BMC Leafmark; after removing the LM pad tests with elevated emission levels, there was no clear trend between emissions and BMC Leafmark across the OES and Aftermarket NAO tests.

Vehicle-Level Mass Results

Each test measured the PM emissions from a single wheel from either the front or rear axle. This section aggregates the test results to estimate vehicle-level emissions. For a given vehicle model, friction material, and test weight, the average front and rear emissions are added together and doubled to estimate 4-wheel emissions rates for each combination. Results presented in this section use only the PM mass measurements made by the 100S4 system.

Figure 47 presents the vehicle-level PM10 mass emission rates for each vehicle and test weight combination. Values are calculated as applicable for those friction materials that were tested on both front and rear assemblies within each model. Values range from approximately 3 mg/mi for the Prius OES material to nearly 30 mg/mi for the F-150 when heavily loaded with aftermarket low metallic pads.

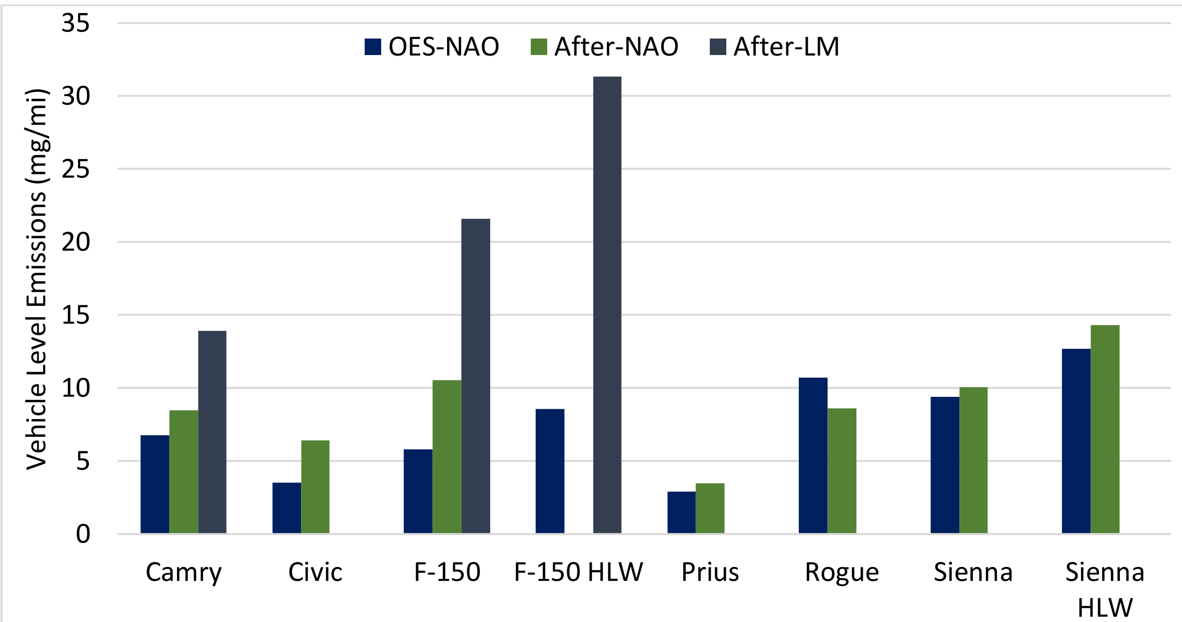

Figure 47. Vehicle-level PM10 mass emission rates for each vehicle, test weight, and friction material combination.

Next, these (along with the corresponding PM2.5) values are aggregated to estimate a single, average, on-road emission rate for each model at each PM size classification. These estimates will be based on the LINK breakdown of in-use pad materials on the road. A single emission value at each size classification for each model will be estimated for potential use as an emission factor in EMFAC. The estimate begins with the data provided by LINK regarding in-use balances of different materials based on their business intelligence. Those surveys involved estimates of pad material balances by vehicle model at 3 years old and 11 years old; those values were averaged to yield a simple estimate at 7 years of vehicle age. The estimated friction material balance by model at various vehicle ages is presented in Table 21. Note that aftermarket low metallic pads are only present in the estimate for those vehicles for which those materials were tested. The OES and aftermarket NAO materials are normalized to 100% for the other vehicles given that the test matrix did not involve testing these material/model combinations. One key assumption was necessary to develop the table; ERG assumed that when brake services are performed on vehicles in-use, that front and rear pads are typically replaced at the same time. This assumption was made based on looking at pad material wear rates as a percentage of total pad mass during each test. Front and rear pads generally lost approximately equivalent percentages of their total weight during the burnish and test cycle.

Table 21. Estimated balance of friction materials by model for vehicles models at 3 and 11 years old.

Age	Model	OES NAO%	AM NAO%	AM LM%
3 years old	Camry	29.8	57.8	12.5
3 years old	Civic	29.8	70.2	N/A
3 years old	F-150	78.8	8.8	12.4
3 years old	Prius	29.8	70.3	N/A
3 years old	Rogue	29.8	70.3	N/A
3 years old	Sienna	29.8	70.3	N/A
11 years old	Camry	22.4	43.6	34.0
11 years old	Civic	22.4	77.6	N/A
11 years old	F-150	59.4	6.6	34.0
11 years old	Prius	22.4	77.6	N/A
11 years old	Rogue	22.4	77.6	N/A
11 years old	Sienna	22.4	77.6	N/A

These values were then used to calculate overall average by-model PM emission rates for these models in the in-use fleet. The values presented in Table 22 are multiplied by the in-use fleet balance to calculate an estimate of in-use emissions for each model and test weight combination at an average age of 7 years.

Table 22. Measured in-use brake emission rates by model, estimated for 7 year old vehicles.

Model	Estimated In-Use PM2.5 Emission Rate (mg/mi)	Estimated In-Use PM10 Emission Rate (mg/mi)
Camry	1.7	9.3
Civic	1.1	5.7
F-150	2.0	9.8
F-150 HLW	2.6	13.9
Prius	1.0	3.3
Rogue	2.0	9.2
Sienna	2.1	9.9
Sienna HLW	2.7	13.9

Results by Vehicle Average Speed

The EMFAC model uses speed correction factors (SCFs) to adjust modeled pollutant emission rates for trips of varying average speeds. The CBDC was developed for this work and is comprised of three different segments representing microtrips falling in average speed ranges of 0-21 kph, 21-69 kph and above 69 kph. The CBDC was designed such that the relative distance traveled in each speed segment approximates the relative distances traveled by all microtrips within each speed range in the Caltrans dataset so that the overall cycle emissions represent real-world driving. So, the test cycle overall is representative of California light-duty driving, but the three speed segments can be used for initial refinement based on three trip average speed bins. However, the measurements from the continuous instruments used in this study can also be analyzed to further resolve differences in emissions by speed bins into smaller-sized speed bins. Analysis on the a basis of more than just three speed bins was desirable for populating EMFAC (the CBDC could not be designed to include more than three distance weighted speed segments as it would have become too long in duration to meet the one test per day goal).

The QCM measures cumulative PM2.5 mass throughout each test and is a measurement that allowed for resolving the changing emission rates throughout each test (the 100S4 and 47mm Teflon systems were used only for total measurements over the whole cycle, not by speed segment). The QCM logged its cumulative collected PM mass once per minute during the test. In this study, the QCM was considered a relative measurement; ERG did not use the absolute masses logged by the QCM for any final test results. This is because the mass values logged by QCM were generally much lower than that measured by 100S4 or the Teflon system; however, the QCM response was reasonably linear when compared to those measurements so the instrument was still determined to be useful for relative measurements. To use it as a relative measurement only, ERG used the QCM results only to develop factors to ratio against the 100S4-measured PM2.5 mass.

The APS was also used to make continuous particle measurements. This unit reported a particle size distribution (0.5 µm to 18 µm) on a second-by-second basis. This tool was useful for estimating particle volume emissions on a by-event basis as well as for estimating the emitted volume ratio of PM2.5 to PM10, which allowed for an estimate of PM10 emission mass based on the PM2.5 mass measurements of the QCM. In general, the APS-calculated PM2.5 to PM10 size ratio agreed reasonably well with the 100S4-measured ratio, which further validated this approach.

This section describes ERG's analysis of the effect of vehicle average speed on emissions based on the following three analysis methods. ERG investigated each of the following three methods and then selected the best method to generate SCFs.

Method 1. Using the QCM to resolve the average emission rates into three bins based on the ranges of the three speed segments

Method 2. Using the QCM on a minute-by-minute basis to resolve all brake events into more than three speed bins
Method 3. Using the APS on a second-by-second basis to resolve the emission rates of each brake event on a particle volume basis into more than three speed bins

Method 1: Using QCM to Generate Three Speed Bins

This method involved using the QCM to determine the percentage of the total test PM mass emitted in each speed segment. These percentages were used to apportion the total 100S4-measured test mass to each segment. The factors were then corrected for the represented distance of each segment to determine emission rates by speed on a per-distance basis.

In this method, ERG used the APS size distribution to also estimate the ratio of PM10 to PM2.5 mass to develop factors to estimate PM10 trends based on the QCM-measured PM2.5 results. ERG took the following steps to perform this estimation using the APS data:

- Gather the APS data that indicates the particle size distribution (by counts) in the range from 0.52-20 μm.
- Assume that particles are spherical, then calculate ratio of PM10 particle volume to PM2.5 volume by summing the total particle volume measured at each APS cutpoint (counts of particles multiplied by the volume of a sphere at that cutpoint's diameter)
- Assume particles have a homogenous density such that mass is proportional to volume. Calculate the ratio of PM10 mass to PM2.5 mass for each speed segment and the overall test.
- Multiply the apportioned PM2.5 masses by each segment's ratio to estimate the total PM10 emitted in each speed segment
- Find the PM10 SCFs by determining the ratio of each segments PM10 to the total cycle PM10.

This method required significant assumptions but did allow for the QCM to be used to estimate the PM2.5 and PM10 masses emitted within each speed segment. Figure 48 presents the overall mass emission trend by speed segment observed when averaging all tests. It can be seen that the 21-69 kph speed segment has the highest per-mile emissions, followed by the low speed segment with moderate per-mile emissions, and the high-speed segment has the lowest per-mile emission rate. The error bars in the plot present the 95% confidence intervals based on the variability across all tests. Figure 49 presents, for the same data, the trend in the PM2.5 mass percentage of PM10 averaged across all tests. At higher speeds, the data indicate that PM2.5 makes up an increasing share of PM10 mass emissions.

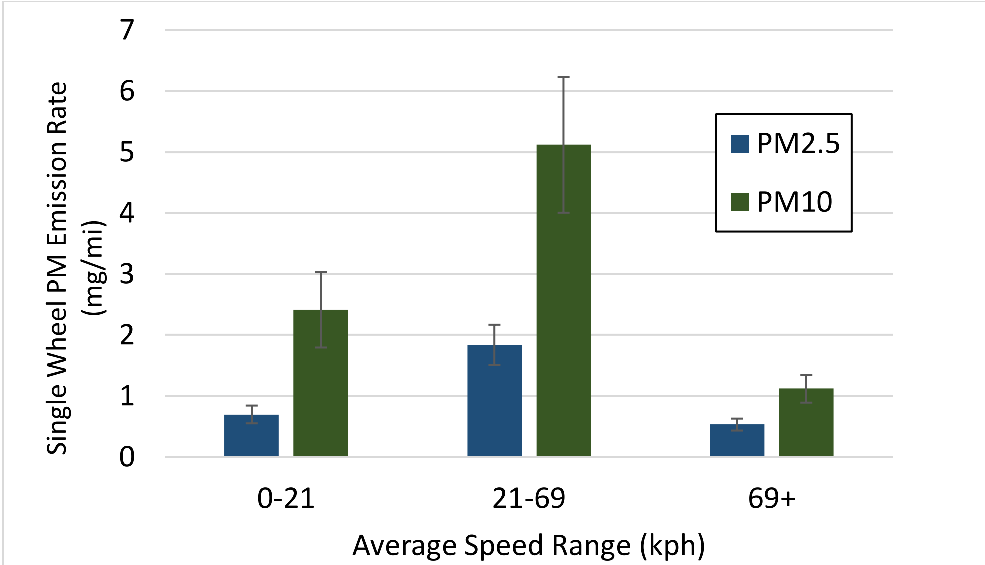

Figure 48. Overall trend in single-wheel mass emission rates over the three different speed segments making up the CBDC overall test cycle (averaged for all tests)

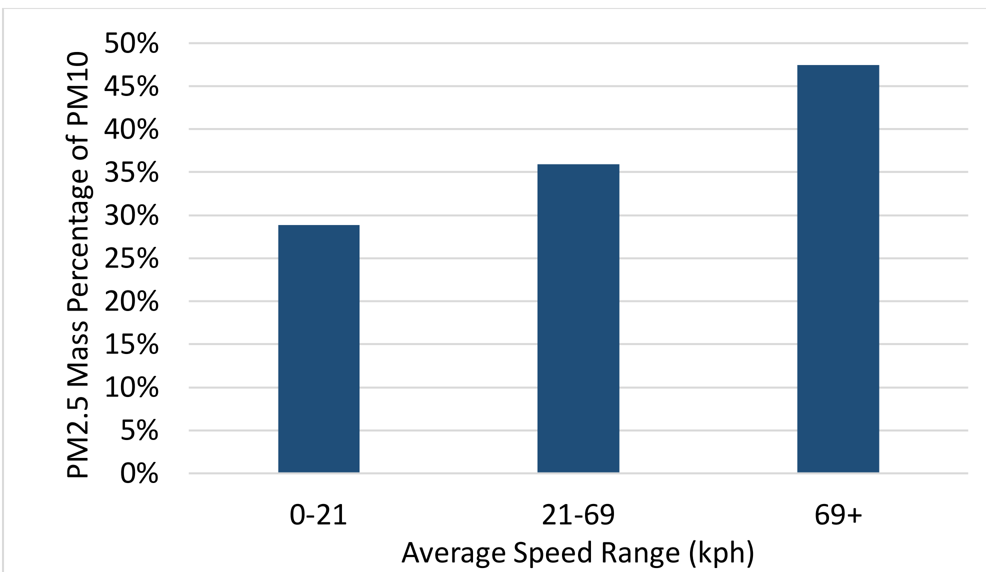

Figure 49. The PM2.5 mass fraction of PM10 for the different speed segments, averaged across all tests.

The speed-based emission results in Figure 48 are not monotonic with increasing speed range. There was discussion among project stakeholders about whether this was an expected result, so ERG further investigated the overall trend presented in the speed segment analysis as a check on the accuracy of that finding. There are some potential factors that confound the agreement between the speed range and emissions, notably the distance represented by each cycle, the number of stops divided by represented distance, the total braking energy divided by represented distance, and the actual duration of braking in each speed segment. Figure 50 presents a bar chart of total braking energy within each speed segment along with the total PM2.5 emission average of all 5 reference tests of the F-150 (axes are scaled differently to determine proportionality). In the high and medium speed segments, the energy and emissions are proportional. In the low speed segment, the relationship trends together (and neither are monotonic) but the energy is high relative to the emissions.

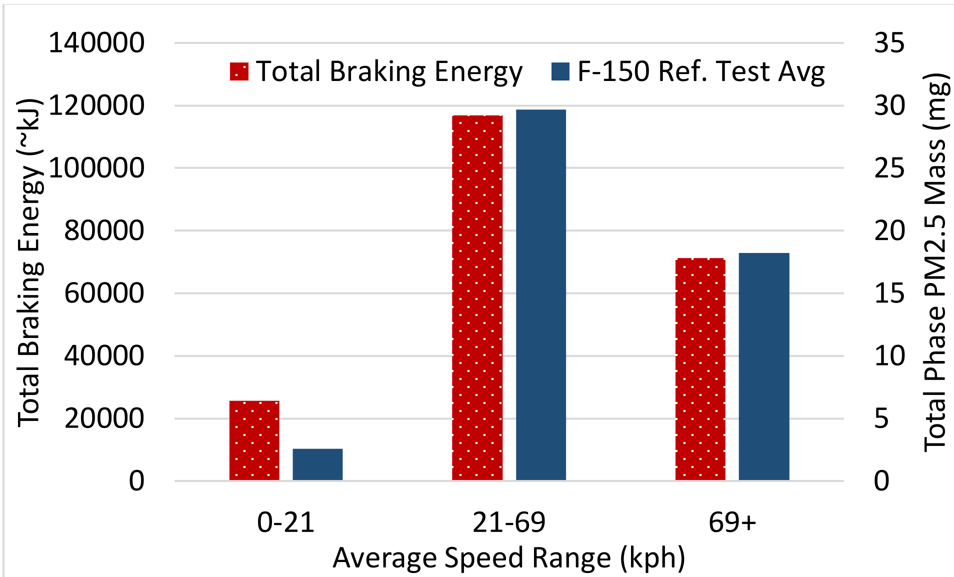

Figure 50. Total braking energy (proportional to kJ) within each speed segment and the F-150 Reference Test Average Total-Cycle PM2.5 emission mass for each speed segment

Figure 51 presents the total PM2.5 emission divided by the total seconds of braking time within each speed segment, averaged over the F-150 reference tests. Presented in this way, the emission measurements are monotonic. A key factor in the interpretation of the SCFs is the cycle-represented distance. Emissions per braking second trend with speed, however accounting for the distance traveled in each speed bin (which is representative of the Caltrans in-use dataset) appears to confound that trend. In general, the investigations presented in Figure 50 and Figure 51 appear to validate the trend in emission rate across different average speeds shown in Figure 48.

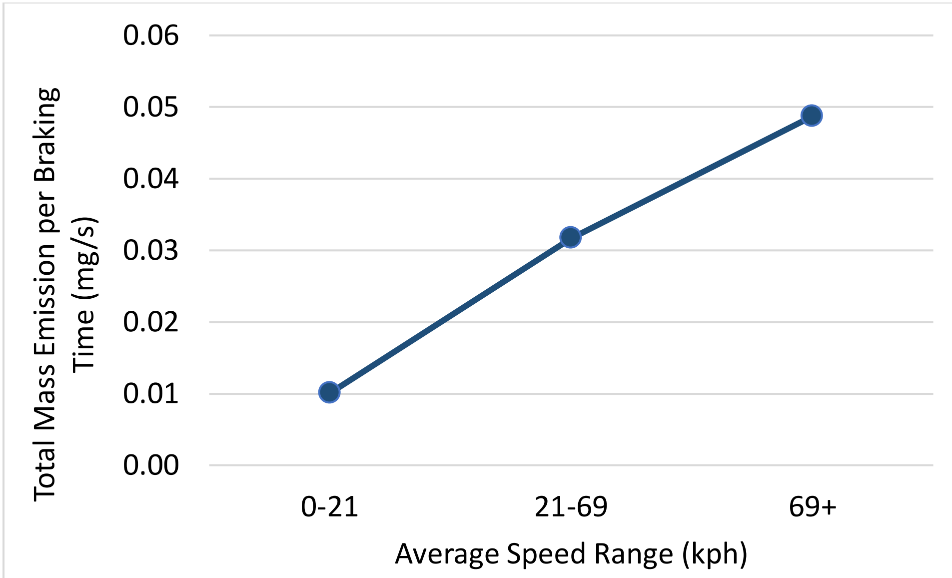

Figure 51. Total PM2.5 emission divided by total braking time in each speed segment, averaged for the F-150 reference tests

Method 2: Using QCM to Generate More than 3 Speed Bins

As a second approach to analyze mass emissions by vehicle average speed, ERG also reviewed the QCM data on a more detailed minute-by-minute basis to potentially increase the speed bin resolution of the analysis. ERG followed the following process for Method 2:

- Note the QCM-logged change in emission mass at each 1-minute interval (the QCM updated its cumulative measurement once per minute).
- Find the mass change of each QCM increment and determine if one or more brake events occurred in the previous minute. If so, determine the total represented distance and the average represented speed for those events. Drop data for minutes that do not contain at least one brake event
- Divide each minute's emission mass by the represented distance of the event(s) in that minute to determine emissions on a per-distance basis
- Bin the emission rate for that minute by the average represented speed of the brake event(s).
- Determine the average emission rate for all minutes in each speed bin on a mass per distance basis
- Determine the overall average emission rate for all minutes containing a brake event, irrespective of speed
- The SCF for each speed bin equals the ratio of the average emissions in each respective bin to the overall average emission rate
- Each SCF will be multiplied by the cycle-level 100S4 emissions to determine the emissions within each speed bin (as with Method 1, the QCM is used only as a relative measurement)

- The APS data was used to estimate the SCFs for PM10 using the same assumptions and procedure as used for the APS in Method 1.

The results of this approach are presented in Figure 52 with the results with different numbers of speed bins presented for comparison (the double line presents the results from Method 1 superimposed over the other Method 2 results). A similar trend to the Method 1 results was observed, with the highest emission rate being associated with medium speeds between 30 and 45 mph. ERG calculated multiple speed bin resolutions to determine which number of bins would be most appropriate for the analysis. It can be seen that the 5 and 7 bin lines are very close to each other. The 14-bin line can be seen to be noisier with oscillations from one bin to the next. ERG selected the 5-bin analysis as the best compromise in bin count.

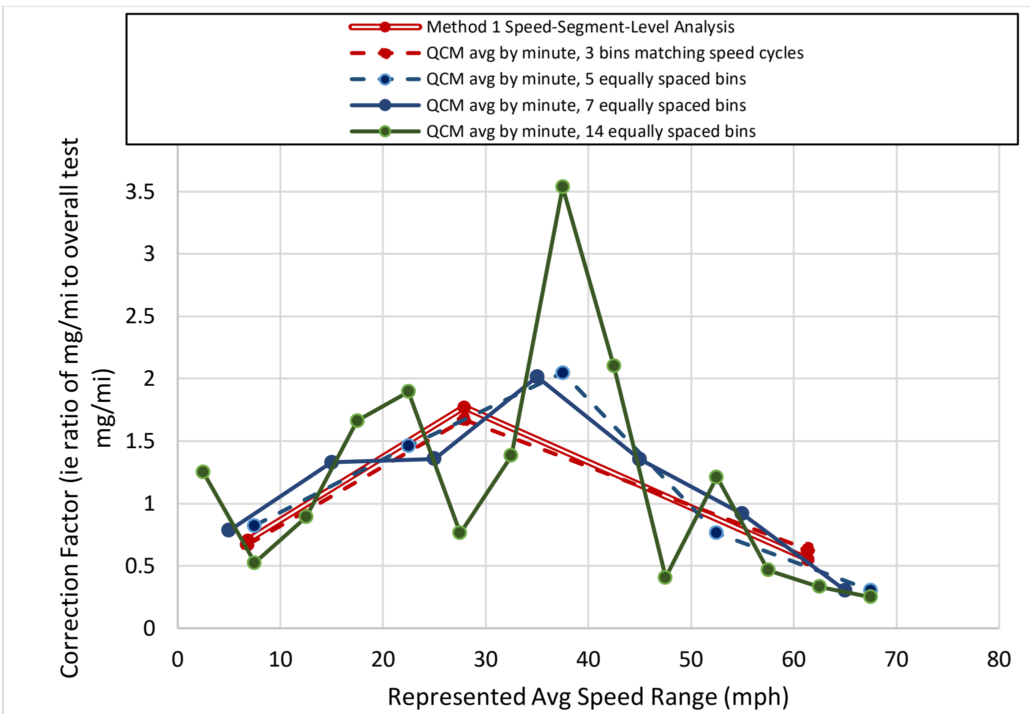

Figure 52. Sample Method 2 SCFs for varying speed bin sizes

Method 3: Using APS to Generate More than 3 Speed Bins

This method is similar to Method 2 but is performed on a volume basis at the 1 Hz time resolution of the APS. ERG employed similar general assumptions (spherical particles, homogenous density, etc.) regarding the APS as used in the other methods. The following process was used:

- Each braking event was analyzed individually. The measured emission volume in the 20 seconds after each braking event was summed and associated with the represented average speed of that event.
- The total volume emissions of each event were grouped by speed bin, then averaged within that speed bin.

The particle volume emission rate based on represented brake event speed is presented in Figure 53. ERG selected 5 speed bins for Method 3 to allow for direct comparison with Method 2. As with the other methods, the middle speed range is clearly associated with the highest volume emission rates.

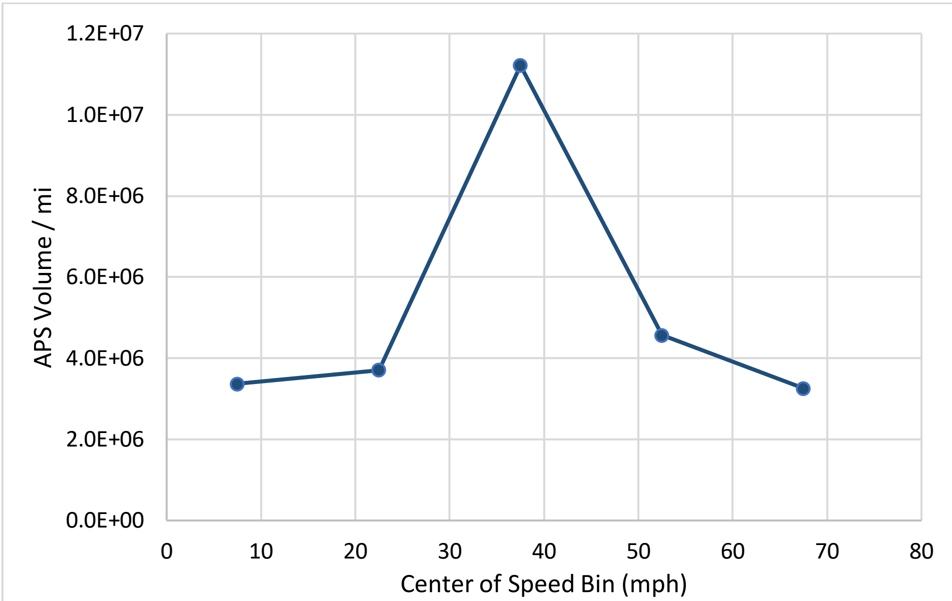

Figure 53. Sample Method 3 SCFs with 5 equally-sized speed bins

Finalizing the SCF Method

The different SCF calculation methods all resulted in a similar general trend of emissions against represented trip average speed. All indicated a peak in emissions in the middle of the speed range near 30-45 mph. However, for recommendation for EMFAC, the method with the greatest accuracy is preferred. Selecting a method allowing for more than 3 speed bins was also preferable if it could be implemented without loss of accuracy.

To select the method utilizing the most accurate instrument, ERG evaluated both the QCM and the APS results for agreement with the 100S4 at the test level. The instrument with the best agreement with the 100S4 is likely to yield the most accurate results. Figure 54 presents the total QCM test collected mass plotted against the 100S4 total collected mass. The R^2 value of a linear fit (shown with the broken line) to this data is 0.62. After review of this plot, ERG and LINK considered the possibility that the QCM was becoming saturated during some tests, because there were no collected masses above 120 µg. Further review indicated that most tests fell within a relatively linear channel (depicted within the solid lines in the figure). The remaining 7 tests were low compared to the 100S4. ERG and LINK were unable to determine the cause of these low values; no other abnormalities were observed. With those 7 tests lying outside of the linear channel dropped, the R^2 of the linear fit increased to 0.81.

The dropped tests were test days 54, 11, 69, 61, 70, 37, and 36 (and did not have any apparent pattern as to why they would be low).

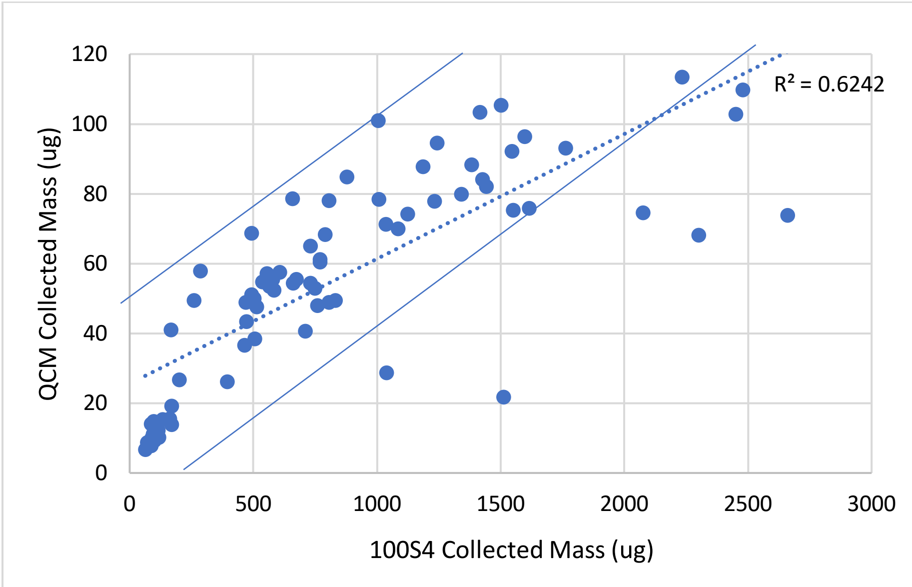

Figure 54. The test-level agreement between the 100S4 and QCM test results.

Figure 55 presents the APS calculated total particle volume by test plotted against the 100S4 total collected mass. The linear fit to this data has an R^2 of 0.73. Unlike the QCM, there was not a group of points that seemed to be outliers as compared to most tests.

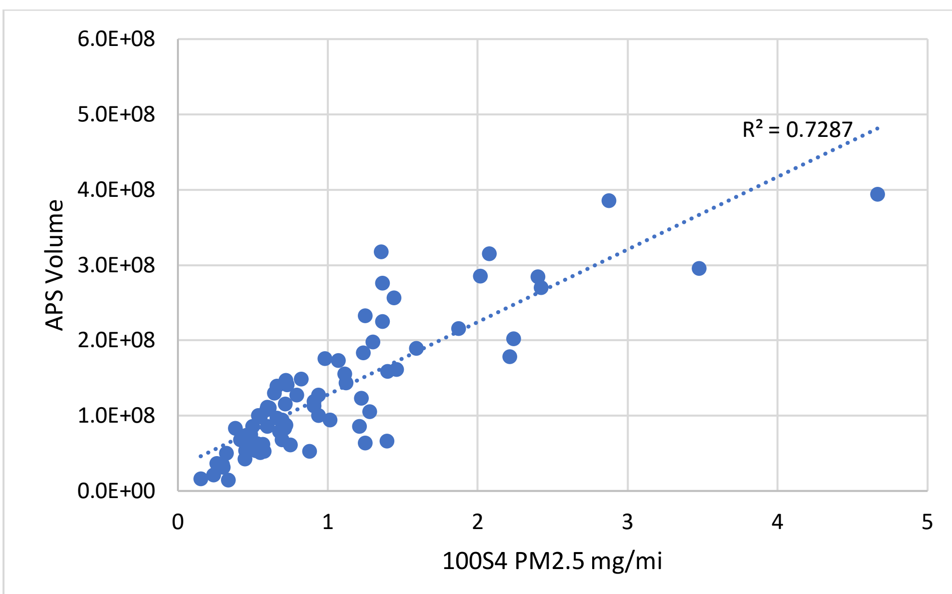

Figure 55. The test-level agreement between the 100S4 mass and APS total particle volume over all tests.

Because it was likely to have the best agreement with the 100S4 mass results, ERG selected the Method 2 approach for generation of the final SCFs. The 7 tests discussed for Figure 54 were dropped for all SCF analyses. The final factors are presented in the Implementation in EMFAC section of this report.

Emission Mass by Vehicle Weight

Figure 56 presents the vehicle-level test emission masses versus the simulated vehicle test weight, categorized by pad material. Labels of vehicle model are shown at the location of each model on the x-axis. The trends within each pad material do appear to be linear, so linear fits are shown by pad material. The fit to the aftermarket LM materials has the highest slope and the OES-NAO has the lowest slope. In this analysis, the fits are not forced through the origin (i.e. intercepts set to zero). The slopes and intercepts for these fits are presented in Table 23. While there may be engineering justification to set the intercepts to zero, there is little justification or utility in doing so as the Civic was the lightest vehicle tested (meaning no data is available near the origin) and is likely to be near the lower limit of weights of any light-duty vehicle to be modeled (meaning any modeling error at a zero vehicle weight will not affect results).

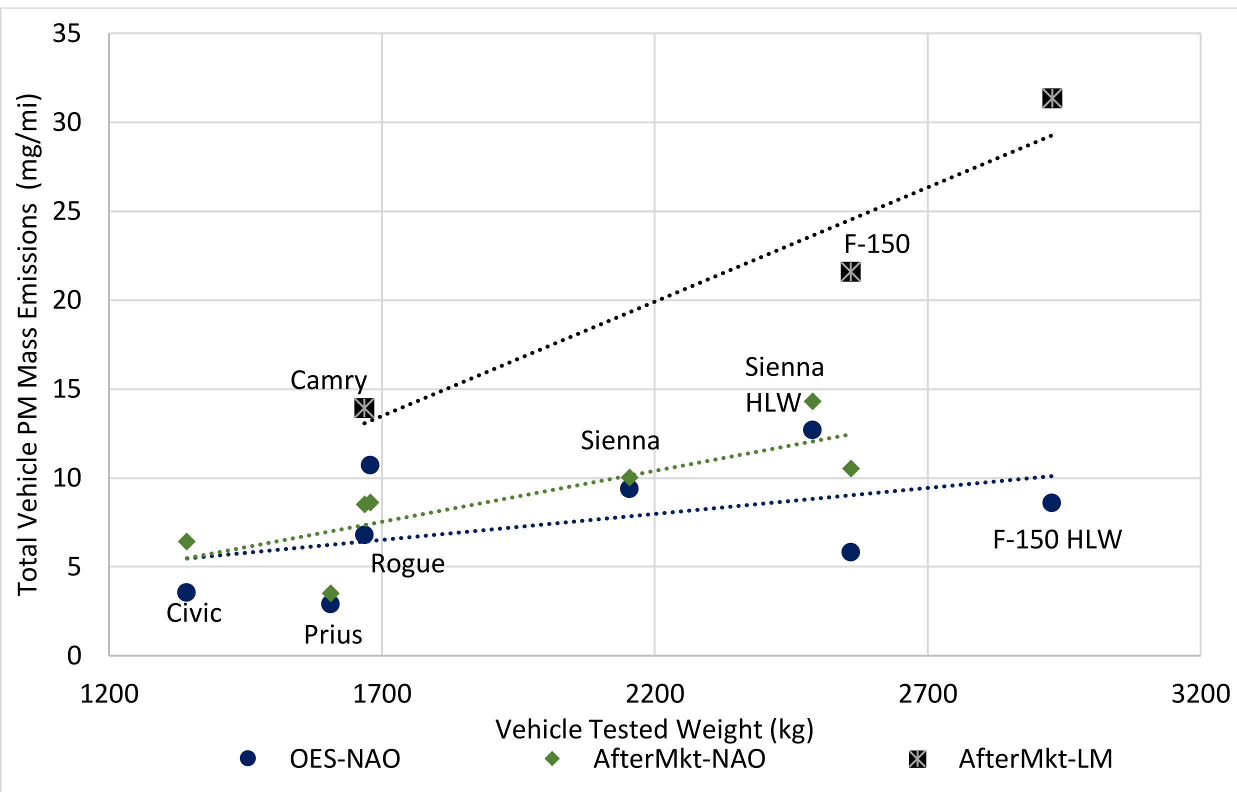

Figure 56. Total vehicle test cycle PM mass emissions vs simulated vehicle test weight, categorized by pad material.

Table 23. Slopes and intercepts for linear fits by material for PM mass emission rate (mg/mi) versus vehicle tested weight (kg)

Material	Slope (mg/kgmi)	Intercept (mg/mi)	Coefficient of Determination (R^2)	P Values, Slope, Intercept
OES NAO	0.003	1.55	0.91	0.23, 0.75
After NAO	0.006	-2.21	0.64	0.03, 0.58
After LM	0.013	-8.37	0.23	0.19, 0.55

Emission Mass and Component Mass Loss During Testing

LINK staff weighed the friction materials before and after each test. Rotors (or drums for the Civic) were weighed separately from pads. This allowed for the calculation of the total mass lost from the components over the course of the burnish and test cycles. Components could not be weighed after the burnish and before the test cycle because removal would have potentially upset the friction couple and nullified the burnishing process. ERG investigated the extent to which the total mass loss was proportional to measured PM mass emissions. This section references the components as pads and rotors generally, but for the Civic rear, the corresponding parts were shoes and drums and they are included.

Figure 57 presents the total PM mass emissions (y-axis) measured during the test cycle plotted against the total mass loss of pads and rotor for each burnish and test. The plot shows PM10 as measured by the 100S4 and has somewhat less noise than that of PM2.5 (though the trends are otherwise similar). Fits are not presented by material as the specific slope of the relationship between the test PM and the pad and mass loss is arbitrary due to the burnish cycle (for which emissions were not quantified by the 100S4). The relationship is presented to show the general level of proportionality.

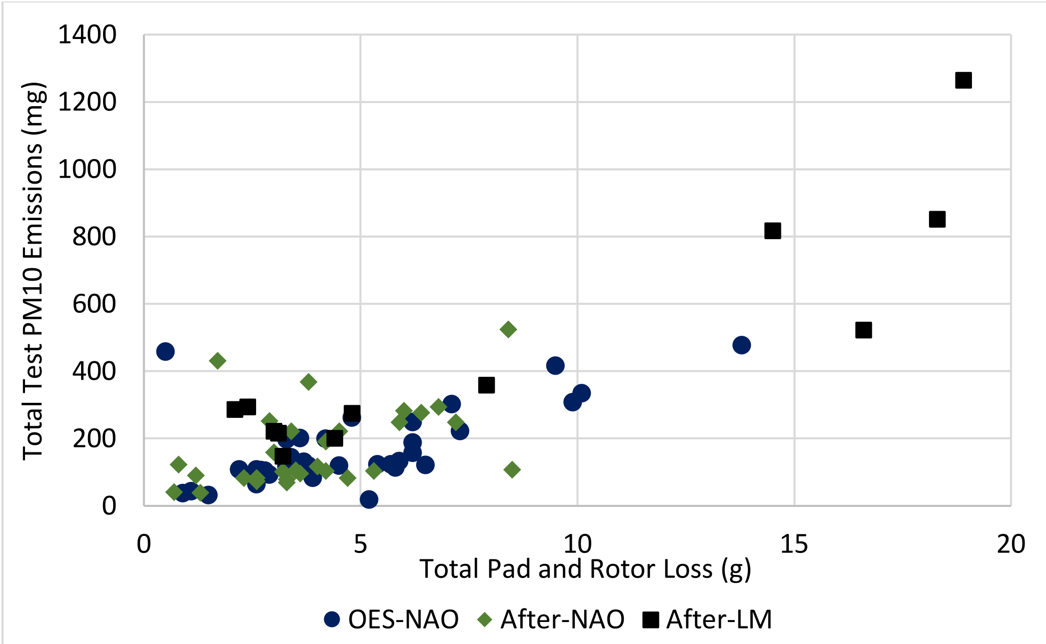

Figure 57. Total test-cycle PM10 emissions plotted against the total mass loss of the pad and rotor during the burnish and test cycle. Each point represents one test.

ERG also investigated whether the PM10 emission rates were more correlated to the mass of pad lost, the mass of rotor loss, or the sum of pad and rotor. Figure 58 presents the PM10 emissions totals for each test against the brake component mass loss for three categories: pad + rotor (same data as Figure 57), pads only, and rotor only. The plot includes R-squared values calculated for a linear fit made to each category. The best linear fit is for the sum of pad and rotor, and the noisiest fit is to the rotor only. This finding indicates that mass losses of both pads and rotors contribute to and are correlated with emitted PM. However, it does appear as though the emitted PM mass is more responsive to the mass of pad lost. This could be because, in most tests, the pad mass loss exceeded that of the rotors. The pad mass loss averaged 3.2 times that of the rotor mass loss across all tests. However, this ratio varied widely across tests did not appear to be sensitive to the friction material type.

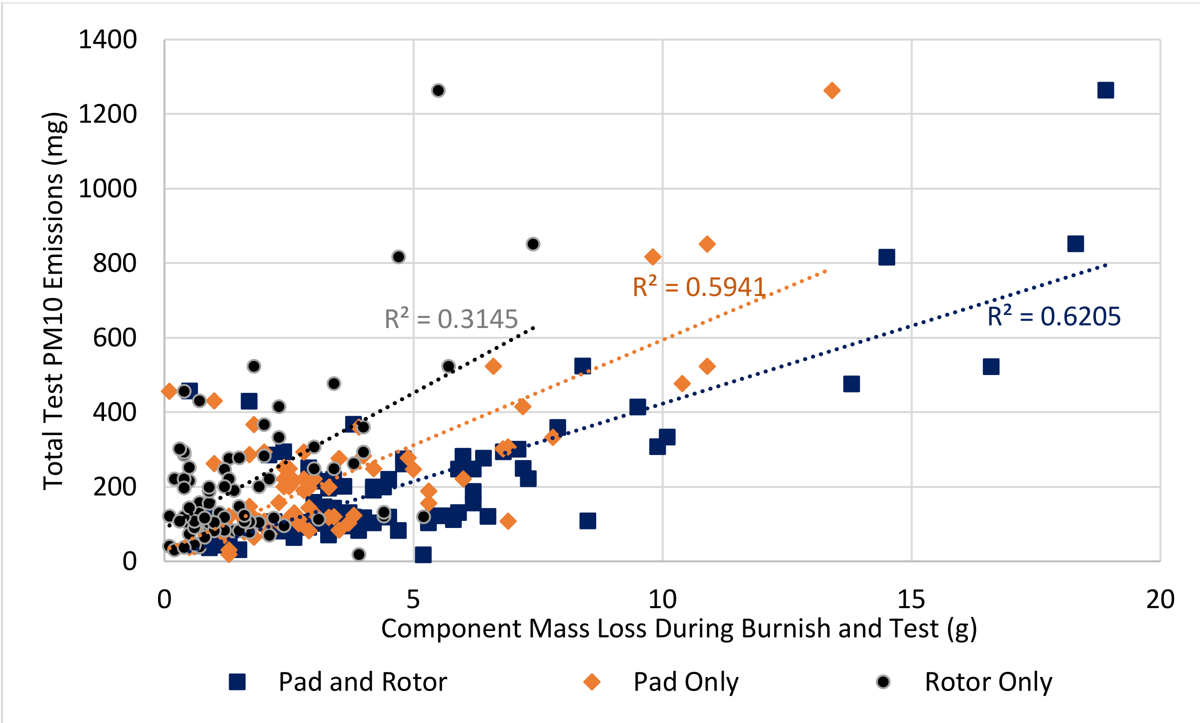

Figure 58. Total cycle PM10 emissions relative to mass lost for pads, rotors, or the sum of pads and rotors. R-squared values are presented for linear fits to each.

Particle Counts

The CPC was used to measure particle counts per unit of sample volume throughout the duration of each test. Particle number totals for each test are included in Appendix
H. Table 24 presents the range, median, and average number of cumulative particles for all CBDC tests on a per-mile basis. In general, there was a weak trend in vehicle weight and particle count; larger vehicles tended to have larger particle counts.

Table 24. Selected statistics for single-wheel particle number counts for all tests (#/mi)

Test Statistic	Particle Number (#/mi)
Average	1.681×10^9
Median	1.258×10^9
Maximum	8.429×10^9
Minimum	3.913×10^8

ERG calculated vehicle-level particle number emission rates by doubling the single wheel emission averages for each model/material/test weight/axle combination. These axle-level values were summed within each model to calculate vehicle-level values. Figure 59 presents these estimates by vehicle model and categorized by pad material type. Compared to the mass results, the spanned range of values across models and pad materials appears lower for particle count results, meaning all vehicles appear to have more similar particle count emissions than they do mass. Generally, the trends otherwise follow those observed for PM mass with a notable exception of the Prius aftermarket NAO material. The elevated values for this combination were caused by high emissions measured in both tests of the front axle; the rear axle emission rates were in line with the other sedans.

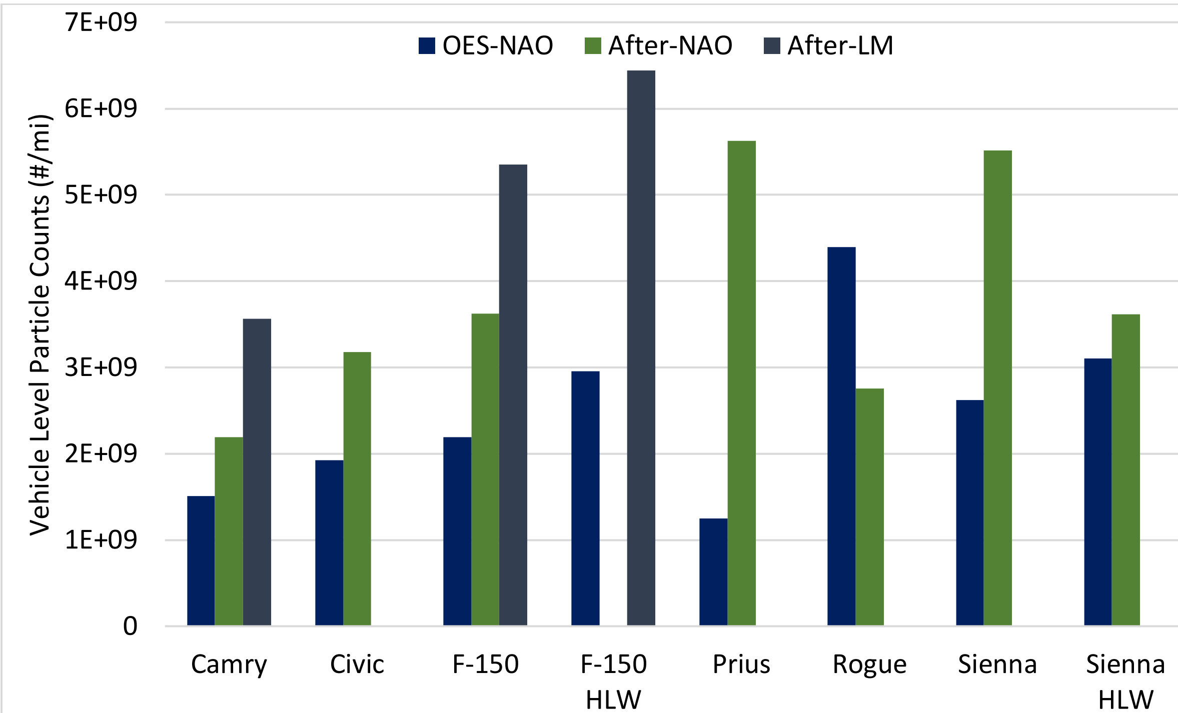

Figure 59. Vehicle-level particle number emission rates for each vehicle and friction material combination

Figure 60 presents the overall trends in single-wheel particle emission rates across the three speed segments. The figure presents the emission rates averaged across all tests. Error bars represent the 95% confidence interval for the mean of the results of all tests. Appendix J presents the corresponding vehicle-level results by individual model.

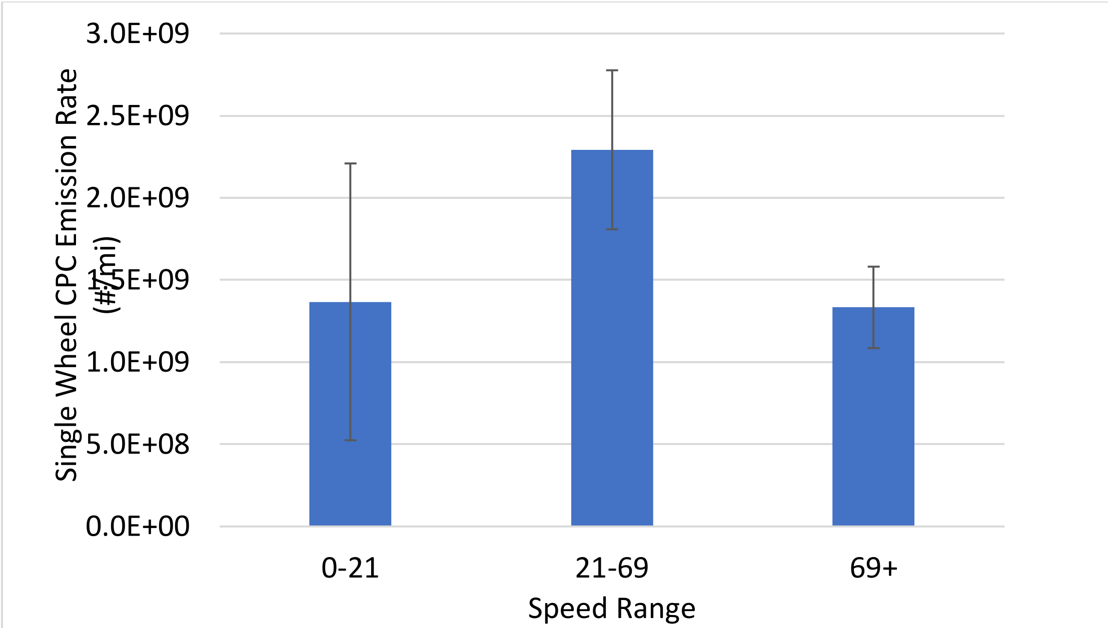

Figure 60. Overall average single-wheel particle number emission rate across the three speed ranges

Particle Size Distributions

Particle size was measured in two size ranges; the EEPS measured from 5.6 – 560 nm, and the APS measured from 0.5 – 20 µm. The APS results tended to show noticeable trends and responses to the test matrix parameters, and their results follow in this section. The EEPS results were more similar across all tests with a lower degree of apparent responsiveness to the test parameters, so EEPS results are presented only in Appendix K. However, results for all tests indicated a multimodal distribution in which at least one peak was present in the APS size range and one peak was present in the EEPS size range. Size distributions are presented in graphs by vehicle and axle, and each distribution is color coded by brake pad material. Note that all distributions in the size distribution figures are normalized to sum to 1. This is to enhance the comparability of particle size without any bias from particle number differences at the test level. Particle number is measured specifically by the CPC so reporting absolute count was not a necessary function of the particle sizers.

The APS reports particle counts in 52 size bins. The smallest bin is intended to include all particles less than 0.52µm in diameter. However, this bin did not resolve any notable differences across tests and generally reported approximately 49% of the particle counts in any given test. So, while this bin was used as a part of the normalization to a sum of 1, the bin is not included in the following APS size distribution plots to keep the scale readable for the remaining bins that resolve differences of interest across the pad materials and vehicle models.

Figure 61 presents the size distribution of particles from the front brake tests of the Camry. It can be seen the test replicate pairs of the three different pad materials follow similar patterns. The low metallic material tends to emit larger particles, and the two NAO materials are relatively similar in particle size distribution.

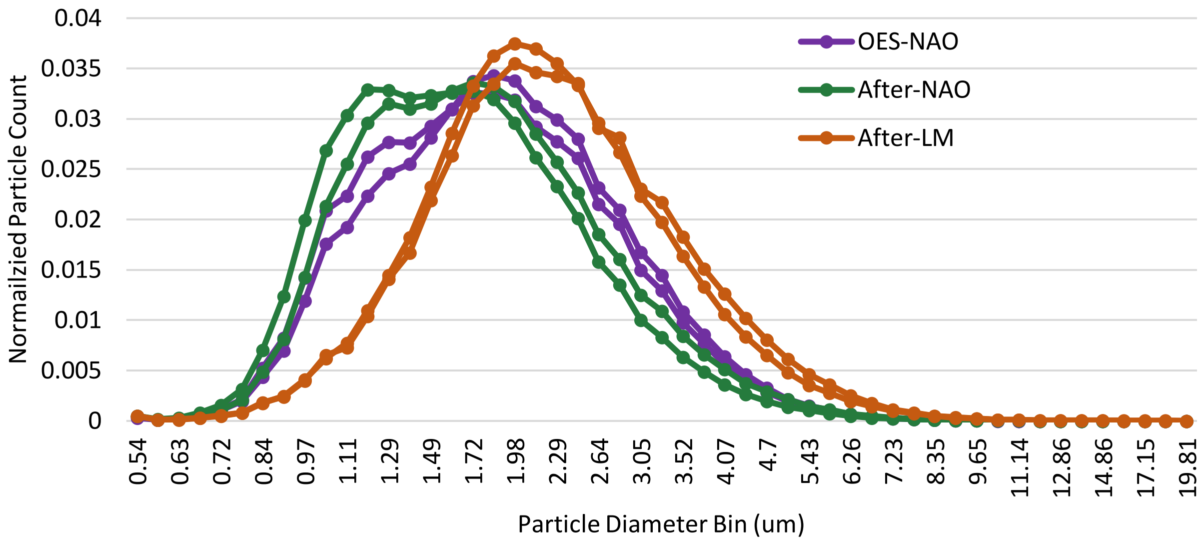

Figure 61. Size distribution of Camry front brake PM as measured by APS

The PM size distribution for the rear brake tests of the Camry is presented in Figure 62. The low metallic material has the largest particle sizes, and the aftermarket NAO tends to have the smallest.

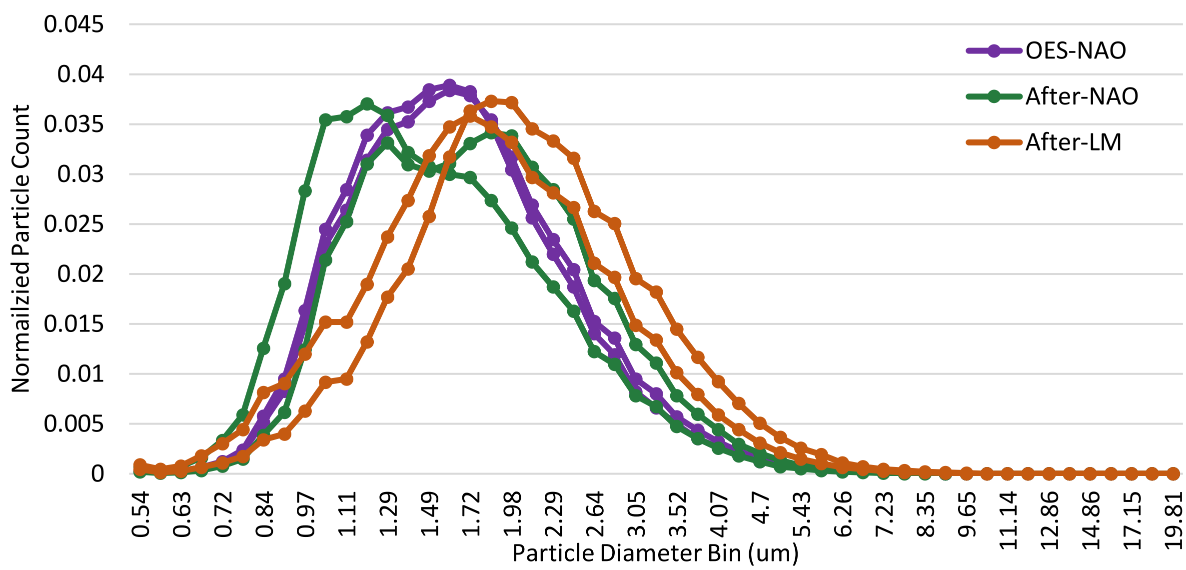

Figure 62. Size distribution of Camry rear brake PM as measured by APS

Figure 63 and Figure 64 present the size distributions for the Civic front and rear, respectively. The OES particles from the front tend to be larger than the aftermarket, but that trend appears to be reversed for the rear drum brake emitted particle size.

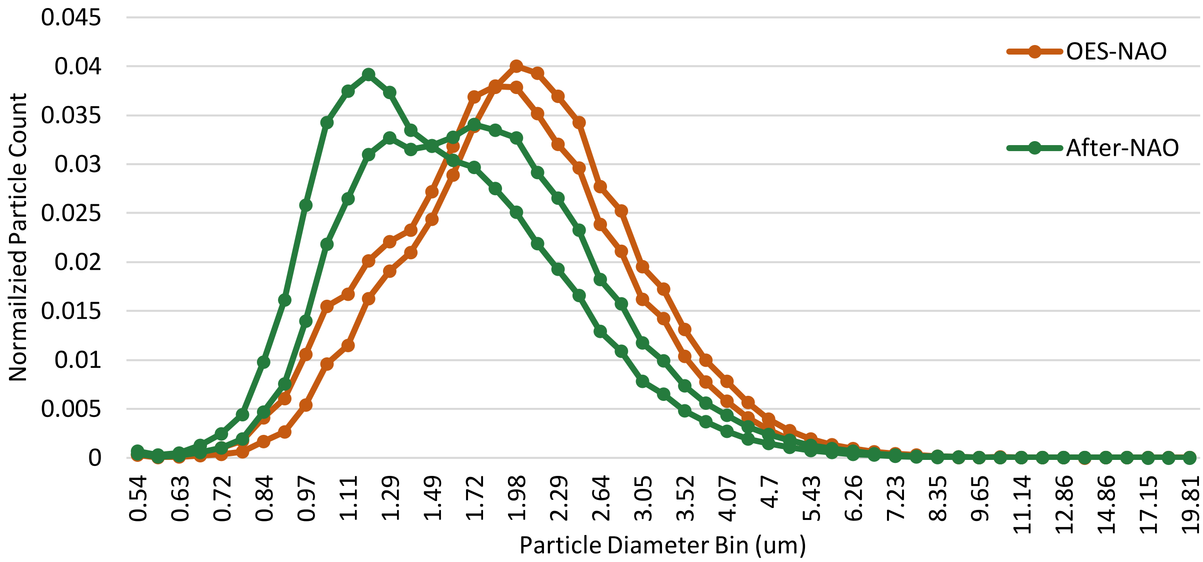

Figure 63. Size distribution of Civic front brake PM as measured by APS

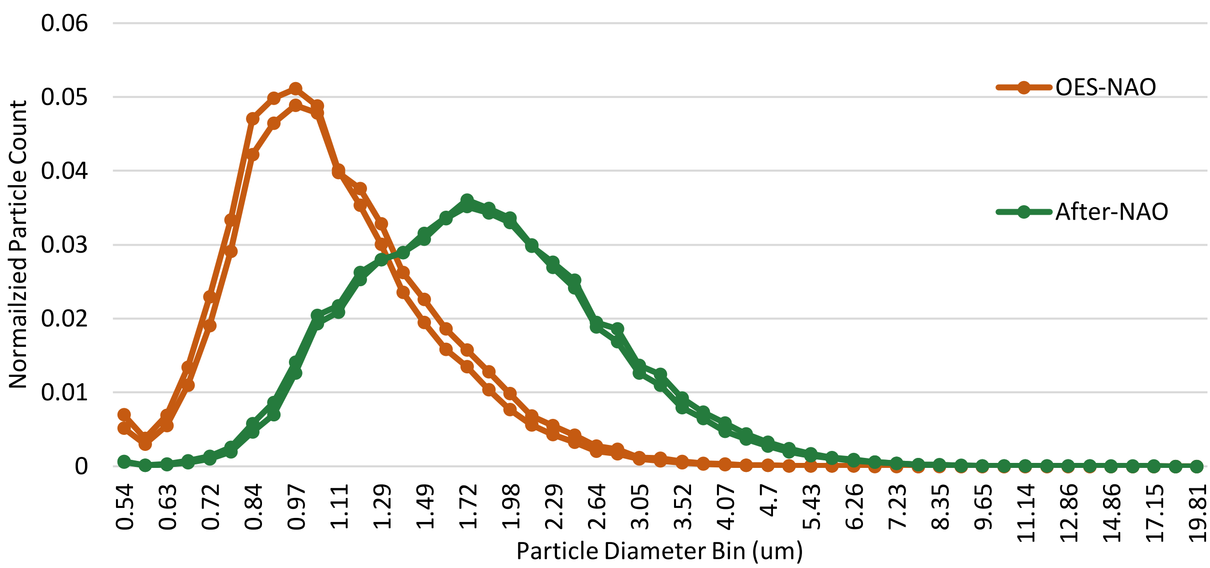

Figure 64. Size distribution of Civic rear brake PM as measured by APS

The size distributions for F-150 front and rear are presented in Figure 65 and Figure 66, respectively. For the front brakes, the low metallic pads have the largest particle size, but the trend is more inconclusive on particle size emitted from the various rear pads.

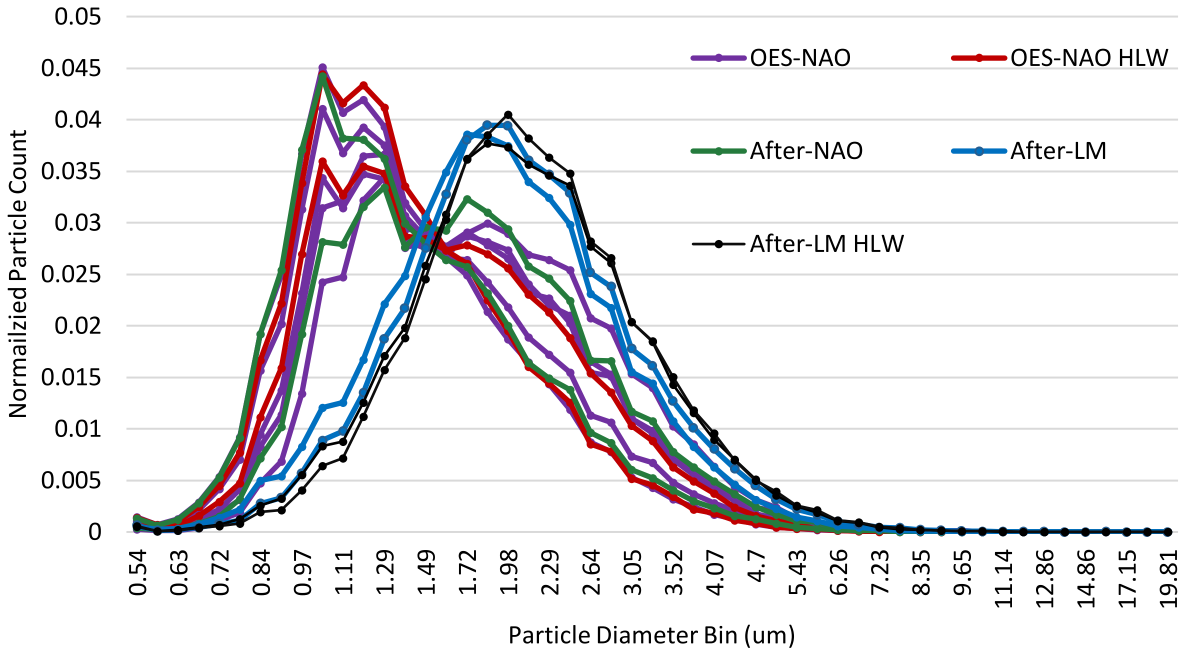

Figure 65. Size distribution of F-150 front brake PM as measured by APS

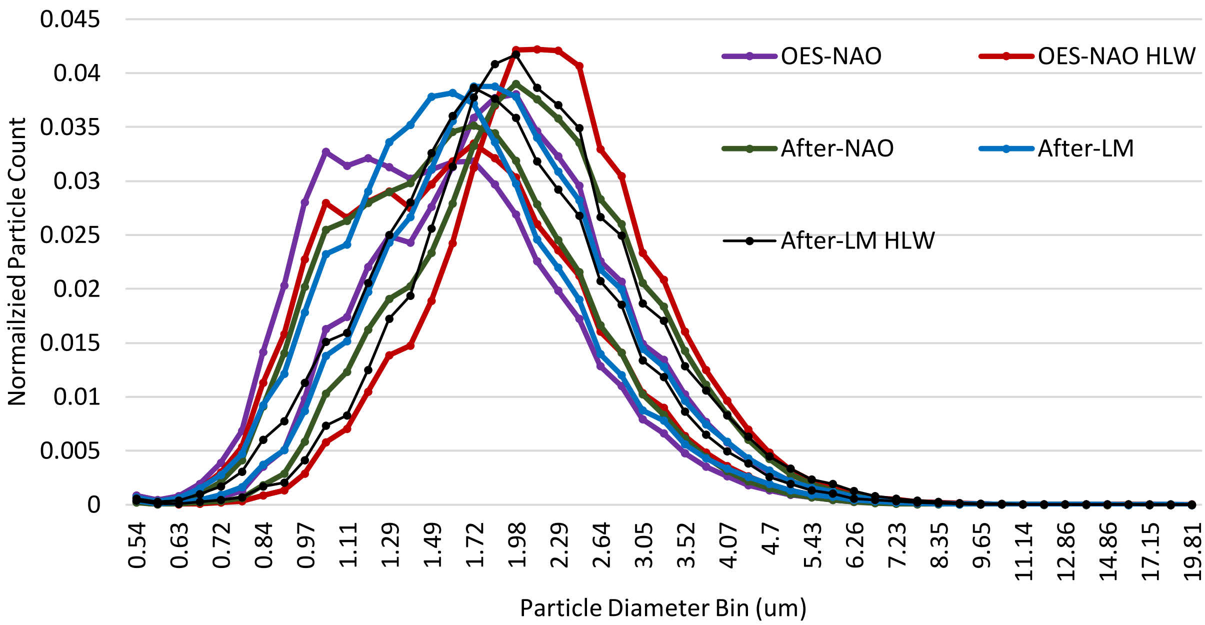

Figure 66. Size distribution of F-150 rear brake PM as measured by APS

Figure 67 and Figure 68 present size distributions for the Prius. The two NAO pad materials are largely overlapped in emissions from both the front and rear assemblies.

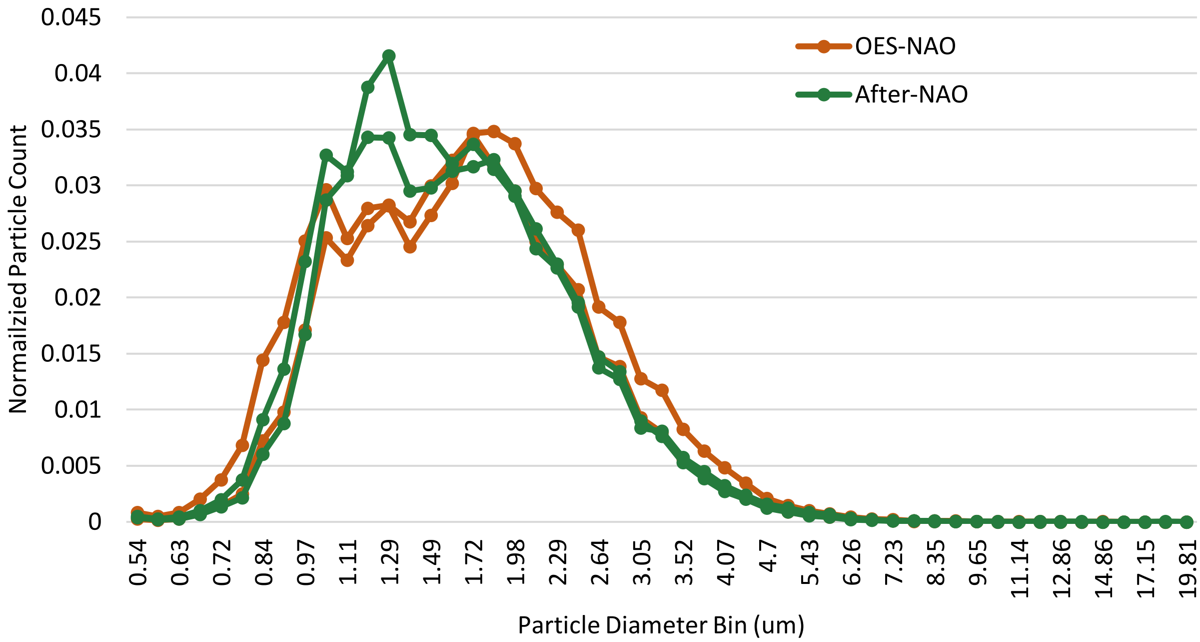

Figure 67. Size distribution of Prius front brake PM as measured by APS

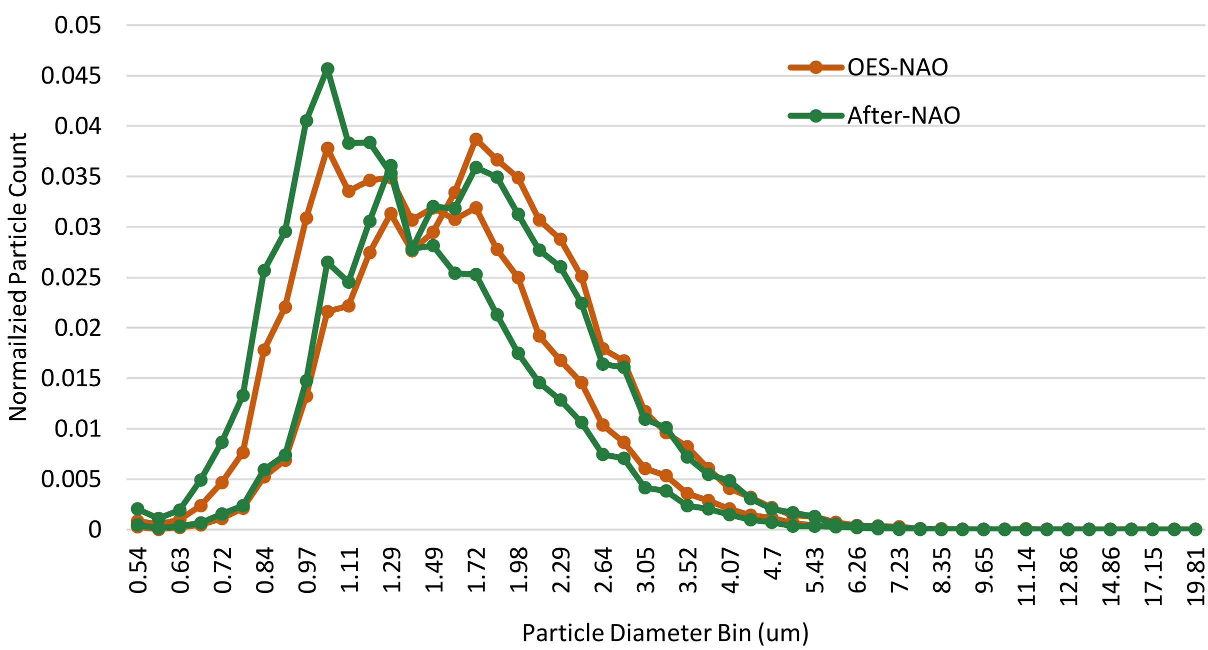

Figure 68. Size distribution of Prius rear brake PM as measured by APS

Figure 69 presents the size distribution of particles from the front brakes of the Rogue. The OES material tends to have a larger particle size than the aftermarket material. Figure 70 presents the findings for the Rogue rear, in which the distributions are largely overlapped.

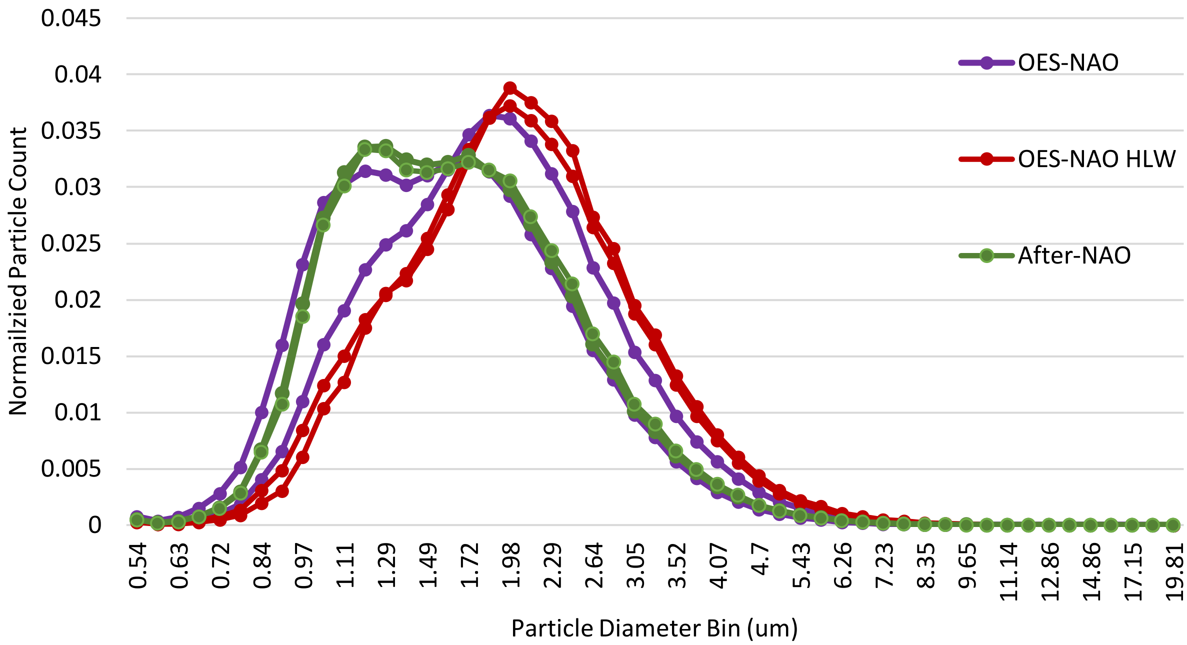

Figure 69. Size distribution of Rogue front brake PM as measured by APS

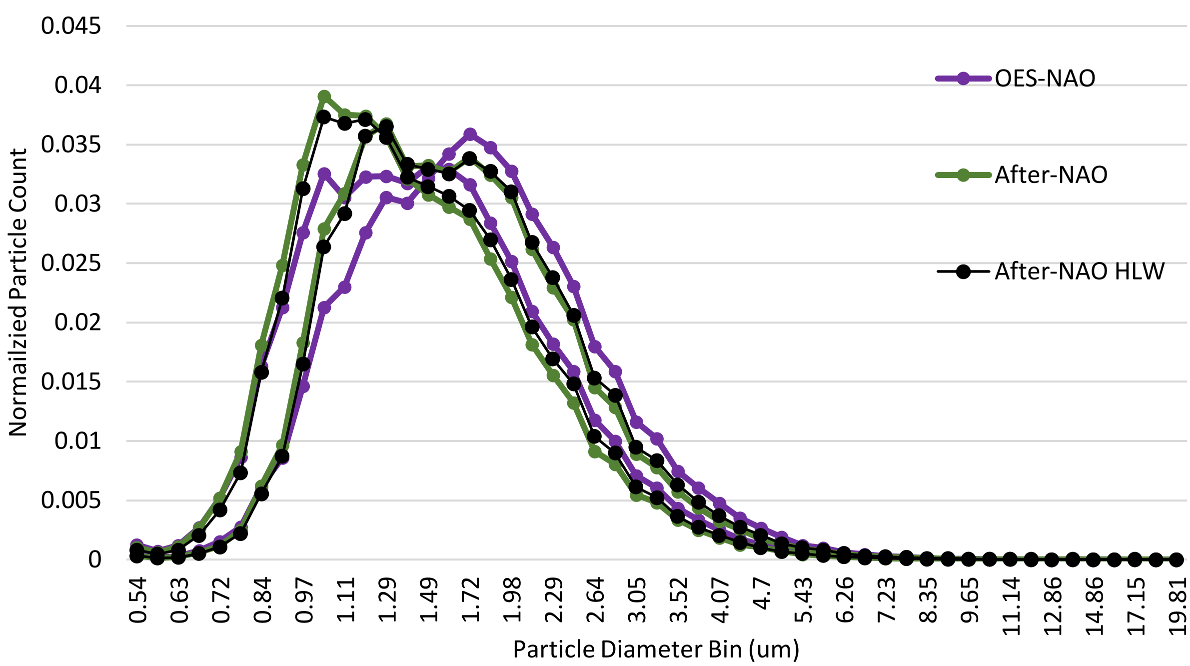

Figure 70. Size distribution of Rogue rear brake PM as measured by APS

Figure 71 and Figure 72 present the size distributions for the Sienna front and rear, respectively. Both display significant overlap in the size distributions of the different friction materials and test weight. Both the front and rear distributions tend to have a minor bimodal effect, with a major peak at 1.98 µm and a minor peak at 1.29 µm.

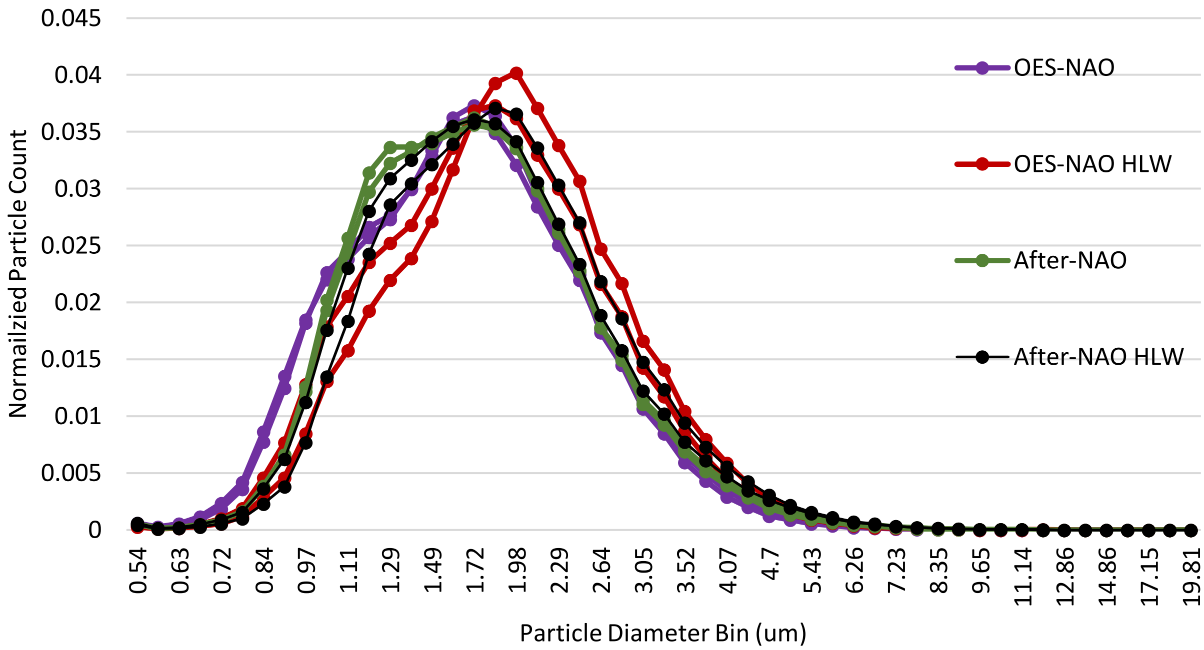

Figure 71. Size distribution of Sienna front brake PM as measured by APS

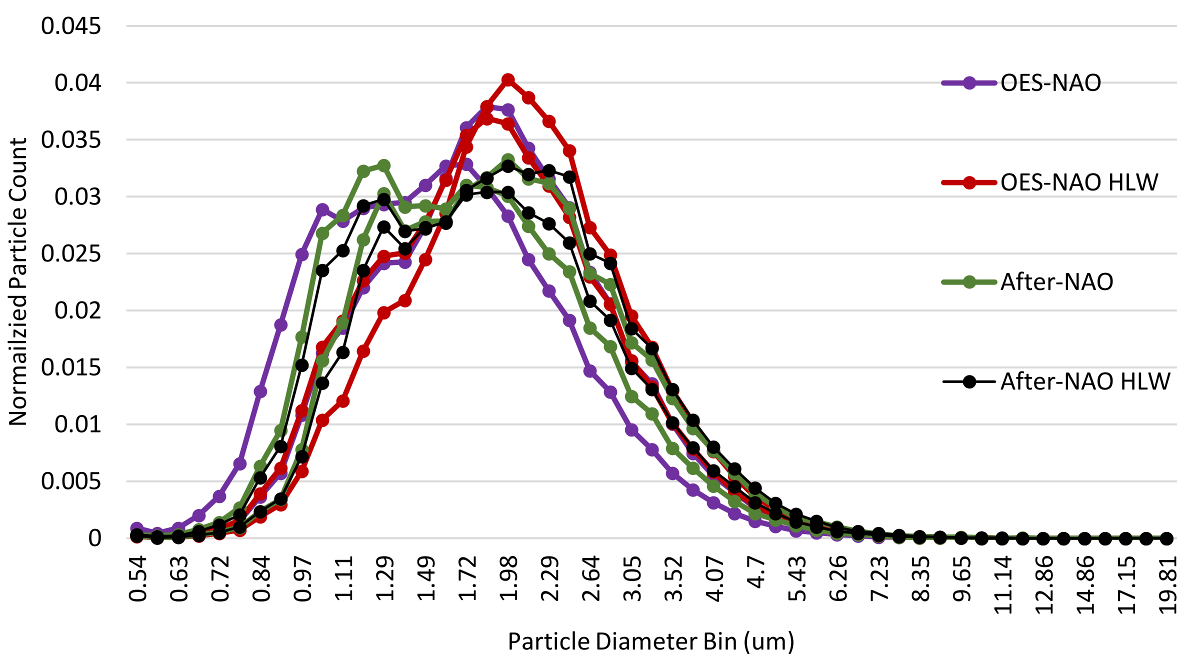

Figure 72. Size distribution of Sienna rear brake PM as measured by APS

Tunnel Blanks

LINK conducted two tunnel blank experiments, one early in the test program and the other late in the test program. Tunnel blanks involved running a complete CBDC test cycle without brake pads mounted or the brake hydraulic pressure active to help determine the level of background PM present during a test. Table 25 presents the results of the tunnel blank experiments as compared to all other brake assembly tests for particle counts and mass measurements. Mass measurements of PM10 were conducted with both the 100S4 as well as the two parallel 47 mm PTFE filter holder systems (note that in normal tests only 1 of the filters was directly measuring PM using a PTFE filter). The particle counts during blanks averaged approximately 0.2% of the test average. The 100S4 blank measurement was about 1% of the average test mass, and the PTFE filters averaged approximately 2.8% of the average value when including a single outlying high value during Tunnel Blank 2. No corrections were applied to the test results based on the tunnel blank findings. The main concern was that one of the mass measurements was an outlier in the 100S4 vs PTFE results by test. ERG and LINK were concerned that performing corrections based on an outlying point would have a detrimental effect on all results.

Table 25. PM counts and mass measurements for the two tunnel blank procedures as well as the averages for all brake emissions tests

	Test Day	CPC #	100S4 PM10 (mg)	47mm PM10 1 (mg)	47 PM10 mm 2 (mg)
Tunnel Blank 1	17	9.5x10^{7}	1.4	2.7	2.3
Tunnel Blank 2	66	2.1x10^{8}	2.7	3.7	12.5
Overall Test Average	All Others	1.3x10^{11}	208.3	192.3[1]	192.3[1]

[1]-Only 1 filter holder was used during non-blank dynamometer tests of brake components, so the average of those values is presented for both holders.

Figure 73 presents the particle size distributions measured by the APS during the two tunnel blank experiments. The measured size distributions are generally similar to the brake component tests with a peak around 1.6-2 µm. The similarity in shape between the tunnel blanks and actual tests may be due to the exchange of particles deposited within the tunnel and the sample airflow; the particles from previous tests that adhere to the surfaces during “seasoning” may be entrained into the sample flow during the blank, leaving a similar size distribution even though the total counts are far less. Appendix K includes the tunnel blank measurements from the EEPS. The EEPS measurements during tunnel blanks showed approximately 50% of the counts measured during CBDC tests, and the normalized size distributions were similar between tests and blanks. For this reason, ERG and LINK believe that the EEPS size distribution is strongly affected by the distribution of ambient dust that can pass through the CVS intake filter.

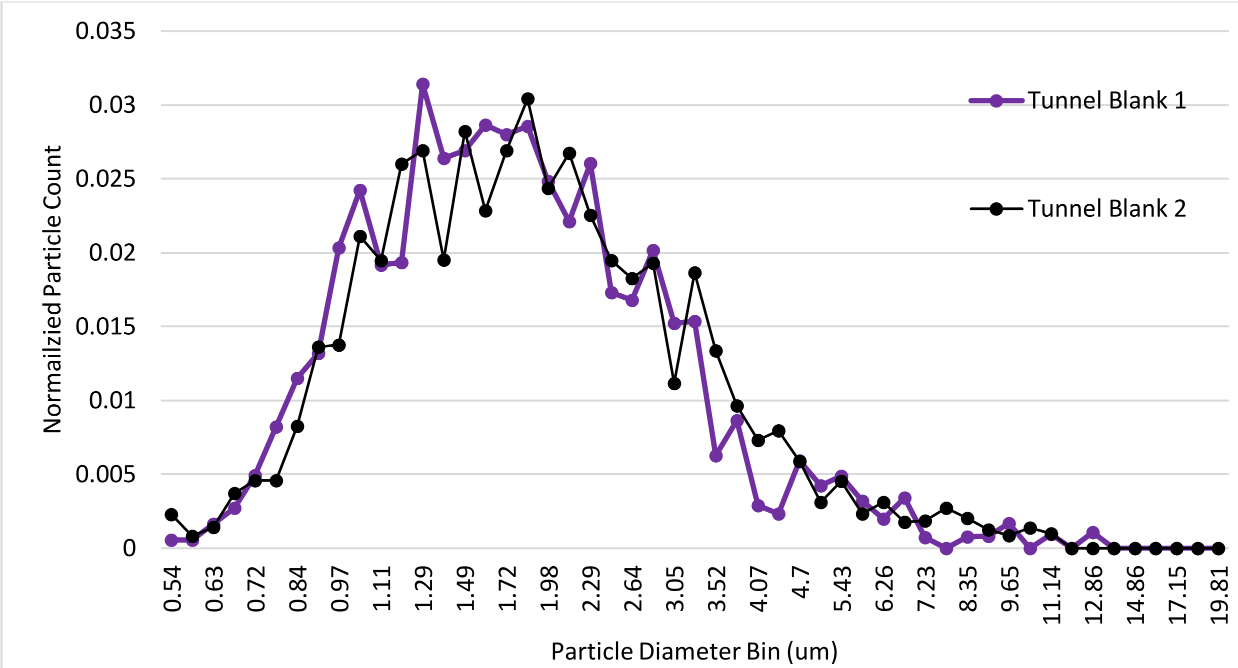

Figure 73. Size distribution of Tunnel Blanks as measured by APS

LINK also performed 6 zero blank experiments, in which filters were weighed, loaded into their respective sampling systems, then removed and re-weighted to determine any trends in weight gain or loss from handling. The weight gain of the PTFE filters during the 6 tunnel blanks averaged approximately 0.5% of the average weight gain measured in the PTFE filters during the CBDC tests. No corrections were applied based on the zero blank findings (as some filters gained weight and some lost weight during the zero blank process). The complete listing of zero blank results is presented in Appendix L.

Trends in Individual Brake Events

In addition to test level and phase level analysis, ERG also reviewed emissions for individual brake events. The QCM measured instantaneous mass and the CPC measured instantaneous particle count and findings of each are presented in this section.

For these analyses, event emissions for each measurement type are calculated as the sum of each deceleration event plus the emissions captured in the cruise or acceleration event following the braking. This segment is added to capture any emissions that might be released in the moments after the brake pressure is released and the friction materials move apart. The QCM data was processed similarly to the method presented in the Results by Vehicle Average Speed section; the QCM was used to estimate the emissions percentage of the 100S4-measured total PM2.5 across each brake event. These analyses present only findings for PM2.5 so no factor was used to estimate PM10. The CPC particle data was used directly as measured by the instrument. All analyses presented in this section are on a single-wheel basis.

ERG reviewed plots of the by-event emissions from both instruments as compared to parameters of the event, including the 4 parameters used in test cycle development. ERG reviewed emissions trends as a function of:

- Average vehicle speed during braking event
- Average event deceleration rate
- Brake rotor/drum temperature
- Brake event duration
- Total event braking energy
- Average event braking power

ERG reviewed plots of QCM and CPC data against each of the above parameters for every combination of model, axle, and pad material. No trends were apparent for deceleration rate, and a very weak trend was observed with temperature. Stronger trends were observed for speed, duration, energy, and power. This section presents the results overall for both measurement types across the five parameters in cases where trends were observed. In general, the QCM data appeared to have more noise than the CPC. The QCM appeared to have more noise in both measurement and time alignment. The time alignment noise is largely due to the QCM having a 1-minute time resolution during operation. This resulted in emissions responses that would appear to sometimes lead and sometimes lag the corresponding brake event, making complete time alignment impossible on a by-event basis (though brake events were typically on the order of 1 minute apart). In contrast, the CPC data responded favorably to time alignment. So, in the plots in this section, the CPC data has less overall observed noise. The following by-event plots include all braking events from all CBDC tests in this program.

Figure 74 presents the total brake event particle count against the braking event average speed. Power equation fits were performed by each friction material and are presented in the plot; the LM pads show the highest slope of the three materials. Figure 75 presents the corresponding plot for total event QCM-measured mass by brake event average speed.

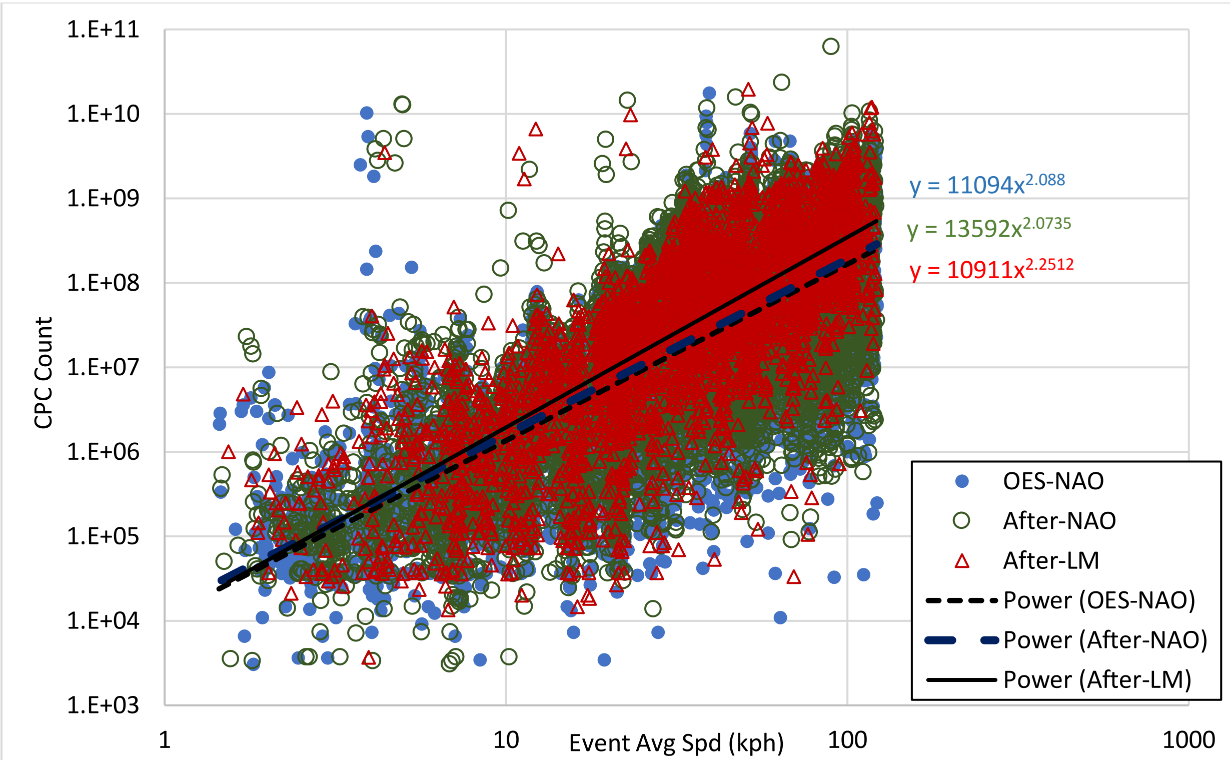

Figure 74. Trends in CPC count against braking event average speed, categorized by friction material

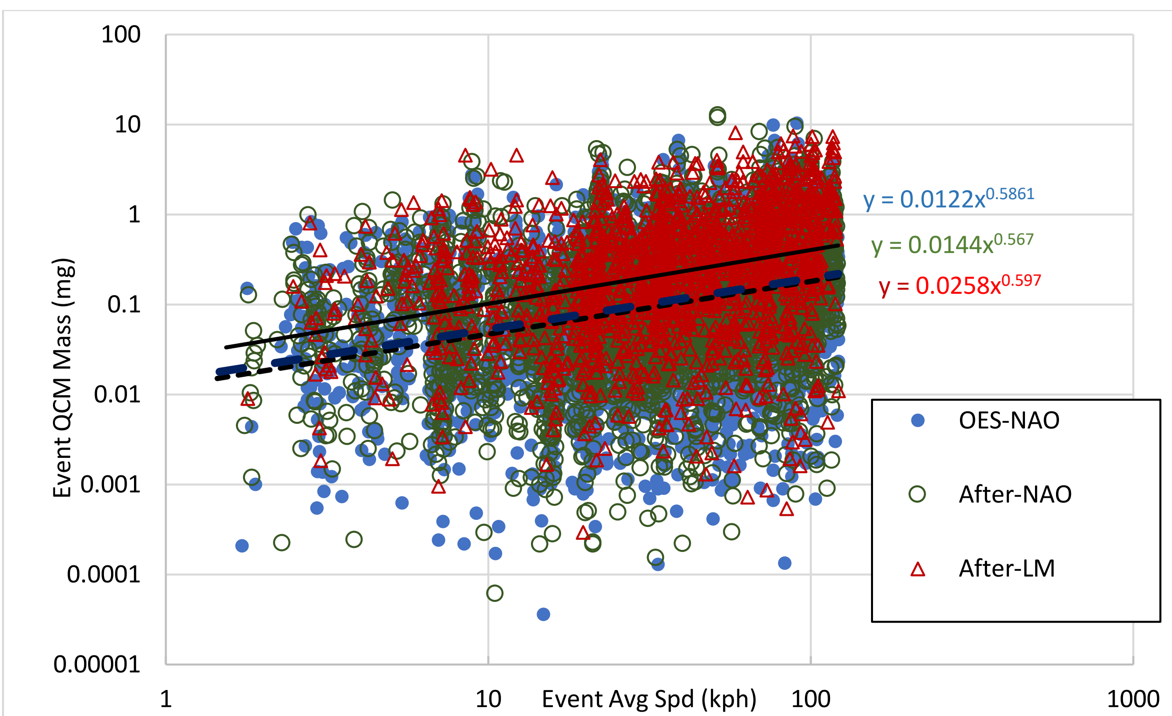

Figure 75. Trends in QCM brake event PM mass against braking event average speed, categorized by friction material

Figure 76 presents the total brake-event CPC count vs brake rotor temperature (note the linear scale of x-axis). Linear fits are applied to the data for reference and to indicate the gradual upward trend. The equations are not given, however, as the R^2 fits were all less than 0.05. Figure 77 presents the QCM-measured total brake event PM2.5 mass against average event rotor temperature. As with the CPC, linear trendlines are presented to show the very shallow increase in emission rate with temperature, but the fits have very low R^2 values. The temperature data in general did not show the level of responsiveness in emission rates as cited in literature. This is likely due to the relatively low temperatures used in this study (that is primarily intended to be representative of normal on-road use). The gradual uptrends in these plots may also be subjected to the confounding factor that the higher-temperature events are likely to be of higher intensity (since the rotor temperature is driven primarily by braking energy). So, it is difficult to draw meaningful conclusions of the effect of brake temperatures on on-road PM emission rates. For completeness, Appendix M presents the data in these two figures as box plots of CPC and QCM results by bins of temperature ranges.

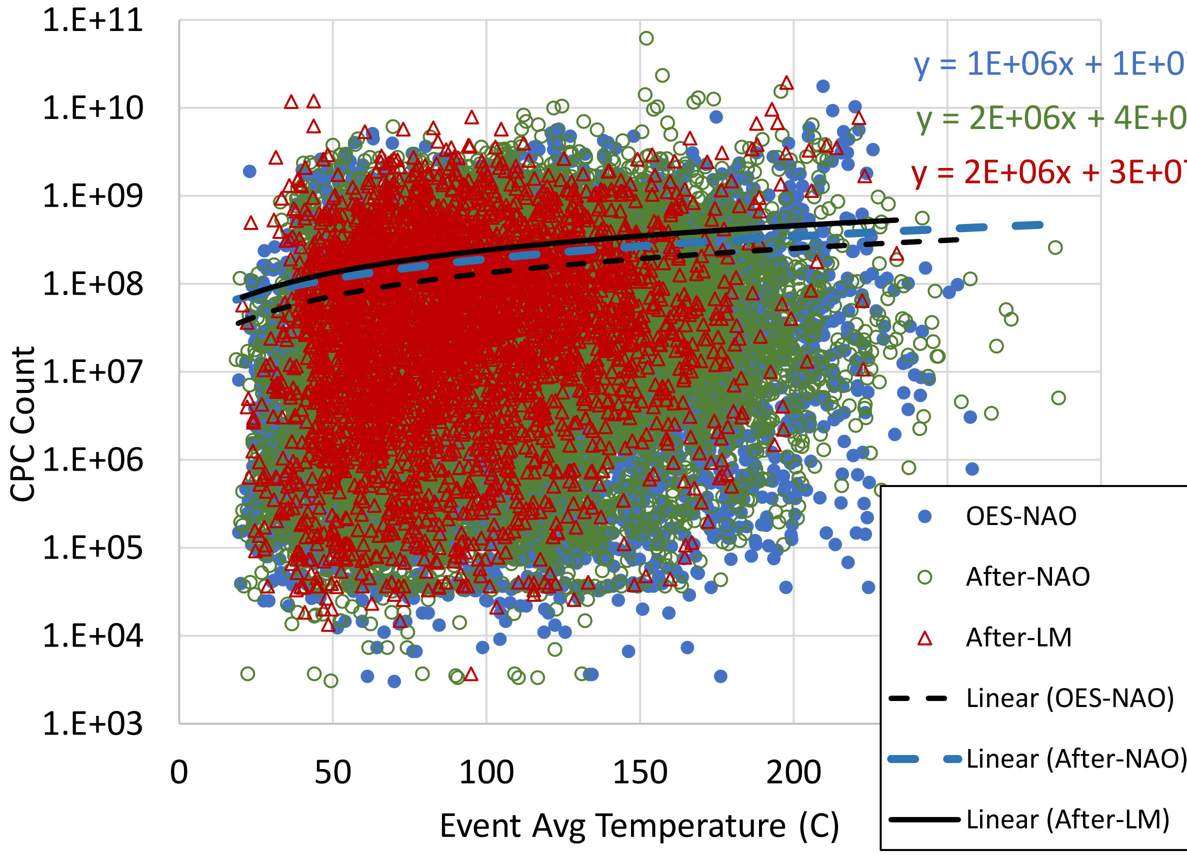

Figure 76. Trends in total braking event CPC count against average rotor temperature, categorized by friction material

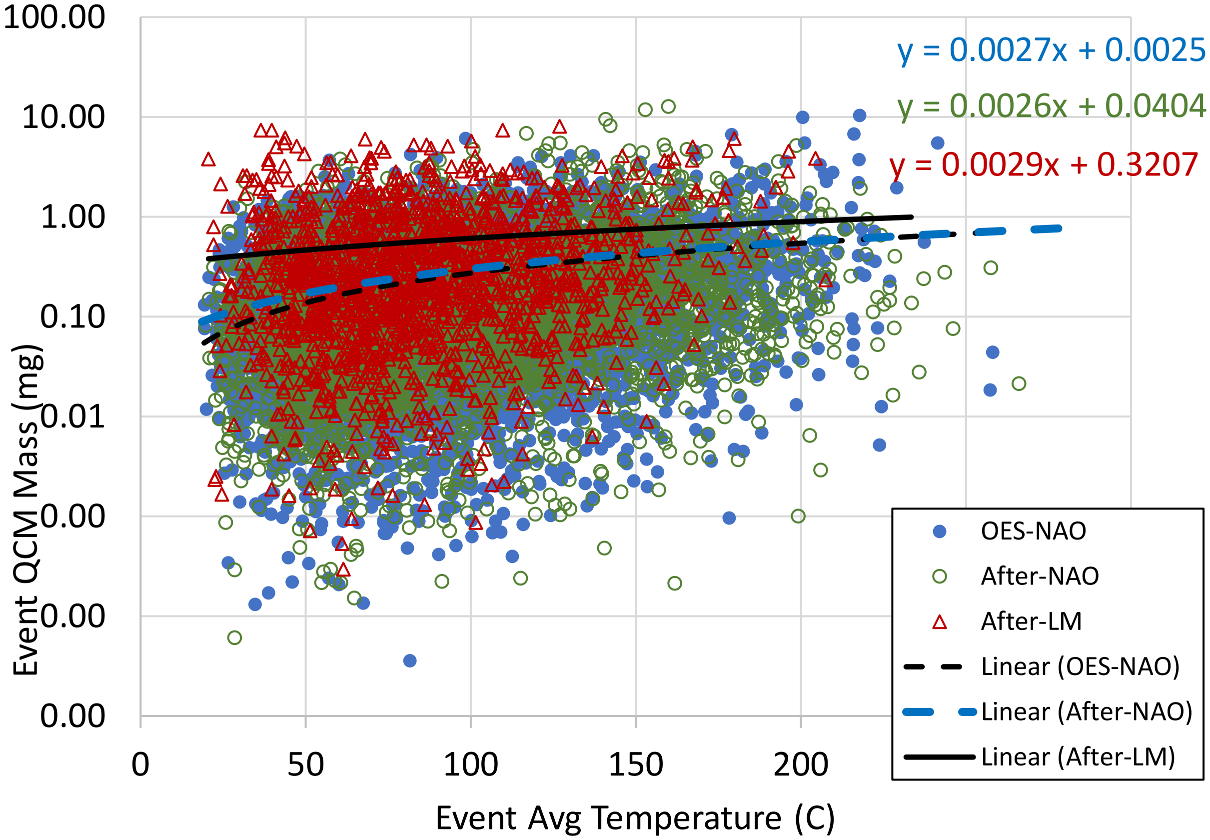

Figure 77. Trends in QCM brake event PM mass against braking event average rotor temperature, categorized by friction material

Figure 78 presents the by-event total particle count plotted against braking event duration. In this plot, it appears that there is less scatter in the data at the longer durations; however, it is likely that this is only because the events with durations over approximately 10 seconds are extremely rare in the tests performed over the CBDC. Analysis of the QCM -by-event PM mass data did not resolve an apparent upward or downward trend in emissions over duration, so that plot is not presented.

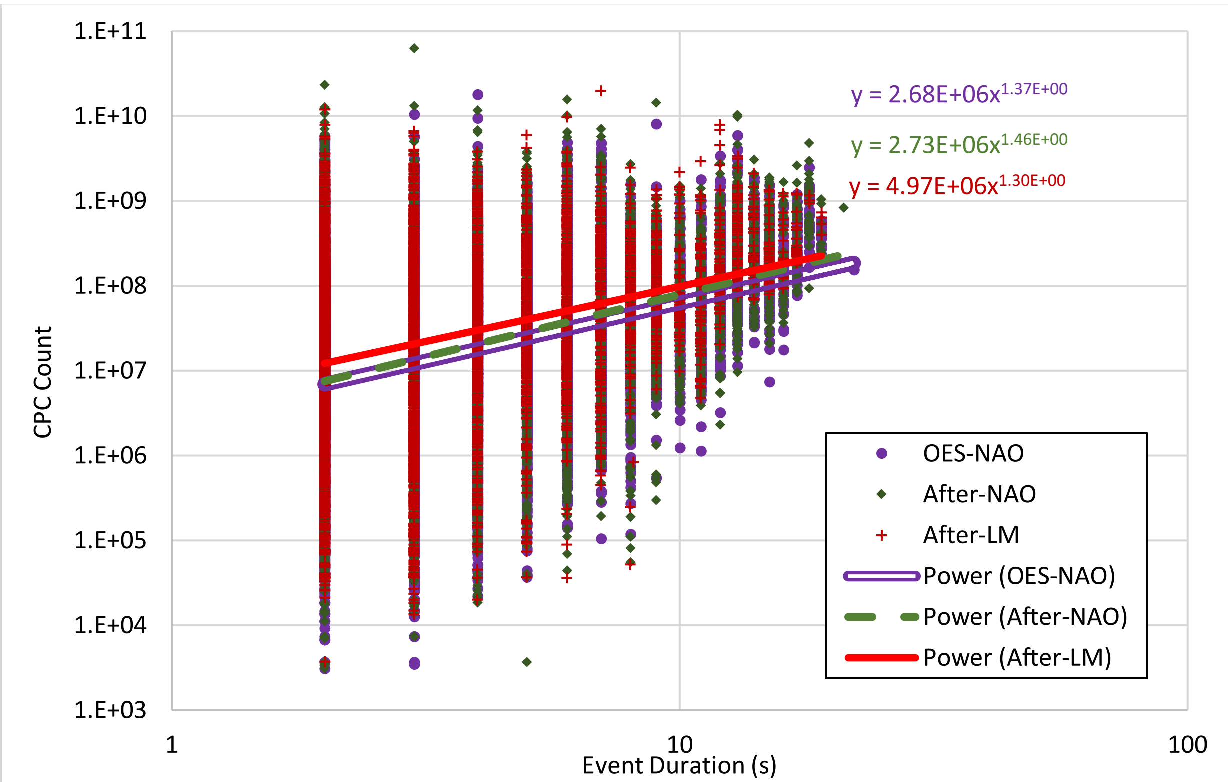

Figure 78. Trends in CPC count against braking event duration, categorized by friction material

Figure 79 presents the by-event total particle count against event total braking energy. The energy calculated in these plots does account for the differences in vehicle mass (it is not calculated purely on the speed change).

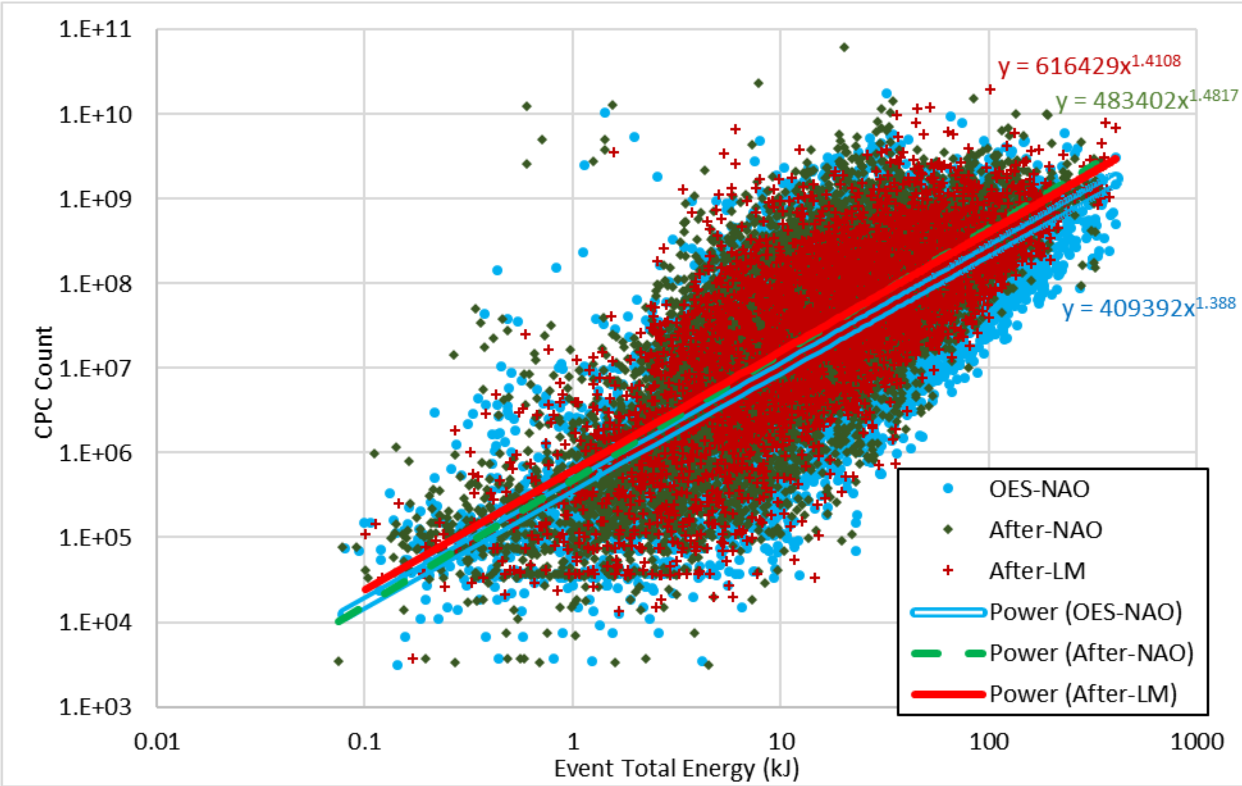

Figure 79. Trends in CPC count against braking event total braking energy, categorized by friction material

Figure 80 presents the by-event PM mass against the braking event total energy. As with the presentation of QCM mass against vehicle speed, it appears that the QCM was less responsive to total braking energy; this could be due to the noise in the instrument, especially in the time domain.

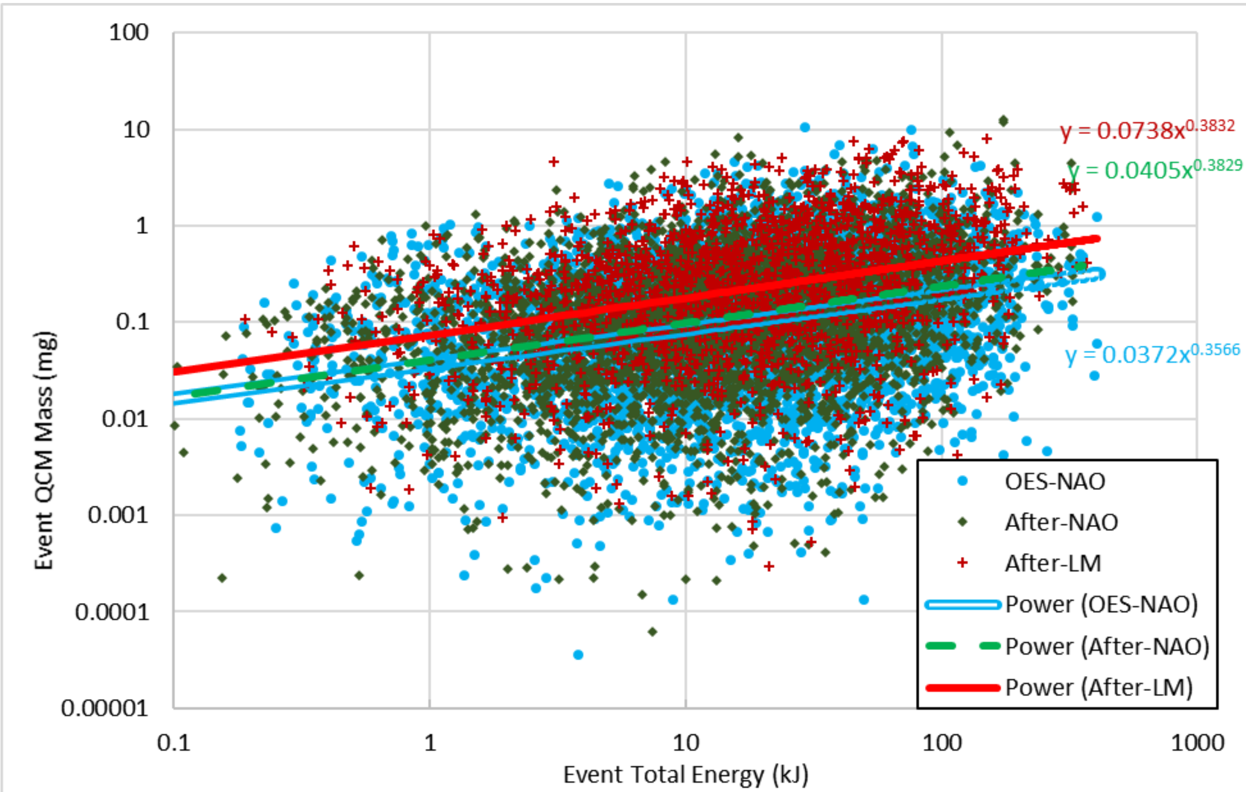

Figure 80. Trends in QCM braking event PM mass against braking event total energy, categorized by friction material

Figure 81 presents the by-event total particle number plotted against the average braking power for the event. It is interesting to see that the event duration, energy, and power all show identifiable responses in emissions. Given that the average power is the energy divided by the duration, it is not completely expected that power would also show such a clear trend.

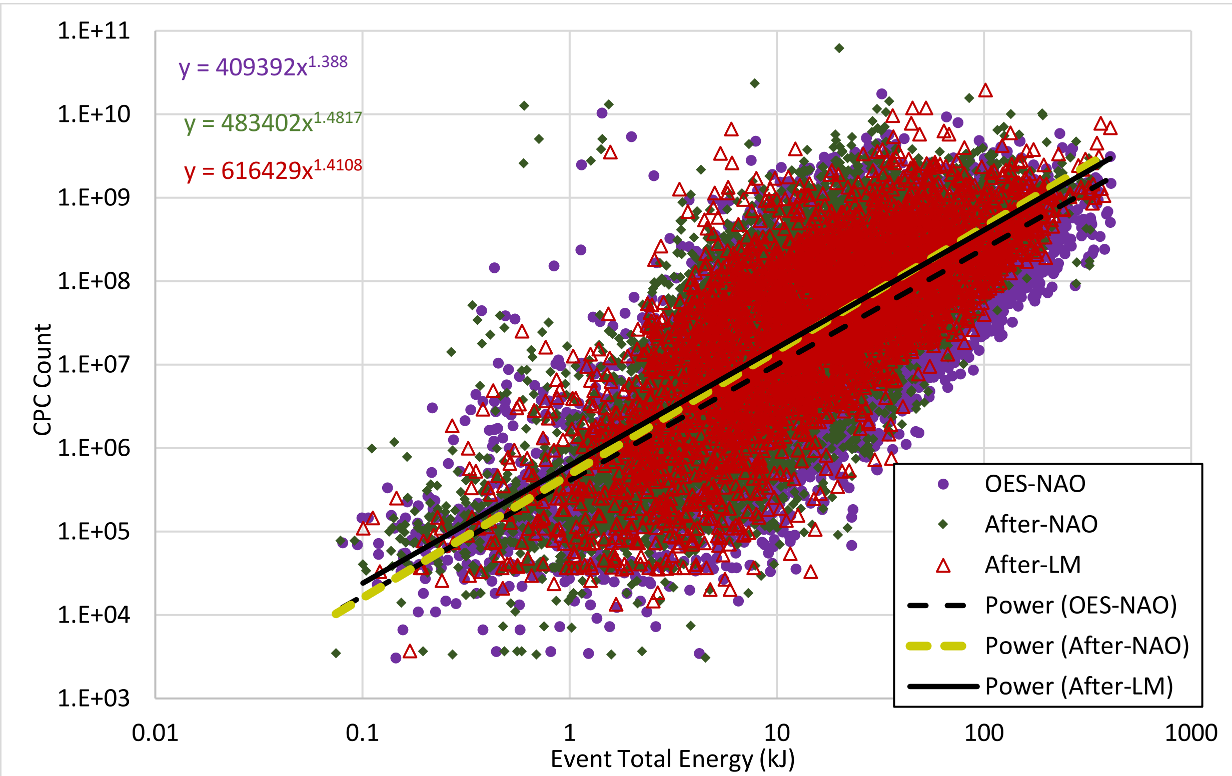

Figure 81. Trends in CPC count against braking event average braking power, categorized by friction material

Figure 82 presents the QCM-measured event PM mass against average braking event power. As with previous plots, the responsiveness appears reduced as compared to the CPC, but there are definite upward trends as shown in the power trendlines.

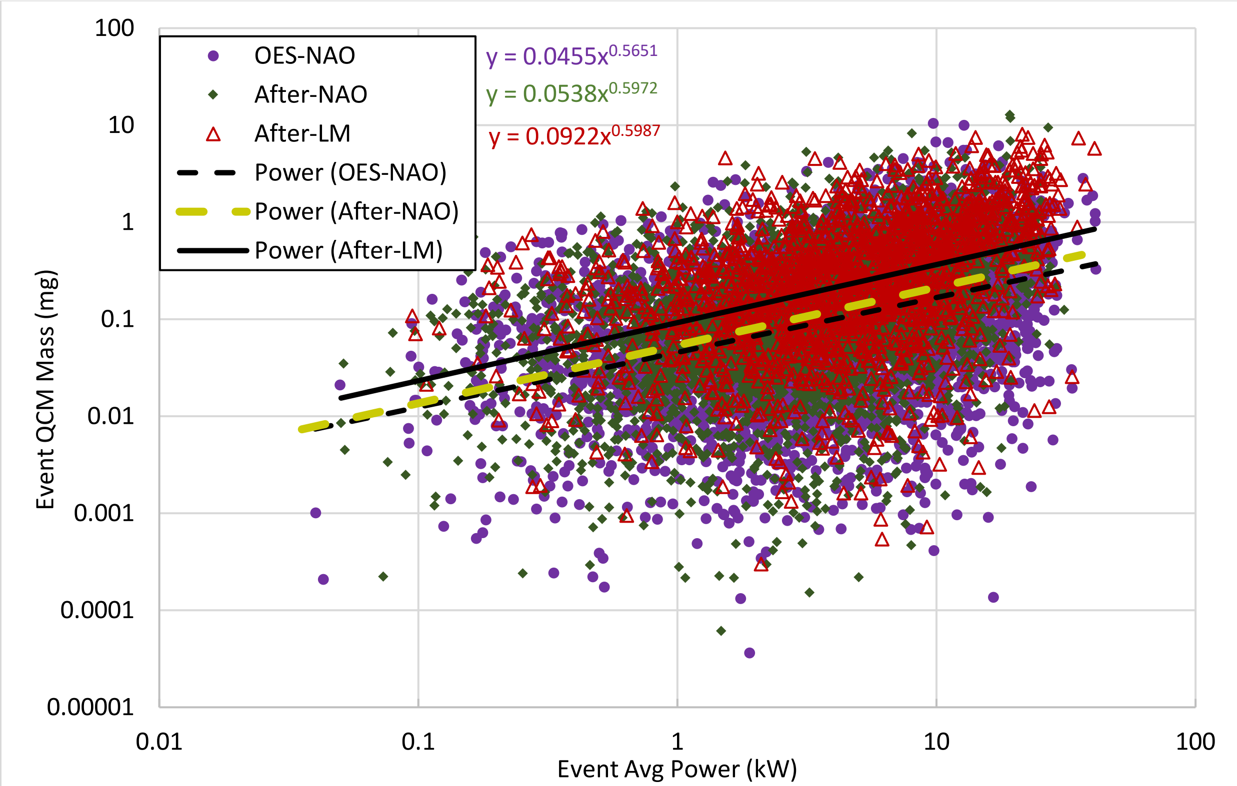

Figure 82. Trends in QCM brake event PM mass against braking event average power, categorized by friction material

It is not immediately clear what differences may have caused the relatively low correlation between emission rates and temperature in this work. Earlier studies, in which brake events were measured using matrix-style cycles instead of representative driving cycles, may have had a confounding factor that the type of braking events necessary to achieve high temperatures would necessarily be high energy events, and these two aspects were correlated in the previous works. There could also possibly be trends in temperature at brake temperatures beyond those encountered in this study, but the Caltrans data suggested that this would be encountered very rarely in on-road use. It is apparent that, of the parameters evaluated in this study, the energy and power are the most correlated to emission rates.

WTLP-Brake Tests

The test matrix included four tests over the WLTP-Brake cycle for the possibility of future benchmarking to other test programs that use that test cycle. Results are presented here primarily to allow for comparison between the WLTP-Brake and the CBDC results. Figure 83 presents a comparison of average emission mass results from the CBDC to two replicate tests over the WLTP-Brake for each of the front OES-NAO friction materials for the Camry and F-150. The WLTP-Brake emissions for the Camry are approximately one third of that over the CBDC; while for the F-150, the results from the two cycles are much more similar.

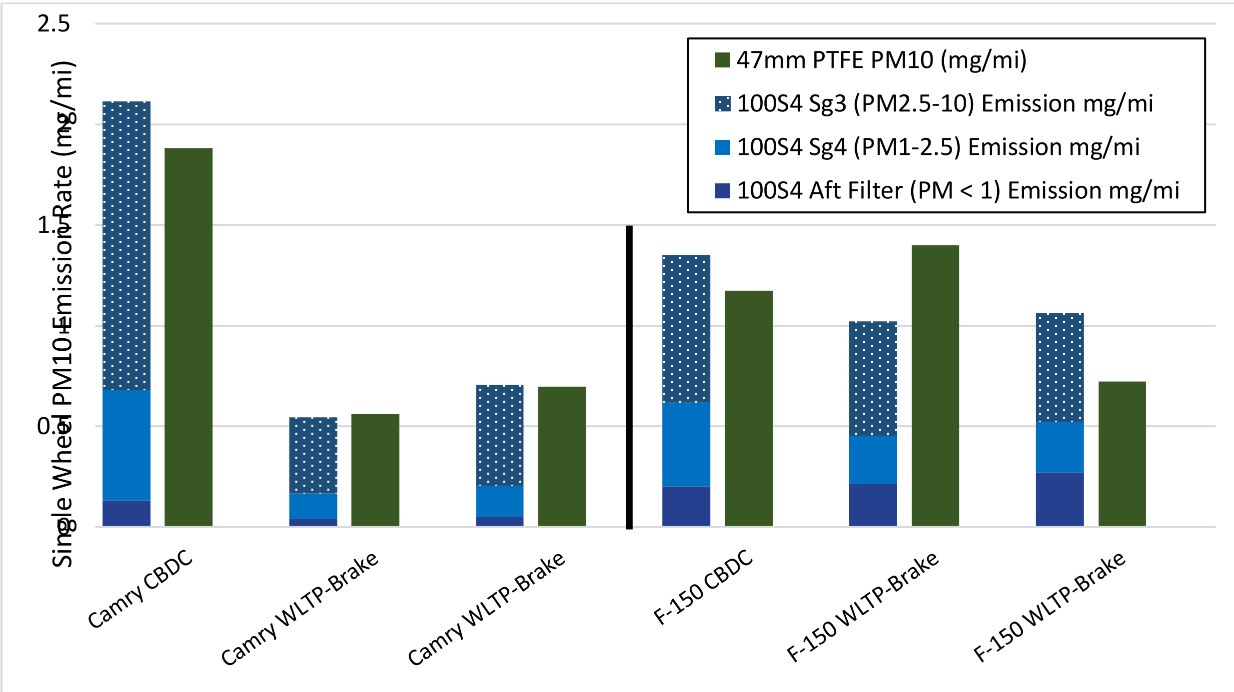

Figure 83. Comparison between the CBDC average results to replicate tests of the WLTP-Brake for the OES-NAO materials for the Camry and F-150 front axles

Discussion

Brake dynamometer testing for drive-cycle based representative particulate emissions is a relatively new concept and few standard procedures existed at the time of the initiation of project 17RD016. During this project, ERG and LINK worked to modify existing exhaust emissions and brake durability testing procedures to create new appropriate and effective brake PM emissions test procedures. Some of these new procedures have already been adapted for use by the PMP within the EU's JRC as they develop brake PM related procedures in parallel with this work.

One early project goal was to be able to perform component installation, burnishing, emissions testing, and assembly removal within a 24 hour period. This goal was created to maximize the number of tests that could be completed during the 17RD016 contract budget. This goal was achieved as LINK was able to conduct almost all tests within this amount of time, and LINK staff could keep a relatively consistent daily schedule throughout the work. In general, testing was reliable and no significant changes to the project plan were needed once testing began.

The results in the previous section show that the test setup was sensitive to the various parameters varied in the test matrix. The different vehicle platforms, brake pad materials, and test weights resulted in appreciable differences in PM mass emissions. This section aims to evaluate and discuss the experimental design, test methods employed, and test results.

Instrument Agreement in Mass Measurements

Generally, there was good agreement between the 100S4 and the 47mm Teflon filter mass measurement. Figure 84 presents a plot of the 100S4 vs the Teflon filter mass measurements, categorized by all emissions tests and the tunnel blanks. Note that two tunnel blanks were performed. In each, a single measurement of the 100S4 took place, and PTFE filters were placed in both legs of the filter system for parallel measurement. Both results for each blank are included as separate points with the same 100S4 value.

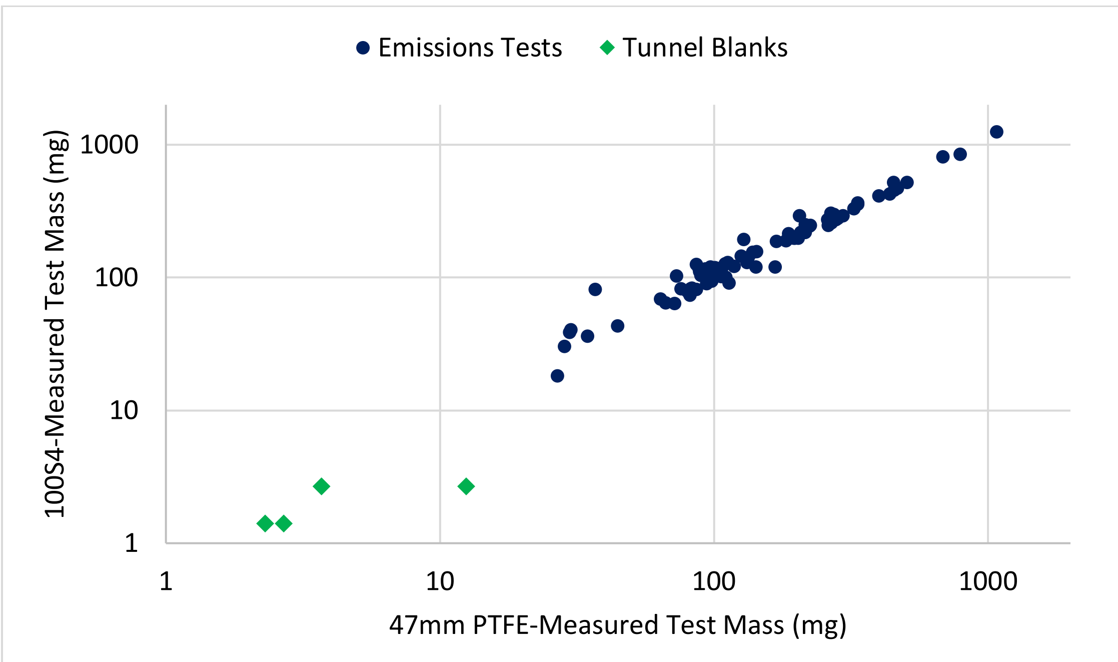

Figure 84. Agreement between 100S4 mass measurements (Y-axis) and 47mm PTFE mass measurements (X-axis) for all tests and tunnel blanks

Evaluation of the Burnish Procedure

The burnish procedure and dynamometer cycle were developed by ERG specifically for this work. The development of the cycle involved applying engineering judgement to early PMP burnish guidelines. This section is presented to evaluate the burnish procedure to determine the effectiveness of the cycle and inform any changes that may improve future testing. During burnish cycles, LINK operated the APS, EEPS, and logged brake temperature and hydraulic pressure data. LINK also ran the CPC during some burnish cycles but did not run that unit during all test days to reduce the amount of cleaning and maintenance required and prevent any delays to the test schedule. LINK did not run the QCM during the burnish cycle as that would have risked the unit becoming overloaded and losing data during the subsequent test cycle. So, plots of particle size, particle count, and the logged parameters of hydraulic pressure, speed, and brake temperature are available to evaluate the burnish cycle. For brevity, not all combinations of plots are shown; a representative plot is presented in this section for each vehicle model. The burnish cycle can be evaluated by determining where in the cycle the measured values become stable (given that the cycle is made up of many repeats of the same speed trace)

Camry. Figure 85 presents the cumulative particle count measured during the burnish cycle on Test Day 59. This test day was the Camry rear assembly, equipped with aftermarket low metallic pads. The CPC trend stabilizes around 18,000 seconds into the test cycle (approximately 40% through the cycle).

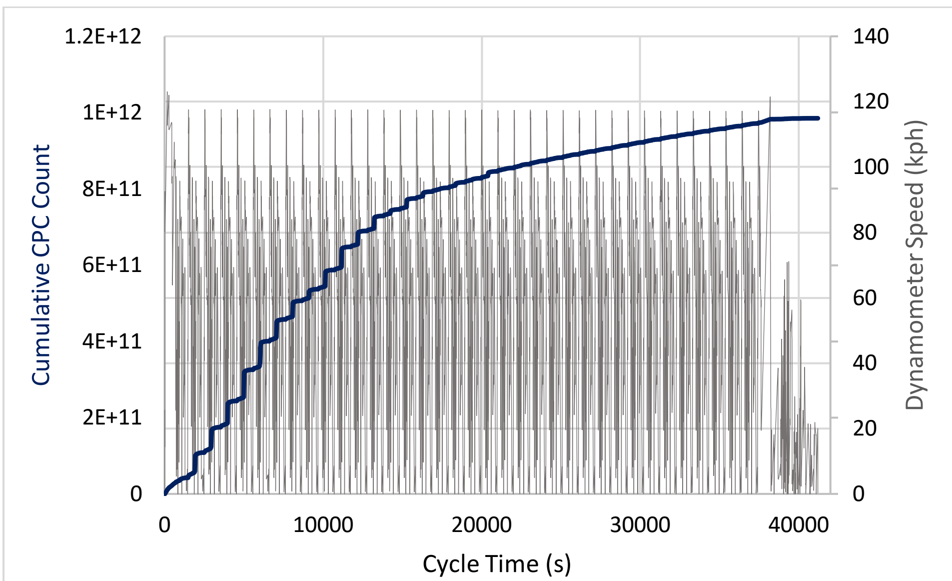

Figure 85. Cumulative CPC Particle Count Measured during a burnish of the Camry rear Aftermarket LM pads

Civic. Figure 86 presents the cumulative particle count measured during the burnish cycle on Test Day 84. This was a burnish of the Civic front assembly with OES-NAO friction materials installed. The particle count trend appears to stabilize at approximately 13,000 seconds (approximately 32% through the cycle).

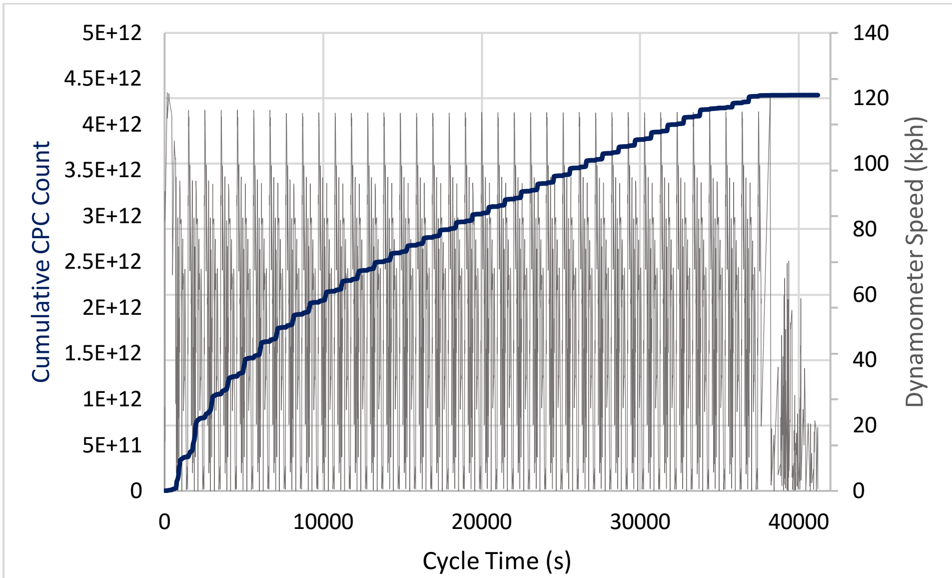

Figure 86. Cumulative CPC Particle Count Measured during a burnish of the Civic front OES-NAO pads

F-150. Figure 87 presents the calculated brake effectiveness over the burnish cycle of the F-150 front assembly during Test Day 63. Brake effectiveness is calculated by the deceleration torque divided by the brake hydraulic pressure and is proportional to the coefficient of friction between the pads and rotors. Each point on the plot represents the average effectiveness during a single braking event. This burnish took place with aftermarket metallic pads installed. The trend in effectiveness appears to stabilize at around 22,000 seconds (approximately 53% through the cycle). Note that the values are only an approximation of coefficient of friction and so they have a repetitive scattering across the different braking events. This is likely because there is some internal resistance in the hydraulic system that must be overcome such that the effectiveness is disproportionately lower in low intensity braking events (i.e. a larger proportion of the hydraulic pressure is used only to move the caliper pistons and pads prior to making significant contact with the rotors).

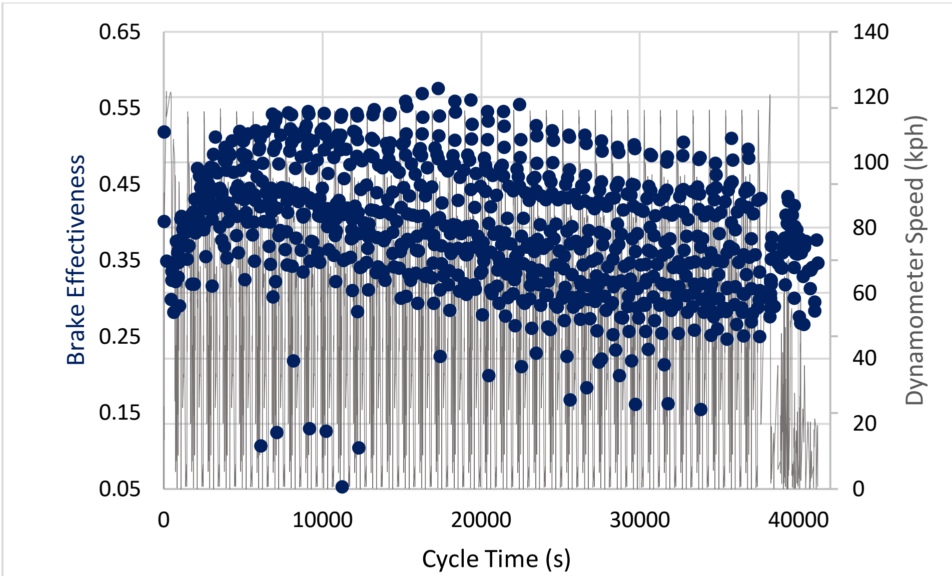

Figure 87. Calculated brake effectiveness (proportional to coefficient of friction) during a burnish of the F-150 front aftermarket metallic pads

Prius. Figure 88 presents the calculated brake effectiveness during the burnish of Test Day 49. This was a test of the front assembly with aftermarket-NAO friction materials installed. The effectiveness trend appears to stabilize at approximately 10,000 seconds into the cycle (24% through the cycle). The burnish of the Prius was a point of concern given that the burnish cycle was developed based on an assumed total amount of braking energy required. Given the simulation of the Prius' regenerative braking system, the friction materials for this vehicle did not receive the same amount of relative burnish energy as did the materials of the other vehicles. To further investigate this concern, Figure 89 presents another plot for the Prius, the cumulative particle count during the burnish for Test Day 27. This test day was a test of the rear assembly with OES-NAO materials. The figure indicates that the stabilization took place later in the cycle than that shown for the previous vehicles. It appears to stabilize at around 35,000 seconds (85% though the cycle. In future tests, to mitigate this potential concern, it may be beneficial to turn off the regenerative braking simulation during the some or all of the burnish cycle of regenerative braking-equipped vehicles.

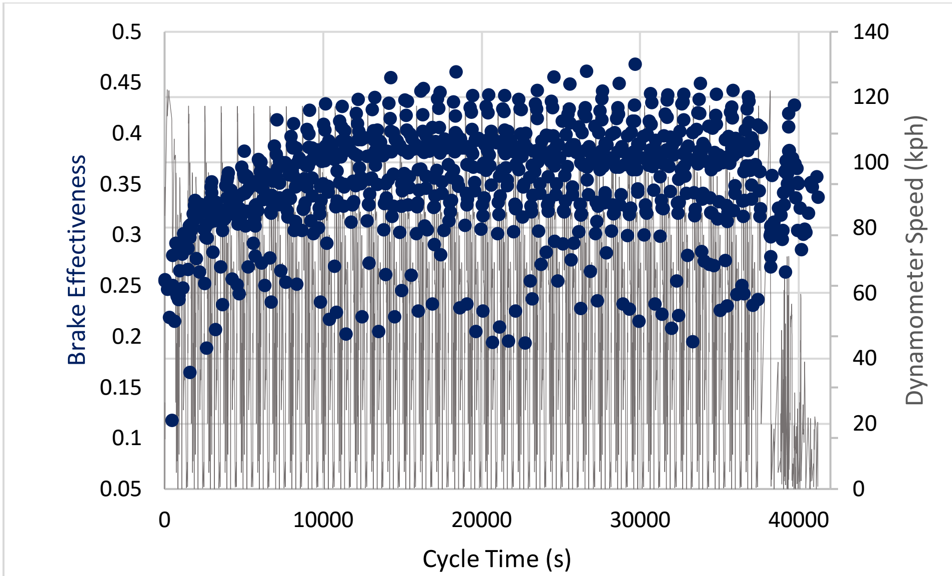

Figure 88. Calculated brake effectiveness (proportional to coefficient of friction) during a burnish of the Prius front aftermarket NAO pads

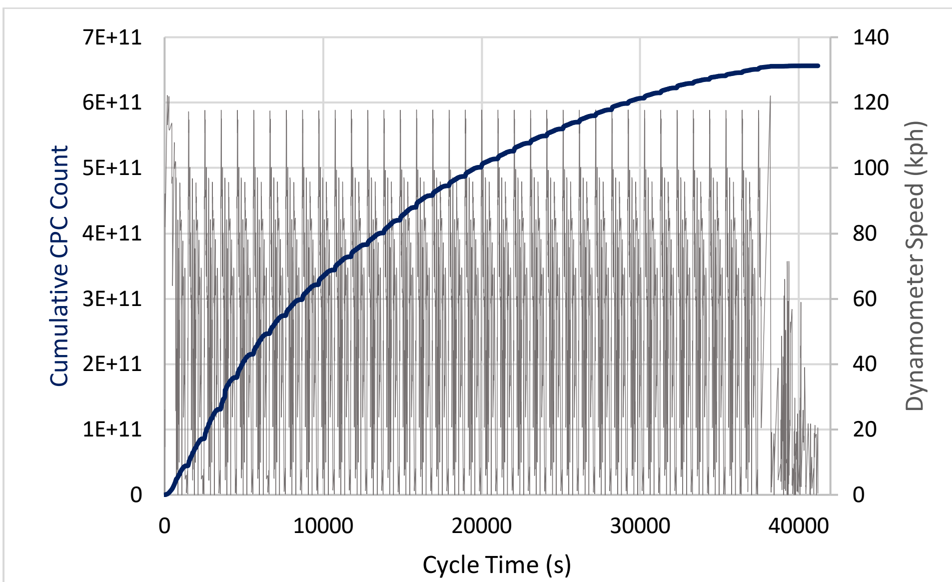

Figure 89. Cumulative CPC Particle Count Measured during a burnish of the Prius rear OES-NAO pads

Rogue. Figure 90 presents particle size data for the burnish cycle of Test Day 38. This test was a front-assembly test of the aftermarket-NAO pads for this vehicle. The APS size distribution (color coded by particle count) is the upper plot, and the EEPS side distribution (also color coded by count) is the lower plot. APS data appears to stabilize around 25,000 seconds (60% of the cycle), and the EEPS appears to stabilize around 30,000 seconds (73%).

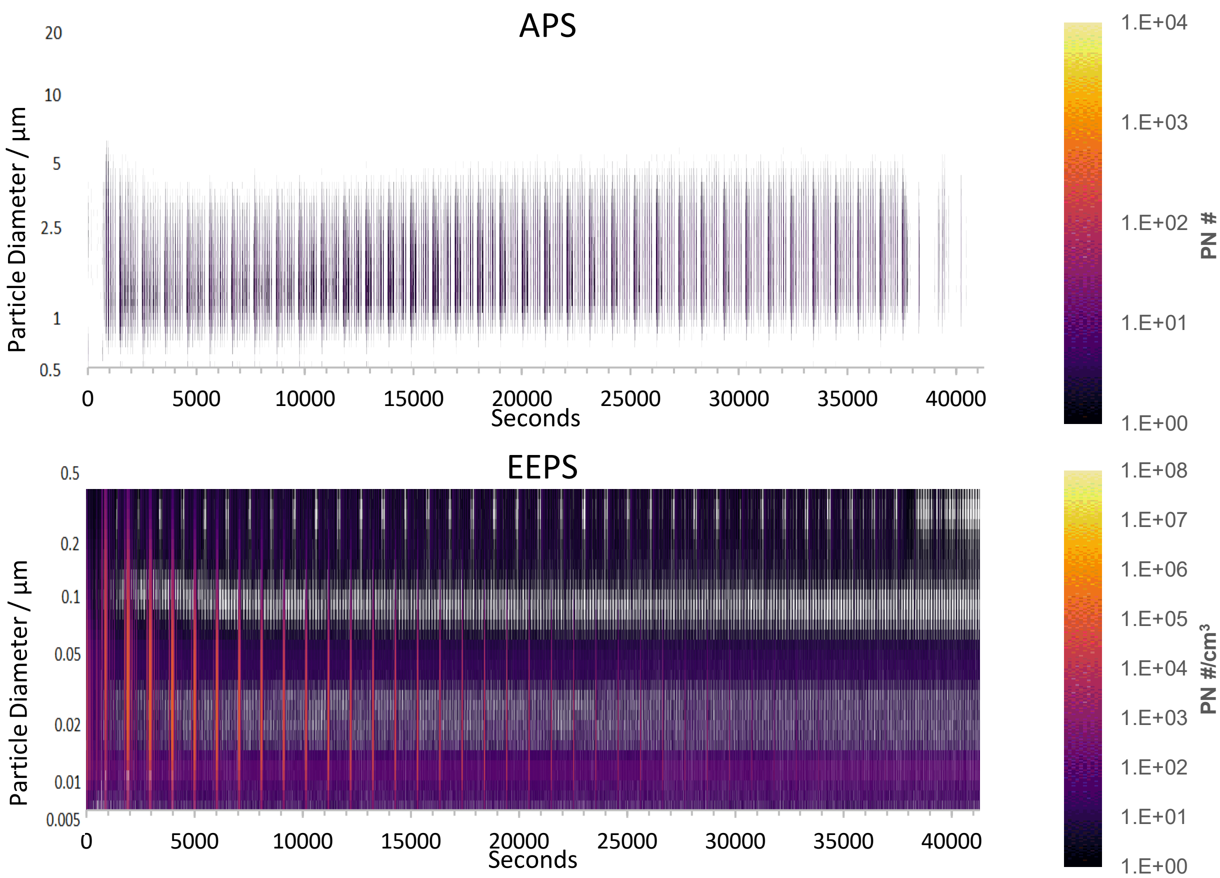

Figure 90. Particle size data during the burnish cycle of the Rogue front aftermarket-NAO pads. The upper plot presents the APS result and the lower presents the EEPS.

Sienna. Figure 91 presents particle size data for the burnish cycle of Test Day 13. This test was a rear-assembly test of the OES-NAO pads for this vehicle. The APS size distribution is the upper plot, and the EEPS side distribution is the lower plot. The APS data appears to stabilize around 20,000 seconds (49% of the cycle), and the EEPS appears to stabilize around 27,000 seconds (66%).

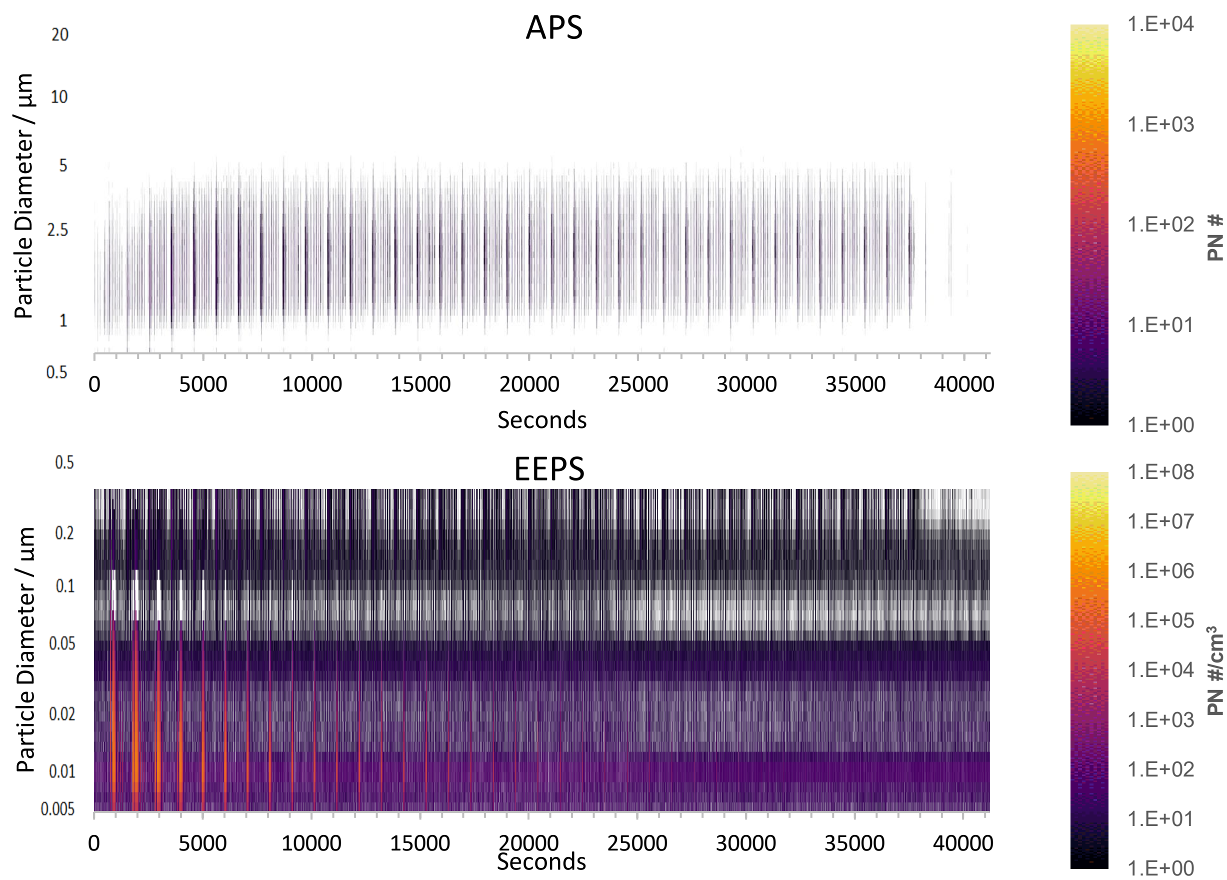

Figure 91. Particle size data during the burnish cycle of the Sienna rear OES-NAO pads. The upper plot presents the APS result and the lower presents the EEPS.

The burnish cycle appears to have included a large enough amount of braking energy for all friction materials to reach a stable condition from the various metrics presented in this section. The Prius rear assembly was a point of concern because it appeared to reach a stable level just as the burnish cycle was ending. This concern could be mitigated by disabling regenerative braking simulation during burnish of this type of vehicle in future testing. For all other vehicles, stabilization appeared to be reached at or before 30,000s into testing. So, the burnish cycle could potentially be reduced in length by up to approximately 3 hours and still achieve the desired level of stability for conventional-braking vehicles.

The CPC plots indicate that particle count emissions are elevated during the early stages of burnish after installation. Given that the duration of time that this elevated emission rate was observed (~5-6 hours typically), it is not likely that the burnishing process in-use has an appreciable effect on the overall emissions inventory given that brake pads typically last for thousands of hours of operation, therefore this portion of brake service will not appreciably affect inventory values.

Evaluation of the Prius Regen Simulation

LINK used their internal 'DutyCycleRegen' program for the simulation of the Prius on the dynamometer. Given that brake dynamometer testing for emissions is a relatively new field, and the Prius (and most other regenerative braking equipped vehicles) operate using a proprietary algorithm, there is not a common or recognized procedure or approach for simulation of the regenerative system on a brake dynamometer. This section aims to evaluate the accuracy of the regenerative system used in this work. The Prius ETW was 1,606 kg in this work, and the Camry was the closest vehicle in weight at 1,668 kg ETW and so it is presented as the non-regenerative benchmark for comparison.

The first comparison is between the overall average brake torque measured during all dynamometer tests. Table 26 presents the overall average brake torque for Camry and Prius for front and rear assemblies. For direct comparison, only OES-NAO and Aftermarket-NAO pads are included (as the Prius was not tested with metallic pads). It can be seen that the Prius braking torque averages less than half of that of the Camry due to the simulation of the regenerative braking system.

Table 26. Comparison of Overall Average Measured Brake Torque for Camry and Prius

Test Vehicle	Avg. Front Brake Torque (nm)	Avg. Rear Brake Torque (nm)
Camry	138.4	48.3
Prius	55.9	20.5
Prius % of Camry Torque	40.4%	42.5%

Figure 92 presents an example instance of the source of the difference in torque trends between the Camry and Prius. The figure depicts a selected interval of the CBDC test cycle and presents traces of the speed and front brake hydraulic pressure for the two vehicles. The figure shows an example of how the hydraulic brake pressure differs during the same deceleration event, even approaching zero during moments that are most favorable to the regeneration system operation based on the regeneration parameters presented previously.

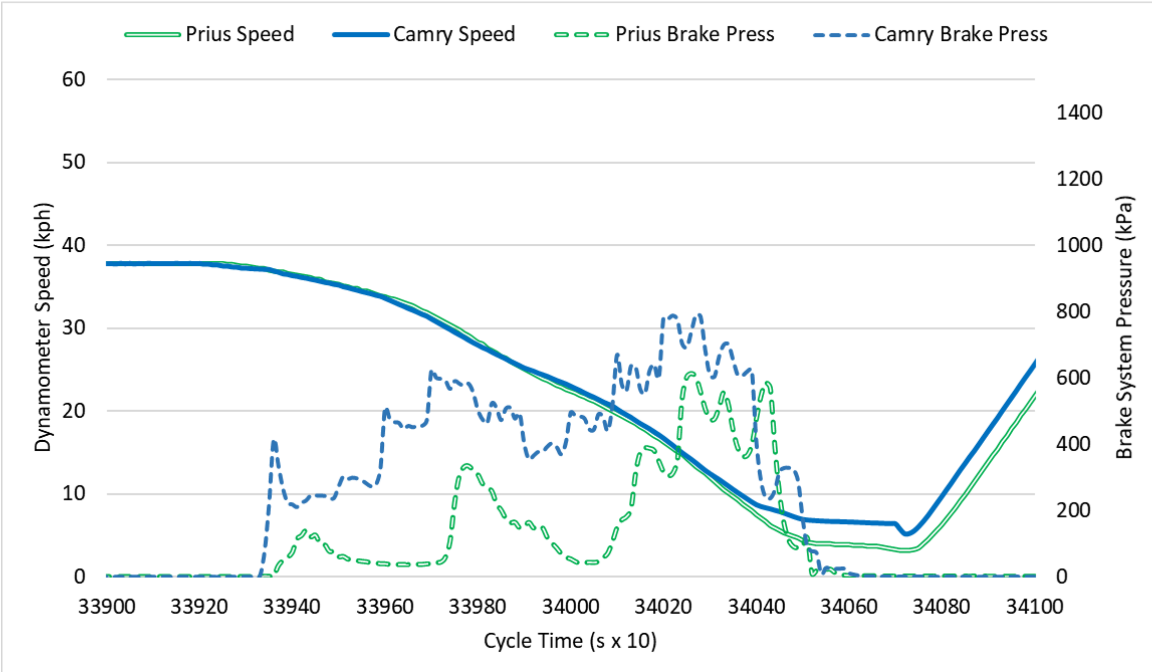

Figure 92. Speed and Brake Pressure traces for a selected point of the dynamometer test cycle for a test of the Camry and a test of the Prius

Another method to evaluate the accuracy and effectiveness of the regenerative system simulation is to make a comparison between the test track experiments and the dynamometer tests. On the test track, all models were driven over the WLTP-Brake cycle to inform the dynamometer cooling air flow setting process. During the cooling air flow setting, the WLTP-Brake Trip 10 was used as the test cycle. Comparing the brake heating trends between the dynamometer and the test track over Trip 10 can give an indication of the accuracy of the regenerative braking simulation. Figure 93 presents temperature traces for the front brake assemblies of the Camry and Prius operating over the WLTP-Brake Trip 10 on the test track and brake dynamometer. It can be seen that the rate of brake heating necessary to follow the same trace is much lower for the Prius than for the Camry. It can also be seen that the heating rates for the Prius are very similar between the test track and brake dynamometer, indicating that the regenerative simulation results in similar brake usage on the dynamometer as on the test track. Figure 94 presents similar data for the rear brake assemblies of both vehicles, and similar results are observed.

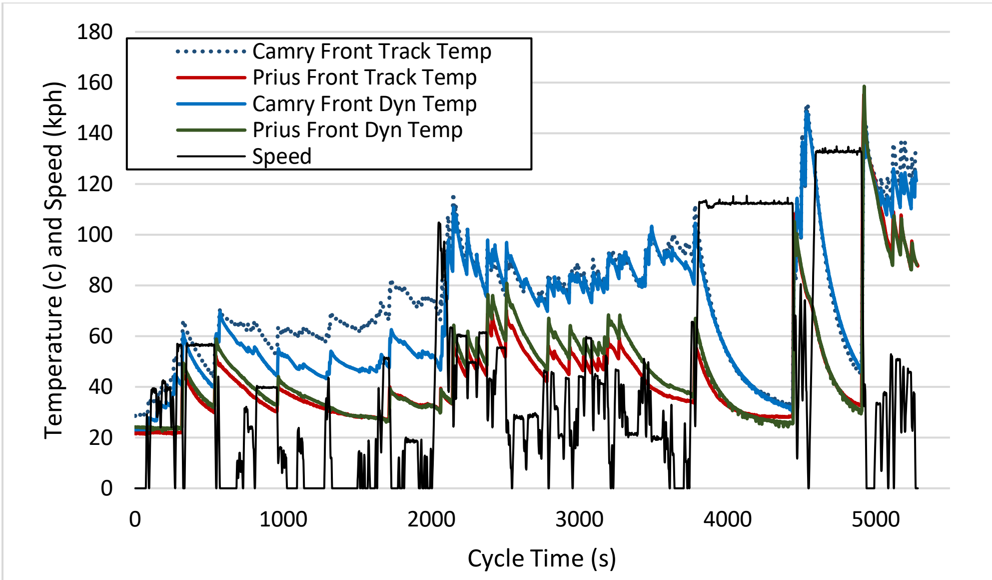

Figure 93. Temperature Traces of the Front Brakes of the Camry and Prius over WLTP-Brake Trip 10, operating on the test track and brake dynamometer

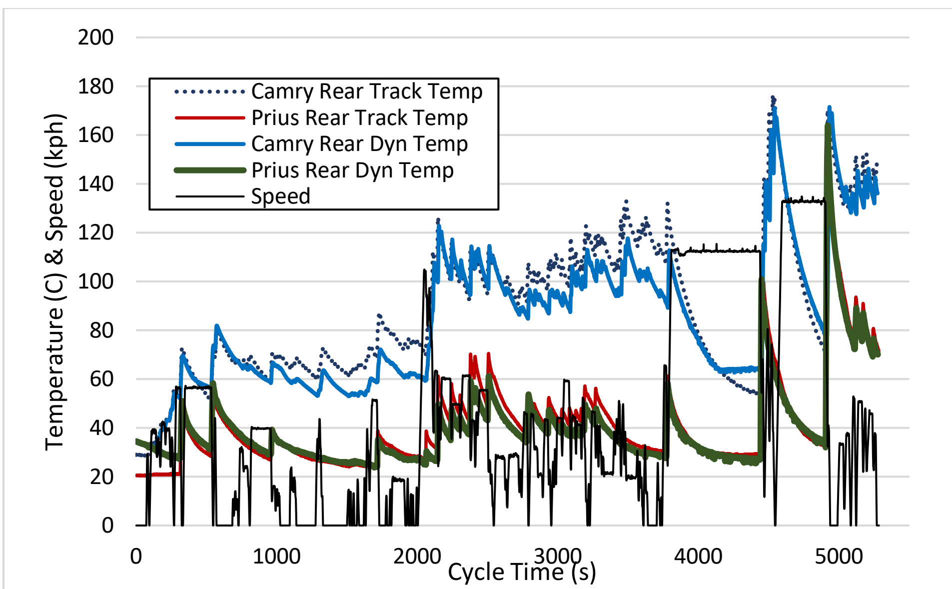

Figure 94. Temperature Traces of the rear Brakes of the Camry and Prius over WLTP-Brake Trip 10, operating on the test track and brake dynamometer

Reference Tests

The test matrix included additional replicate tests of one configuration to be run periodically throughout the program to potentially identify any sources of drift in the testing system. The reference test was chosen to be the front axle assembly of the F-150, equipped with OES-NAO friction materials and operating at ETW test weight. Figure 95 presents mass emission and particle count measurements by date. The original intent was to distribute the reference tests approximately equally throughout the program, however the 4th test was swapped into the middle of the testing program due to a test that was scheduled as a WLTP-Brake being inadvertently run as a CBDC test and therefore matching the reference test parameters.

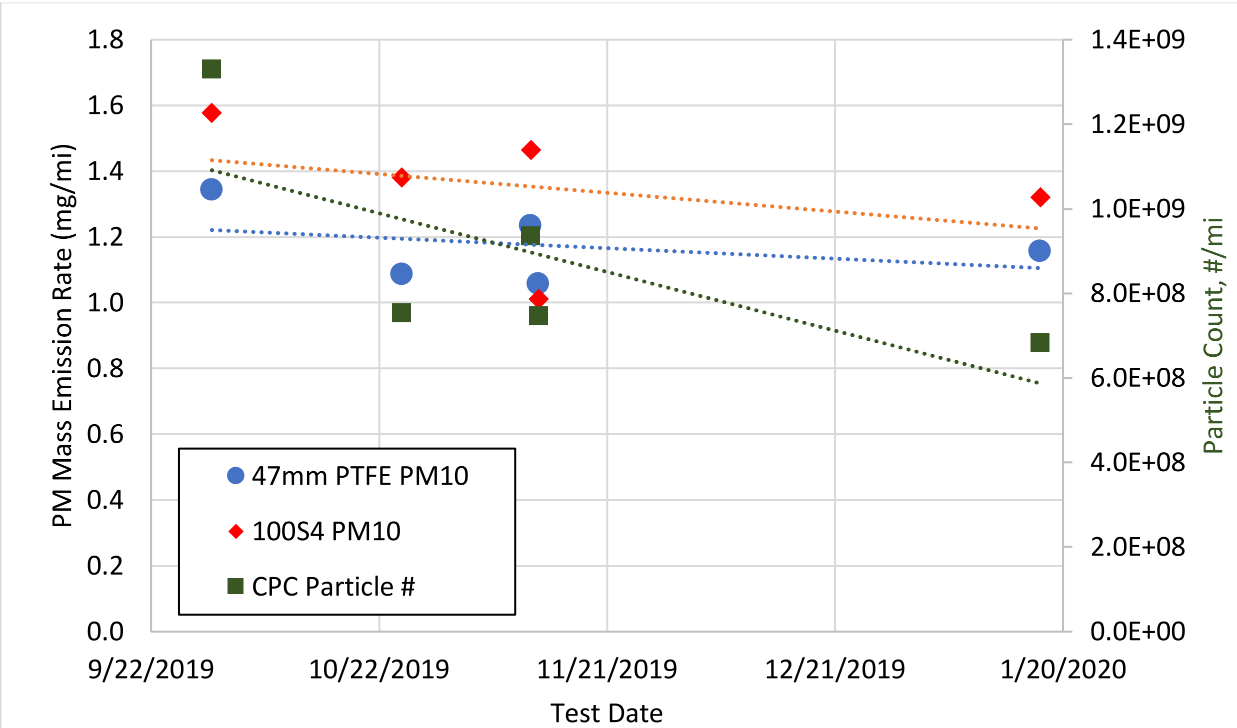

Figure 95. Reference trends by date for the 47mm PTFE and 100S4 PM10 mass measurements (left axis); and CPC particle count (right axis)

Trendlines fit to the test date are included for each of the three sets of values. Both mass measurement types have a minor downward trend over time. This appears to be driven primarily by the first test, which has the highest values for all three measurement types. From the time of the second test date, there is no discernable down trend in either mass measurement. The CPC trend has a steeper apparent down trend; the first value is the highest and the final value is the lowest. However, for both the mass and particle count plots, the noise in each variable appears to be equal or greater in magnitude than the strength of the trends. For this reason, ERG did not apply any corrections to the data based on test date.

Issues encountered

In early November, the humidity controller of CVS airflow loop failed, causing the humidity to eventually exceed the test limits (Limits are 50 +/- 10 %RH). LINK ordered a new control board to solve the problem. In the meantime, LINK continued running only the burnish cycle with the existing humidity controller for multiple upcoming tests without running the test cycle. This interim schedule lasted for approximately 1 week up until the humidity controller was repaired. After this, LINK re-mounted the previously burnished brakes, ran a partial burnish cycle (1 hour) to stabilize the contact surface of friction couple, and measured emissions during the actual test cycle. *This issue resulted in slight downtimes to re-assemble tested parts and run the test cycle separate from the burnish cycle.*

LINK encountered another issue with the dynamometer control computer that aborted a test while conducting the burnish cycle. After troubleshooting this computer with limited staff during the holiday schedule, it was replaced with a new computer. *This issue caused approximately 5 days of delay in the test schedule*.

Comparison of Results to Literature

Studies in literature cite a variety of brake PM emissions test procedures and test cycles. As the concept of brake PM emissions testing for environmental protection is relatively new, there are few standard procedures and a wide variety of estimates of braking PM emissions factors. ERG reviewed a key study that identified a range of published light-duty brake emissions rates.[11] This range of results, converted to mg/veh•mi for comparison to this study, is presented in Table 27. The results for this study tend to be lower in terms of PM2.5 and generally in agreement for PM10 as compared to literature.

Table 27. Ranges of vehicle-level PM emission rates (mg/mi), summarized in literature and for the vehicle models in this study

	Literature Range for Overall LD Emissions Factor (mg/mi)	Range of Emission Rates by Model in this Study (mg/mi)
PM2.5	3.4 – 8.8	1.0 - 2.7
PM10	4.8 – 12.8	3.3 - 13.9

Figure 96 presents a different review of past studies of brake wear emission rates of PM2.5 and PM10 for light- and heavy-duty vehicles.[12] The overlaid rectangles represent the range of vehicle-level emission rates by model in this study. In the figure, squares represent heavy-duty vehicles and circles represent light-duty vehicles (including almost all the same sources as used to generate Table 27). The figure again shows a high level of agreement with literature in terms of PM10, but the literature values are all higher than the range of results of this study for PM2.5. Notably, the findings from this study are lower in both PM2.5 and PM10 than values currently in EMFAC.

[11] Grigoratos, Theodoros & Martini, Giorgio. (2014). Brake wear particle emissions: a review. Environmental science and pollution research international. 22. 10.1007/s11356-014-3696-8.
[12] Sonntag et. al. *Modeling Brake and Tire Wear Emissions in Regulatory Models in the United States*, 2018 ISES-ISEE Joint Annual Meeting

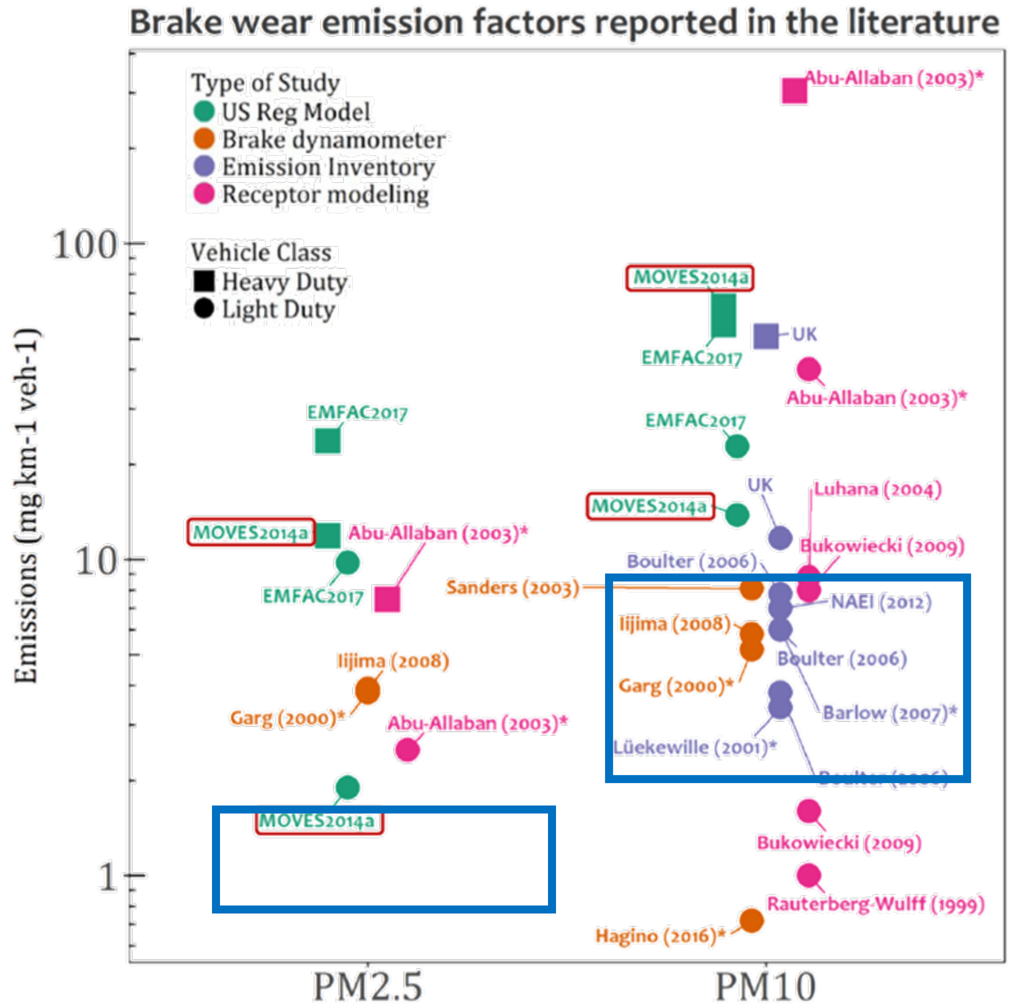

Figure 96. Various literature values for brake emissions, with the ranges from this study overlaid for comparison

PM emission rates cited in literature do appear to be trending down with time. Older emissions models may have been reliant on by-event type brake measurement with much higher temperatures (up to 400 °C), higher deceleration rates, and higher speeds. The prevalence of metallic friction materials is decreasing in the fleet with time and are therefore likely to be less prevalent in recent research. Also, friction material and rotor life has extended significantly in recent years, with current (OES and good quality aftermarket) formulations averaging 50-90k miles of life; based on the presented component mass loss vs PM emission plots, the longer life is indicative of lower PM emission rates.

Implementation into EMFAC

Base Emission Rates

The Test Cycle Development section introduced the concept of the CBDC's represented distance, which is the distance of actual on-road travel that is represented by the braking events in the cycle when accounting for cooling and extended on-road cruises that were abridged to minimize the time required to run the cycle on the dynamometer. Just as the events that make up the CBDC have a represented distance, they also equivalently have a represented time, both for the overall cycle and for each speed segment. These times, along with the represented distances, can be used to calculate represented average speeds to facilitate implementing the results of this work into EMFAC. Units are presented in U.S. Customary to facilitate implementation into EMFAC. Table 28 presents the represented times and distances for the overall CBDC and the speed segments as well as the resulting calculated average speed.

Table 28. Represented time and represented distances for the overall CBDC and each speed segment

Cycle/Segment	Represented Distance (mi)	Represented Time (s)	Represented Average Speed (mi/hr)
CBDC Overall	81.56	11,564	25.39
0-21 kph	3.83	2,911	4.73
21-69 kph	47.31	5,438	19.46
69+ kph	48.33	3,215	54.12

The average overall speed for the CBDC is very near the UC average speed of 24.8 mph. For this reason, ERG recommends treating the overall-cycle results as the base emission rate (BER) for braking for each vehicle type (conceptually treating it similarly to a UC exhaust emission result). However, in this work, the average speed of the cycle does not necessarily reflect the same type of operation that would fall completely in that speed bin. So, the SCF in the 25 mph bin, described in the next section, will not necessarily be set to 1. In this work, with our limited number of test vehicles, results can be averaged for the conventional passenger cars (Civic, Camry, Rogue), the light trucks (F-150 and, based on weight class, Sienna), and the hybrid vehicle with regenerative braking (Prius). Unless cargo-carrying or higher weight operation is to be modeled for light-duty vehicles in EMFAC, only the ETW test results are needed for this approach. The Vehicle-Level Mass Results section presented balances of pad materials at vehicle ages of 3 and 11 years. The BER in EMFAC indicates the new-vehicle emission rates (to be adjusted by deterioration as described below). BERs are developed here by using the fit between 3- and 11-year emission rates and taking only the intercept as the zero-age value. Table 29 presents the BERs (averages for all models within a vehicle type); these new-vehicle values can be used as the basis of EMFAC BERs for light-duty braking PM emissions.

Table 29. The recommended BERs by vehicle type for PM2.5 and PM10

Vehicle Type	PM2.5 BER (mg/mi)	PM10 BER (mg/mi)
Conventional Passenger	1.62	8.18
Light Truck	1.54	6.94
Regenerative-equipped	0.93	3.30

Speed Correction Factors

ERG used the Method 2 approach described in the Results by Vehicle Average Speed section to develop SCFs. This involved using the QCM data on a minute-by-minute basis to determine the PM emission rates in five equally-spaced bins of vehicle average speed. The bins were sized in 15 mph increments in this analysis. Figure 97 presents the resulting overall SCFs for PM2.5 and PM10. The intended use of the brake PM SCFs developed in this work is to multiply the overall test emission rate (considered the BER for the purposes of speed correction) from the 100S4 by the SCFs to determine the emissions from trips with average speeds in each bin range.

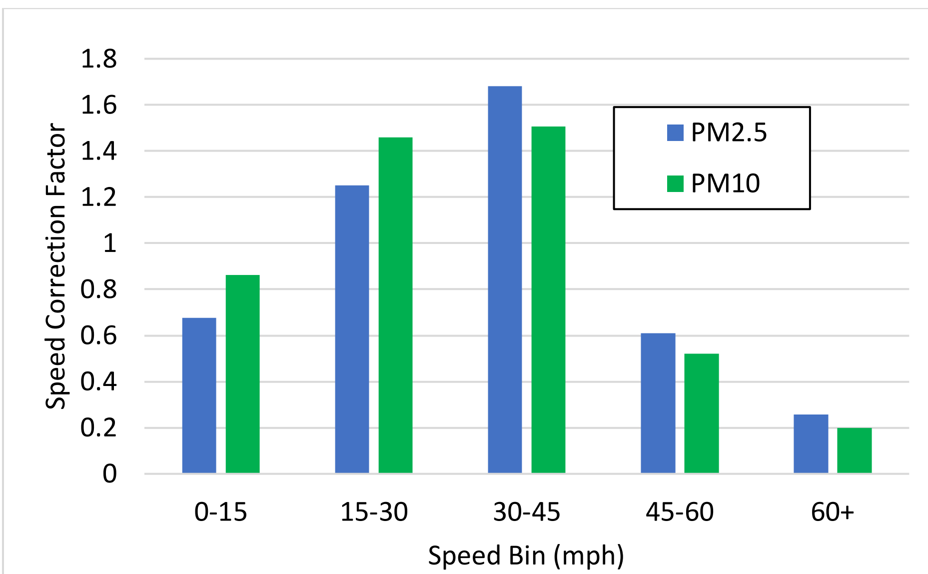

Figure 97. Recommended Overall Speed Correction Factors for PM2.5 and PM10

ERG further divided the SCF data into three vehicle types: passenger cars, light trucks, and regenerative braking equipped cars. The most straightforward method for implementation to EMFAC is to apply piece-wise linear fits to the PM2.5 and PM10 speed bins for each vehicle type. ERG performed these fits to the two PM cutpoints and three vehicle types to determine the SCF values shown in Table 30. The SCFs in the table that can be applied to each overall CBDC result to calculate emission rates for trips of average speeds falling within the different ranges. The factors are given separately for PM2.5 and PM10- these factors are to be multiplied by a given overall test cycle result for PM2.5 and PM10, respectively.

Table 30. Recommended SCFs by speed for PM2.5 and PM10 for three light-duty vehicle types.

Average Speed (mph)	Passenger Cars		Light Trucks		Regenerative Cars	
	PM2.5	PM10	PM2.5	PM10	PM2.5	PM10
5	0.612	0.735	0.604	0.815	0.262	0.399
10	0.786	0.909	0.791	1.014	0.553	0.706
15	0.961	1.082	0.979	1.214	0.844	1.013
20	1.136	1.256	1.167	1.413	1.134	1.321
25	1.314	1.399	1.321	1.495	1.365	1.503
30	1.494	1.513	1.442	1.459	1.535	1.560
35	1.675	1.626	1.563	1.423	1.706	1.618
40	1.567	1.486	1.454	1.256	1.624	1.494
45	1.170	1.093	1.116	0.958	1.290	1.187
50	0.773	0.699	0.778	0.660	0.957	0.881
55	0.516	0.450	0.553	0.459	0.708	0.650
60	0.399	0.345	0.440	0.355	0.543	0.494
65	0.282	0.240	0.327	0.251	0.378	0.339

Recall these SCFs were created using the previously-described Method 2, based on the ratio of the emission rate within the speed bin to the overall cycle (i.e. the BER) emission rate. Note that the SCF for the 25 mph bin does not equal 1; this indicates that operation completely within that bin of trip average speed does not have the same emissions as operation across all speeds even though that wider operation has the same overall average speed.

Deterioration Rates

This study involved testing friction materials that were relatively new; they were purchased new, operated over an aggressive burnish cycle, and then were tested over the CBDC. As a result, the project did not generate emissions measurements indicating the deterioration of friction materials over time. However, vehicles periodically have their friction materials replaced with new components as the vehicle ages, potentially "resetting" the brake PM emission rates as compared to the age of the vehicle. However, the trend in change of installed friction materials was presented in the Representative Test Vehicle and Friction Material Selection section. Trends in the change in installed friction materials over time can be used to estimate deterioration rates in braking PM emissions as vehicles age. LINK business intelligence was used to estimate the balance of materials at vehicle ages of 3 and 11 years, which were presented previously in Table 21. Note that the emissions factors presented previously in Table 22Table 21 were presented on the basis of a 7-year-old vehicle. It is possible to fit a linear interpolation to the emission rates for vehicle ages of 3 and 11 years to yield both a deterioration rate (the slope of the linear fit) and a new-vehicle emission rate estimate (the intercept). The resulting linear fits can be used to model emissions deterioration as a function of vehicle age.

The LINK business intelligence included estimates of the balance of the three friction materials in use based on vehicle age. However, in this test program, only two vehicles were tested with LM brake pads (Camry and F-150), and the migration toward these pads represents a significant effect on the estimated emissions deterioration. Because no data is available for the metallic pads mounted to other vehicles, the Camry data will be used to estimate passenger car deterioration, and the F-150 will be used to estimate truck deterioration. For the estimation of deterioration of regenerative-equipped vehicles, the lack of data regarding metallic pads is less of a concern because of the low replacement rate for these vehicles (and, ERG was not readily able to find any LM pads available for the Prius in the aftermarket at all).

Estimates of the deterioration rate and new vehicle emission rates are presented in Table 31 for PM2.5 and Table 32 for PM10. For the calculation of emission rate at any vehicle age, the deterioration rate is multiplied by age and added to the new-vehicle estimated rate (alternatively, the factors from Table 21 can be used at the 7 year age, and the deterioration rate can be subtracted for each year of age less than 7 and added for each year of age greater than 7). These rates are based only on the estimated changes in installed friction materials as vehicles age.

Table 31. Estimated PM2.5 Deterioration Rates and New-Vehicle Estimated Emission Rates based on Friction Material Trend with Vehicle Age

Vehicle Type	Additive deterioration per year of vehicle age, (mg/mi)	New vehicle estimated emission rate (mg/mi)
Conventional Passenger Car	0.0116	1.62
Light Truck	0.0716	1.54
Regenerative-Equipped	0.0031	0.93

Table 32. Estimated PM10 Deterioration Rates and New-Vehicle Estimated Emission Rates based on Friction Material Trend with Vehicle Age

Vehicle Type	Additive deterioration per year of vehicle age, (mg/mi)	New vehicle estimated emission rate (mg/mi)
Conventional Passenger Car	0.1617	8.18
Light Truck	0.4117	6.94
Regenerative-Equipped	0.0054	3.30

Figure 98 presents the modeled deterioration in emissions factors based on this approach. The vehicle-level emissions factors, calculated for 3 and 11 years of vehicle age, are presented along with the percent of estimated in-use vehicles equipped with LM pads for reference. Regenerative-equipped vehicles are not presented in the figure as they have nearly zero deterioration compared to the other two vehicle classes, and no data is available for that vehicle type on LM pad emissions.

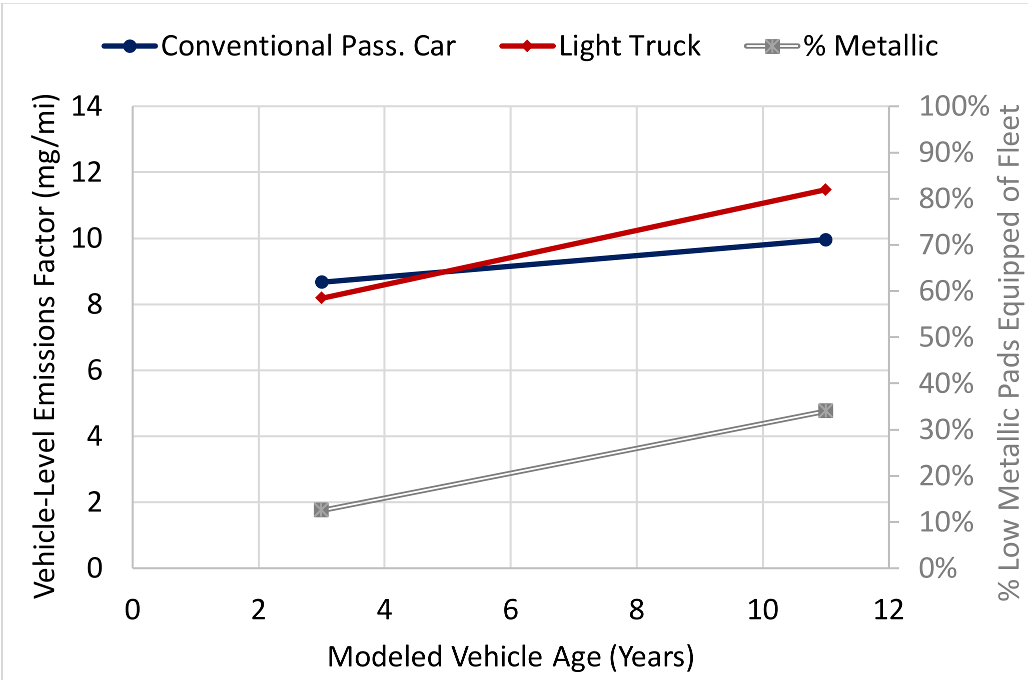

Figure 98. Emission factor deterioration with vehicle age for conventional passenger cars and light trucks. Also presented is the estimated percentage of in-use vehicles at a given age equipped with LM pads (same for both vehicle types).

Summary and Conclusions

This report presented the results from PM emissions testing of light-duty brake assemblies operating on a brake dynamometer. A new brake dynamometer test cycle was developed to represent the operation of real-world vehicles in California based on the Caltrans dataset. ERG adapted a previously developed algorithm to develop a test cycle that would be as similar as possible to the speeds, deceleration rates, temperatures, and braking durations encountered by real vehicles in the Caltrans survey. This new cycle was divided into three speed bins such that emission rates could be differentiated across different ranges of trip average speeds.

Six test vehicles (with common cross-platform brake components) were selected to represent the range of vehicle types in the light-duty fleet. Up to three different friction formulation types were tested for the front and rear assemblies of each model. Replicate tests were conducted for each test matrix combination.

The LINK lab site included a constant volume sampling (CVS) system with an integrated brake dynamometer. Measurements were made in batch and continuously by a variety of instruments including gravimetric sampling in parallel on coated aluminum impactors (TSI 100S4) as well as on 47mm Teflon filters. Instrumentation was also installed to measure particle size distributions, particle counts, and continuous particle mass.

Results were presented for emitted PM mass, particle count, and size distribution from the front and rear assemblies of six test vehicles. The test procedure developed for this work was able to resolve effects on particle mass emissions from the various parameters varied in the test matrix. Particulate mass emissions on a per-wheel-mile basis ranged from approximately 0.5 mg/wheel•mi for the Prius rear brakes operating at ETW with NAO pads up to 15 mg/wheel•mi for the front brake of an F-150 operating with a simulated cargo load and equipped with a low metallic friction material.

In most cases, low metallic friction materials resulted in higher mass emissions than NAO materials. Vehicles tested at higher simulated weights also tended to have higher mass emissions. For a given friction material type, PM emission masses trended linearly with vehicle test weight. Figure 99 presents the average by-vehicle emission mass vs test weight for each vehicle and test weight combination. The F-150 reference vehicle tended to have relatively low PM emissions for its vehicle weight when equipped with OES friction materials (as compared to the other vehicles).

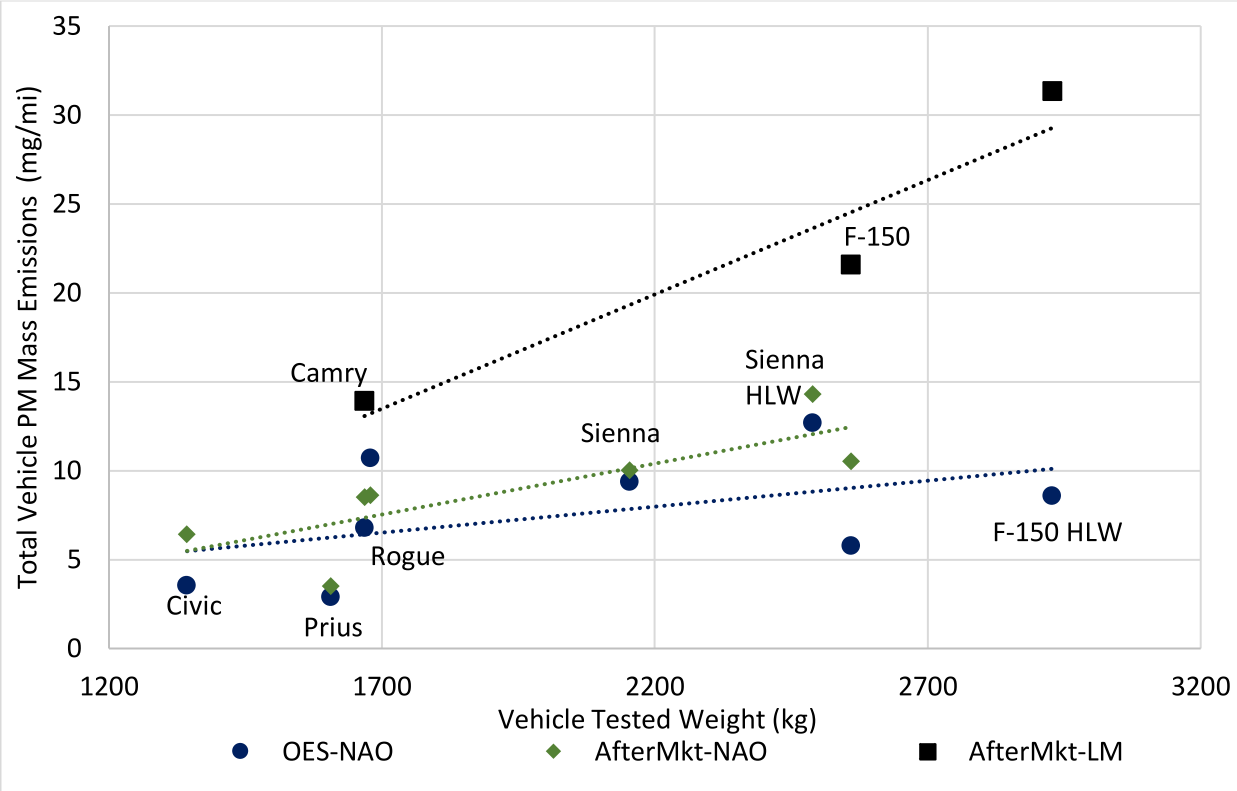

Figure 99. Total vehicle test cycle PM mass emissions vs simulated vehicle test weight, categorized by pad material

ERG used LINK business intelligence to estimate the in-use friction material fractions within each model. Using these fractions, ERG estimated the average in-use emission rates for each model. Table 33 presents these estimated emission rates of PM2.5 and PM10; they represent an inventory-level estimate for in-use emissions assuming an average vehicle age of 7 years.

Table 33. Estimated in-use brake PM emission rates by model (7 years old)

Model	Estimated In-Use PM2.5 Emission Rate (mg/mi)	Estimated In-Use PM10 Emission Rate (mg/mi)
Camry	1.7	9.3
Civic	1.1	5.7
F-150	2.0	9.8
F-150 HLW	2.6	13.9
Prius	1.0	3.3
Rogue	2.0	9.2
Sienna	2.1	9.9
Sienna HLW	2.7	13.9

The test cycle developed for this work included 3 segments representing vehicle trips of different average speeds. The continuous QCM mass data provided the source to resolve differences in emission rates across the three cycles. Using these results, ERG estimated SCFs that may be used to relate the cycle-overall emission masses to trips of different speed bins based on passenger cars and light trucks. Table 34 presents the calculated SCFs by speed bin and vehicle type for PM2.5 and PM10.

Table 34. Recommended SCFs by speed bin for different LDV types for PM2.5 and PM10.

Average	Passenger Cars		Light Trucks		Regenerative Cars	
Speed (mph)	PM2.5	PM10	PM2.5	PM10	PM2.5	PM10
5	0.612	0.735	0.604	0.815	0.262	0.399
10	0.786	0.909	0.791	1.014	0.553	0.706
15	0.961	1.082	0.979	1.214	0.844	1.013
20	1.136	1.256	1.167	1.413	1.134	1.321
25	1.314	1.399	1.321	1.495	1.365	1.503
30	1.494	1.513	1.442	1.459	1.535	1.560
35	1.675	1.626	1.563	1.423	1.706	1.618
40	1.567	1.486	1.454	1.256	1.624	1.494
45	1.170	1.093	1.116	0.958	1.290	1.187
50	0.773	0.699	0.778	0.660	0.957	0.881
55	0.516	0.450	0.553	0.459	0.708	0.650
60	0.399	0.345	0.440	0.355	0.543	0.494
65	0.282	0.240	0.327	0.251	0.378	0.339

This report also presented emissions results for particle size distribution and particle counts. Particle count emissions generally trended with overall mass, however the observed range from the lowest to highest emitter was reduced as compared to measured mass. In general, low metallic pads resulted in somewhat larger particle sizes than did NAO pads.

Recommendations

The Project 17RD016 proposal included a task in which ERG and LINK would use the experience in this work to develop recommendations for future work in the development of measurement techniques for non-exhaust PM emissions from vehicles.

Realistic Emissions Factors

The brake dynamometer system intentionally represents idealized braking particulate emission circumstances as compared to braking systems mounted on vehicles. They are idealized in that there is not a wheel/tire mounted, there is only the minimum hardware necessary for support of the components in the airflow, and there are not bodywork or vehicle frame elements in the airflow. This is intentional to maximize the repeatability of testing and to ensure that the maximum percentage of generated particles reach the point of sampling. The goal is to understand the particles generated at the friction couple, so it is important that the test setup maximize the sensitivity to particles originating at that point. In actual on-road use, however, some amount of brake-generated particulate settles on or adheres to vehicle components and surfaces. As a result, brake dynamometer testing may result in measurements that overestimate real in-use braking emissions.

ERG did not find any recent literature regarding the level of PM losses from settling. The Sanders (2003) study indicated estimates of the fraction of PM mass remaining airborne on a real vehicle being in the range of 50% - 70% of the emitted mass from the friction couple.[13] However, there was also some level of loss present in the dynamometer sampling system. The Arizona dust experiment indicated recovery percentages around 90%. **Accounting for this, a reasonable estimate for in-use emission rates would be 66% of the emission factors determined in this work.**

Further testing may help to inform a better understanding of the particle losses from settling, transient behavior like coagulation (and potential increased settling as a result), other dispersion considerations for brake particles, and temperature or meteorological effects on vehicle emissions in-use.

LINK and ERG recommend the following testing ideas for CARB’s continued investigation into brake emissions:

Long-term effects. In this work, the tested friction materials were relatively new as they were tested after approximately 11 hours of burnishing. While the friction materials used in a given pad or shoe are likely to be homogenous throughout in terms of chemistry, it may be beneficial to determine whether there is a PM emissions trend as the pad or shoe proceeds through its life toward end-of-life. Also, the friction materials in this program were free of corrosion or any other wear outside of that caused by the burnish cycle. It may be beneficial to determine any effect of corrosion (especially for metallic materials) or other environmental effects on PM emissions. This could potentially be done by working with vehicle fleets to make an agreement to acquire their used brake components for testing. A more costly option would be to conduct a full aging program in which the aging, corrosion, and/or wear would be conducted as a part of the experimental design.

Meteorological effects. Weather can affect both driving habits as well as the morphology of particles as they are released into the atmosphere. The Caltrans travel survey that formed the basis for the development of the CBDC test cycle was a wide-

---

[13] Sanders, Paul G. et. al. “Airborne Brake Wear Debris: Size Distributions, Composition, and a Comparison of Dynamometer and Vehicle Tests.” Environmental Science & Technology 37 (2003): 4060–4069

ranging project that would have captured various weather events across the state, however the weather was not logged or noted so no analysis is possible on that basis. Additionally, rain may have a large effect on mitigating PM emissions (though this would be likely to shift air quality effects of PM to watershed effects). Understanding these effects, taken with climate data for the state, may allow for a correction to be applied to the brake PM factors in EMFAC based on weather.

(Urban) Geographic location. There may also be reason to prioritize the analysis of urban environments (and their associated driving styles) in which vehicle and pedestrians would be grouped together in large numbers and close proximity. The test cycle in this work represented vehicle use across the state, but PM emissions may be a higher priority in urban areas due to population density. The low-speed portion of the CBDC reflects the driving in low-speed trips from across the state, not necessarily those from urban environments.

By event analysis. To further inform the understanding of the mechanisms and physical causes of varying levels of braking events, it may be of interest to conduct testing over a prescribed or gridded set of stops instead of the representative driving cycle used in this program. It could resemble the Heating and Cooling Matrix used in this work to develop the brake temperature model. A series of the same engineered stops could be performed repeatedly and characterized as a group. This could reduce the noise observed in the Individual Brake Event analysis in this work.

Alternative brake dynamometer setup. For dynamometer testing in which the intent is not necessarily to attempt to capture all of the PM from the brake friction interface, minor changes from the design used in this work may be beneficial. For example, with a slightly larger brake enclosure, it may be feasible to mount a "dummy wheel" to the tested brake rotor to determine whether it would collect a measureable amount of PM (i.e. measurably less PM would reach the point of sampling). The dummy wheel could be a typical vehicle wheel with just the spokes and inner drum, with some of the outer drum machined off so that it would fit in the enclosure. Depending on the design, it may also need to have a hole drilled out at the center to accommodate the dynamometer's brake hub support. Likewise, it may be possible to add an inner fender shape to the enclosure to disturb the airflow to determine if there is a measurable amount of particle loss. These are speculative ideas but potentially worth investigating.

Empirical/numerical models for transport losses. LINK developed a model of the transport losses of the CVS and sampling train setup used in this project. This was a relatively simple model assuming little turbulence and gradual curves in sample ducting. It may be of benefit to pursue modeling of transport losses in greater detail to create estimates of particulate settling on in-use vehicles, though this would require a much more complicated model than that used by LINK in analyzing the smooth surfaces of the setup used in this work.

Heavy Duty Vehicles

This work focused on light-duty vehicles ranging in size from a Honda Civic up to a Ford F-150. For EMFAC modeling, however, the heavy-duty vehicles operating in California may be the source of a significant amount of PM emissions from the on-road vehicle fleet. The increased weight of these vehicles means that braking energy to stop from a given speed is much higher than that for a light-duty vehicle. As a result, even though the population of these vehicles is lower than that of light-duty, the total emissions may be equivalent or even higher. One confounding factor is that heavy duty vehicles are more often equipped with drum brakes than their light-duty counterparts. In this study, the Civic rear axle was drum brake equipped and emitted at lower rates than the other vehicles, likely due to particles being trapped within the drum assembly. So, it is possible that heavy duty brake PM emissions do not completely scale up with weight at the same slope as the light-duty vehicles in this study.

Since the time of the 17RD016 request for proposal, Caltrans has initiated a parallel project to measure the PM emissions associated with heavy duty vehicle braking. One of the key challenges to this work involves the wide variety of vehicle types and vocations in the heavy-duty fleet. Additionally, heavy duty vehicles tend to have multiple axles (including trailer axles) that all may have different braking characteristics and associated emission rates. The Caltrans project will include 36 dynamometer tests from different axles of Class 8 tractor trailers, refuse trucks, beverage haul trucks, and urban buses. The results of this project will better inform the need for and direction for potential further testing. Additionally, in recognition of the potential differences in braking emissions between regenerative-braking equipped hybrid vehicles and regenerative-braking equipped electric vehicles, the Caltrans project will include brake PM testing of one light-duty electric vehicle. This will help determine whether there are differences in the regeneration strategies of the two vehicle types (both of which are becoming more prevalent in the in-use fleet) that measurably affect PM emission rates during on-road operation.

Tire Wear

The other potentially significant source of non-exhaust PM from vehicles is that of tire wear. The tire slip between the tire and roadway during operation results in abrasion of both sides of the friction couple. Rolling tires can also lift roadway debris and cause it to become airborne, and it is not always possible to determine whether the source of particulate is the tire, roadway material, or settled debris without chemical analysis. For the sake of measurement of all PM emission caused at the tire/road interface, the source is not important as all three directly contribute. However, if reductions are to be made possible, awareness of the source (either the roadway material or tire material) is critical to informing possibilities for reduction. Tire formulations generally consist primarily of styrene butadiene rubber, natural rubber, and polybutadiene. To enhance the engineering properties of the tire, zinc oxide is often present at levels of approximately one to two percent, and this zinc can comprise some percentage of the emitted particulate. Roadway surfaces vary more in material formulation, including stone/mineral matter, bituminous binder, sand, and various binders.[14]

The most common research publications discussing tire and roadway PM emissions are roadside or tunnel studies of the ambient air around vehicles traveling the roadway. These types of experiments reflect real in-use values but do not have the same level of control over vehicle types, tire materials, and driving styles as a dynamometer study in which a complete test matrix can be prescribed. Because many literature references describe roadside studies, many of the available emissions factors relate to ambient air on a by-volume basis, not to a per-mile basis as needed for informing EMFAC.[15,16]

Some studies have used a test vehicle with an onboard portable emissions measurement (PEMS) system mounted in such a way that it draws in tire and road or brake PM. These types of measurements generally involve a funnel-shaped capturing device with a sample pump that draws the air and PM into the system for measurement. Depending on the size and shape of the funnel, it can sample either tire/road interface PM or brake PM (with some risk of cross-contamination). These types of measurements allow for control of the test vehicle operational conditions and the tire and roadway materials. This type of testing is also subject to environmental conditions and contaminations, unlike the controllable conditions in a lab.

There have been studies involving various laboratory dyno systems that simulate the tire/road interface within controlled laboratory conditions. Like the brake dynamometer, these systems were generally developed for testing other tire parameters (such as tread life or noise) and were then adapted to PM testing. It is challenging to develop a representative laboratory simulation of the tire/road interface, however. Two existing designs are the system used by the German Federal Highway Research Institute (BASt), in which a large cylinder is fabricated, and the inside surface is made of roadway material. A wheel and tire combination is driven around the inside of this loop in a manner similar to a planetary gear in a gearset. Turning loads, tire scrubbing, acceleration, and deceleration can all be simulated with this design, and the volume within the confines of the cylindrical enclosure can be sampled for emitted PM.

[14] Ntziachristos and Boulter. (2013). EMEP/EEA air pollutant emission inventory guidebook - 2013: 1.A.3.b.vi Road vehicle tyre and brake wear.
[15] Panko, Julie & Hitchcock, Kristen & Fuller, Gary & Green, David. (2019). Evaluation of Tire Wear Contribution to PM2.5 in Urban Environments. Atmosphere. 10. 99. 10.3390/atmos10020099.
[16] Sommer et. Al. (2018). Tire Abrasion as a Major Source of Microplastics in the Environment. Aerosol and Air Quality Research. 18. 10.4209/aaqr.2018.03.0099.

Another method is a flat circular roadway surface with a centrally mounted arm that supports a wheel and tire traveling around the roadway surface. Acceleration, deceleration, and scrubbing can also be simulated with this design; however, the constant turning may emit a greater number of particles due to shear than would be emitted while traveling along a straight path. This type of laboratory setup has been used by the Swedish National Road and Transport Research Institute (VTI).

There is also the design that operates more like a light-duty chassis dynamometer in which a wheel and tire rides on the outside of a large textured drum, such as a 48" dynamometer roll. This interface can be mounted within an enclosure and the generated particles drawn and sampled from that enclosure. Because the tire is riding against a round surface, the tire stresses, deformation, and likely PM emissions would be higher than that from driving along a flat surface.[17] Some adjustment factor to account for this would be necessary. Of the various laboratory designs, this design appears to be the most cost-effective to fabricate, especially in a lab already containing a chassis dynamometer and PM sampling equipment.

The literature reveals a wide range of particle emissions estimates and wear factors. One aspect that adds complexity is that tires can sometimes separate larger particles up into the ~1mm range. These particles settle immediately so do not become airborne particulate, but they are a part of the mass represented by reported "wear factors."[18] So, literature review must take care to specify the type of emission of interest. This difference contributes to the wide range of observed values for tire wear in literature. ERG has attempted to compile some estimates of tire and road wear and they are presented in Table 35. The table presents two emission sources, tires only or the tire and road interface. For comparison, value ranges are given for PM2.5, PM10, and all wear. Some values are given in literature on a per-tire basis and some are given at the vehicle distance traveled level, indicated by vkm.

[17] Dalmau, Eugenia & Augsburg, Klaus & Wenzel, Felix & Ivanov, Valentin. (2017). Tire particle emissions: Demand on reliable characterization.
[18] Sommer et. Al. (2018). Tire Abrasion as a Major Source of Microplastics in the Environment. Aerosol and Air Quality Research. 18. 10.4209/aaqr.2018.03.0099.

Table 35. Selected light-duty tire and roadway PM emission factors from literature

Emission Source	PM2.5	PM10	All Mass
Tire Only			0.02-0.11 g/vkm[19];
Tire + Roadway	0.31-0.5 ug/tire•km	0.54-0.95 ug/tire•km; 3.5-9.0 mg/vkm[20]	3.5-6.4 mg/km (>PM10)[21]

Based on literature, there appears to be a wide variety of research into measuring particulate emissions from tires, however there does not appear to be a consensus or any standardization of test processes. One potential avenue of work would be to conduct a survey or poll from various researchers to start developing a consensus on what can be agreed upon and standardized to start moving toward a test method that can be widely accepted.

[19] Ntziachristos and Boulter. (2013). EMEP/EEA air pollutant emission inventory guidebook - 2013: 1.A.3.b.vi Road vehicle tyre and brake wear.

[20] PMP – Particle Measurement Program UNECE Informal Group, Non-exhaust traffic related particle emissions. Non-exhaust traffic related particle emissions (brake and tyre/road wear). Informal document GRPE-73-14 73rd GRPE, 6-10 June 2016. https://www.unece.org/fileadmin/DAM/trans/doc/2016/wp29grpe/GRPE-73-14.pdf

[21] Aatmeeyata, D.S. Kaul, Mukesh Sharma,*Traffic generated non-exhaust particulate emissions from concrete pavement: A mass and particle size study for two-wheelers and small cars*, Atmospheric Environment, Volume 43, Issue 35, 2009, Pages 5691-5697

References

Mathissen, M. et. al., A novel real-world braking cycle for studying brake wear particle emissions, Wear, Volumes 414–415, 2018

Garg, Bhagwan D. et. al. "Brake Wear Particulate Matter Emissions." Environmental Science & Technology 34.21 (2000): 4463–4469

Sanders, Paul G. et. al. "Airborne Brake Wear Debris: Size Distributions, Composition, and a Comparison of Dynamometer and Vehicle Tests." Environmental Science & Technology 37 (2003): 4060–4069

Marcel Mathissen, Jaroslaw Grochowicz, Christian Schmidt, Rainer Vogt, Ferdinand H. Farwick zum Hagen, Tomasz Grabiec, Heinz Steven and Theodoros Grigoratos, A novel real-world braking cycle for studying brake wear particle emissions, Wear, https://doi.org/10.1016/j.wear.2018.07.020e

EPA Annual Certification Data for Vehicles, Engines, and Equipment https://www.epa.gov/compliance-and-fuel-economy-data/annual-certification-data-vehicles-engines-and-equipment

Society of Automotive Engineers (SAE) Standard J2789, Inertia Calculation for Single-Ended Inertia-Dynamometer Testing
https://www.sae.org/standards/content/j2789_201008/

Grigoratos, Theodoros & Martini, Giorgio. (2014). Brake wear particle emissions: a review. Environmental science and pollution research international. 22. 10.1007/s11356-014-3696-8.

Ntziachristos and Boulter. (2013). EMEP/EEA air pollutant emission inventory guidebook - 2013: 1.A.3.b.vi Road vehicle tyre and brake wear.

Panko, Julie & Hitchcock, Kristen & Fuller, Gary & Green, David. (2019). Evaluation of Tire Wear Contribution to PM2.5 in Urban Environments. Atmosphere. 10. 99. 10.3390/atmos10020099.

Sommer et. Al. (2018). Tire Abrasion as a Major Source of Microplastics in the Environment. Aerosol and Air Quality Research. 18. 10.4209/aaqr.2018.03.0099.

Dalmau, Eugenia & Augsburg, Klaus & Wenzel, Felix & Ivanov, Valentin. (2017). Tire particle emissions: Demand on reliable characterization.

PMP – Particle Measurement Program UNECE Informal Group, Non-exhaust traffic related particle emissions. Non-exhaust traffic related particle emissions (brake and tyre/road wear). Informal document GRPE-73-14 73rd GRPE, 6-10 June 2016. https://www.unece.org/fileadmin/DAM/trans/doc/2016/wp29grpe/GRPE-73-14.pdf

Aatmeeyata, D.S. Kaul, Mukesh Sharma,Traffic generated non-exhaust particulate emissions from concrete pavement: A mass and particle size study for two-wheelers and small cars, Atmospheric Environment, Volume 43, Issue 35, 2009, Pages 5691-5697

Glossary of Terms, Abbreviations, and Symbols

100S4 – The TSI instrument used in this work to measure gravimetric PM mass at various size classifications using coated aluminum impactors

APS – Aerodynamic Particle Sizer, the TSI instrument used to measure particle size distributions in the range from 0.5 – 20 μm

Brake Event – In a driving trace, the period of time from the initial application of the brakes until the brakes are either released or the vehicle comes to a stop

BWI – Brake Wear Index (or Indices), a measure of the amount of brake emissions potential from a given vehicle or brake component, weighted by friction material mass and the counts in-use in the fleet

California Brake Dynamometer Cycle (CBDC) – The new brake dynamometer test cycle developed and used during this test program

EEPS – Engine Exhaust Particle Sizer, the TSI instrument used to measure particle size distributions in the range from 5.6 to 560 nm

ETW – Equivalent test weight, the simulated test weight used for most tests in this program; corresponds to curb weight + 300 lbs.

Generalized Coastdown Curve – The estimated coastdown curve, derived from the average of the road load coastdowns of the 6 test vehicles in this program, used to identify braking events in the Caltrans dataset (any decelerations greater than this curve were flagged as braking events)

Heating and Cooling Matrix – The test matrix of standardized braking events and cruise intervals followed by each vehicle on the test track while recording brake temperatures in order to provide inputs to the temperature model.

HLW – Heavily laden weight, the test weight used in some tests of the cargo-carrying vehicles amounting to two thirds of the difference between the curb weight and gross vehicle weight

LM – Low metallic friction materials used in some tests of the Camry and F-150 assemblies. Indicates the materials have a larger amount of metal than NAO

Microtrip – An identified portion of the Caltrans driving trace consisting of the time that a vehicle starts moving, through the cruise and lasting until the next stop.

NAO – Non asbestos organic friction materials, the most common friction material and that comprising all OES pads

OES – Original Equipment Service, the friction material specified in dealer-sourced replacement parts

PM – Particulate Matter, often classified by PM2.5, indicating particulate up to 2.5μm in diameter, and PM10, particulate up to 10μm in diameter

QCM – Quartz Crystal Microbalance, the TSI instrument used to measure continuous PM2.5 mass

Represented distance – the distance represented by the CBDC for inventory purposes; the cycle consists of braking events extracted from real trips as well as engineered cruises added for cooling, neither of which has distance basis in real use; represented distiance also includes the actual distance traveled between each braking event

SCC – Speed Correction Cycles, the EMFAC speed cycles used to factor UC emission rates into the different EMFAC speed bins

SCF – Speed Correction Factors, the values provided in this work that may be used to to factor the overall vehicle-level emission rates found in this work into groups of EMFAC speed bins

UC – The EMFAC Unified Cycle, the standard basis for exhaust emissions factors in EMFAC

WLTP-Brake – The World-Harmonized Brake cycle, developed recently in Europe in cooperation with the JRC; a new cycle designed specifically for measuring brake PM emissions.